



DEVELOPMENT OF PLIER-LIKE CATIONIC NIOSOMES FOR GENE
DELIVERY AGAINST BREAST CANCER CELLS



A Thesis Submitted in Partial Fulfillment of the Requirements
for Doctor of Philosophy (PHARMACEUTICAL TECHNOLOGY)
Department of PHARMACEUTICAL TECHNOLOGY
Graduate School, Silpakorn University
Academic Year 2020
Copyright of Graduate School, Silpakorn University

การพัฒนานีโอโซมประจุบวกที่มีลักษณะคล้ายคีมสำหรับนำส่งยีนเพื่อต้านเซลล์มะเร็ง
เต้านม



วิทยานิพนธ์นี้เป็นส่วนหนึ่งของการศึกษาตามหลักสูตรปรัชญาดุษฎีบัณฑิต
สาขาวิชาเทคโนโลยีสารสนเทศ แบบ 1.2 ปรัชญาดุษฎีบัณฑิต
ภาควิชาเทคโนโลยีสารสนเทศ
บัณฑิตวิทยาลัย มหาวิทยาลัยศิลปากร
ปีการศึกษา 2563
ลิขสิทธิ์ของบัณฑิตวิทยาลัย มหาวิทยาลัยศิลปากร

DEVELOPMENT OF PLIER-LIKE CATIONIC NIOSOMES FOR
GENE DELIVERY AGAINST BREAST CANCER CELLS



By
MISS Supusson PENGNAM

A Thesis Submitted in Partial Fulfillment of the Requirements
for Doctor of Philosophy (PHARMACEUTICAL TECHNOLOGY)
Department of PHARMACEUTICAL TECHNOLOGY
Graduate School, Silpakorn University
Academic Year 2020
Copyright of Graduate School, Silpakorn University

Title DEVELOPMENT OF PLIER-LIKE CATIONIC NIOSOMES FOR
 GENE DELIVERY AGAINST BREAST CANCER CELLS
By Supusson PENGNAM
Field of Study (PHARMACEUTICAL TECHNOLOGY)
Advisor Professor PRANEET OPANASOPIT , Ph.D.

Graduate School Silpakorn University in Partial Fulfillment of the
Requirements for the Doctor of Philosophy

.....Dean of graduate school
(Associate Professor Jurairat Nunthanid, Ph.D.)

Approved by

.....Chair person
(Associate Professor TANASAIT NGAWHIRUNPAT,
Ph.D.)

.....Advisor
(Professor PRANEET OPANASOPIT , Ph.D.)

.....Co advisor
(Associate Professor Theerasak Rojanarata , Ph.D.)

.....Co advisor
(Assistant Professor Samarwadee Plianwong , Ph.D.)

.....External Examiner
(Associate Professor Boon-ek Yingyongnarongkul , Ph.D.)

59353801 : Major (PHARMACEUTICAL TECHNOLOGY)

Keyword : GENE DELIVERY SYSTEMS, siRNA, NIOSOMES, CATIONIC LIPIDS, APOPTOSIS

MISS SUPUSSON PENGNAM : DEVELOPMENT OF PLIER-LIKE CATIONIC NIOSOMES FOR GENE DELIVERY AGAINST BREAST CANCER CELLS THESIS ADVISOR : PROFESSOR PRANEET OPANASOPIT, Ph.D.

In this study, novel synthesized plier-like cationic lipids (PCLs, i.e., PCL-A, -B and -C) were used to formulate plier-like cationic niosomes (PCNs) for nucleic acid delivery. The molar ratio of PCL-A was primarily optimized in formulations. The PCN-A composed of Span 20: cholesterol: PCL-A (2.5: 2.5: 2 mM) were successfully prepared, resulting in niosomes with a positive charge and the nano-sized range. The weight ratios of PCNs: DNA or PCNs: siRNA affected the efficiency were also studied. The result indicated that PCN-A/DNA or PCN-A/siRNA at the weight ratios of 1: 1 and 5: 1 showed the highest efficiency in the delivery of DNA and siRNA, respectively. Among the cationic niosomes, PCN-B gave the highest transfection efficiency and silencing efficiency compared to PCN-A and PCN-C. The internalization pathway of PCN-B for siRNA delivery was found to be endocytosis which was almost the same as DNA delivery. Cholesterol on the cellular membrane is important for cell membrane ruffle formation which involved in endocytosis pathways. PCNs presented pH-sensitive properties which might contribute to intracellular endosomal escape for gene delivery. PEGylation of PCN-B at 0, 2 and 5% were evaluated on cellular activity and physical stability. PEGylation at 2% significantly reduced cytotoxicity and improved efficiency for pDNA and siRNA delivery in HeLa cells. PEGylation significantly improved storage stability. Therefore, the recommended storage condition of PCN-B was 4 °C for 1 month, whereas PEGylated PCN-B could be stored at 4 °C or 25 °C for at least 4 months. Moreover, PCN-B and PEGylated PCN-B gave high transfection and silencing efficiency with minimal cytotoxicity, even in the presence of serum. Here, the anticancer effect of siRNA against anti-apoptotic genes, namely, Mcl-1, Bcl-2 and survivin, was screened in breast cancer cell line MCF-7 and MDA-MB-231. PCN-B was successfully employed as siRNA carriers for anti-apoptotic mRNA targets that could deliver and release siRNA to the desired target site and silence mRNA targets in both MCF-7 and MDA-MB-231 cells. The silencing of Mcl-1 mRNA noticeably reduced the cell viability by approximately 30% in MCF-7 cells. This finding suggested that Mcl-1 downregulation might be a potential target in MCF-7 cells for apoptosis induction. However, the study of cationic niosomes for gene delivery still needs more studies in translational research. This study revealed that PCN-B could be an effective and safe alternative transfection reagent for not only pDNA but also siRNA delivery.

ACKNOWLEDGEMENTS

It would not have been possible to complete this dissertation without the help and support from everyone around me. Firstly, I would like to express my sincere gratitude to my thesis advisor, Prof. Dr. Praneet Opanasopit, for the continuous support of my Ph.D study and related research, for his motivation and immense knowledge. Her guidance helped me in all the time of research and writing of this thesis.

My sincere gratitude also goes to my thesis co-adviser, Assoc. Prof. Theerasak Rojanarata and Assist. Prof. Samarwadee Plianwong for the helpful support, invaluable suggestion, and kindness given to me during my study. I am very much indebted to them. I could not have imagined having a better advisor and co-advisor for my Ph.D study.

Besides my advisors, I would like to thank the rest of my thesis committee: Assoc. Prof. Dr. Tanasait Ngawhirunpat and Assoc. Prof. Dr. Boon-ek Yingyongnarongkul, for their insightful comments and encouragement, and the hard question that incited me to widen my research from various perspectives.

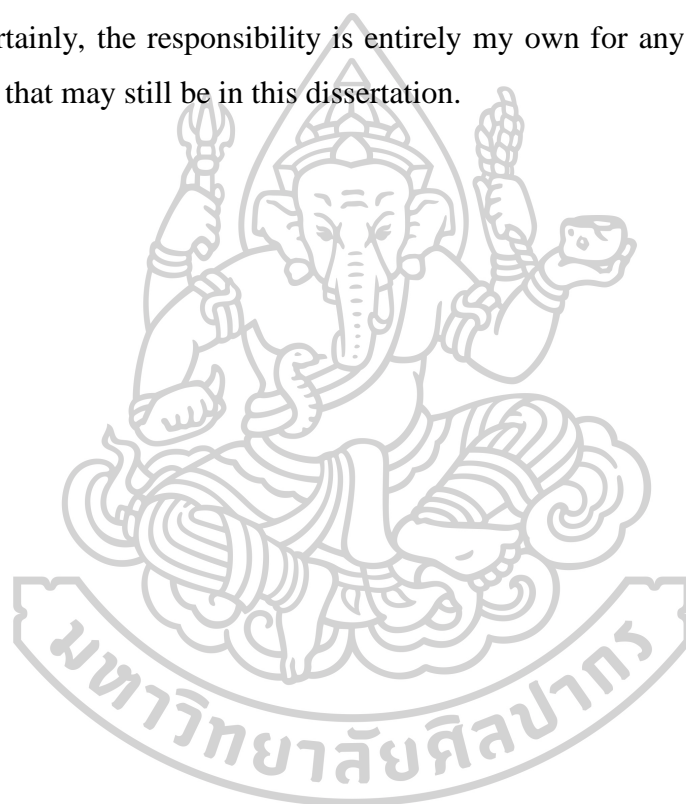
My special appreciation goes to Asst. Prof. Dr. Prasopchai Patrojanasophon, Asst. Prof. Dr. Siripan Limsirichaikul valuable advice, support, and kindness throughout this research. I would like to thank my collaborators at the Faculty of Sciences, Ramkhamhaeng University, for helping me synthesized the cationic lipids used in this work.

My sincere thanks also go to Assoc. Prof. Dr. May Xiong, who provided me an opportunity to join their team as visiting researcher in his laboratory at the University of Georgia, Athens, Georgia, USA. I really appreciate her professional and excellent guidance and value everything I have learned from her. My special thanks are extended to Dr. Zhi Liu and Xiong's lab members for their helping and caring during my living in the USA.

My next gratitude and appreciation go to the Commission of Higher Education (Thailand), the Thailand Research Sciences and Innovation (TSRI) through the Royal Golden Jubilee Ph.D. program (Grant No. PHD/0047/2559), for financial support during my study as well as Faculty of Pharmacy, Silpakorn University for facility support and partial financial support.

My special thanks go to my friends and members of the Pharmaceutical Development of Green Innovation Group (PDGIG), especially Miss Areerut Sripattanaporn, Dr. Teeratas Kansom and Dr. Worranan Rangsimawong, for valuable laboratory techniques and their support. Last but not least, I would like to give the greatest appreciation to my beloved family: Mr. Sirichai Pengnam, Ms. Suwanna Thuamklud, Ms. Siriruk Phainpanitporn, Mr. Pravit Phattarapaisarn and my father's friend family for their spiritual supports, understanding, encouragement, and unconditional love in me, as always, for which my mere expression of thanks likewise does not suffice.

Certainly, the responsibility is entirely my own for any mistake or inadequate information that may still be in this dissertation.



Supusson PENGNAM

TABLE OF CONTENTS

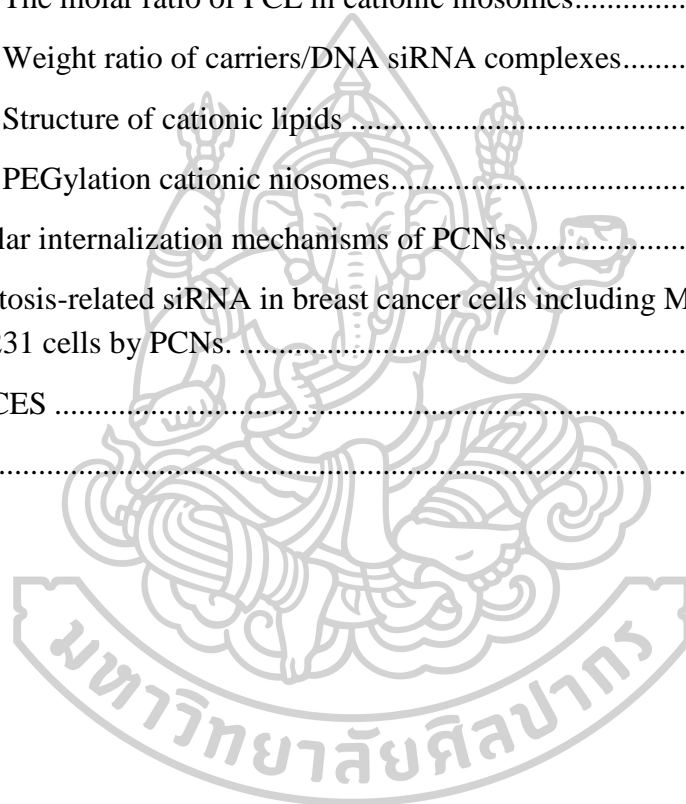
	Page
ABSTRACT.....	D
ACKNOWLEDGEMENTS.....	E
TABLE OF CONTENTS.....	G
LIST OF TABLES.....	L
LIST OF FIGURES.....	M
LIST OF ABBREVIATIONS.....	1
CHAPTER 1.....	4
INTRODUCTION.....	4
1.1 Statement and significance of the research problem.....	4
1.2 Aims and objectives.....	9
1.3 The research hypothesis.....	9
CHAPTER 2.....	10
LITERATURE REVIEWS.....	10
2.1 Introduction of gene therapy.....	10
2.1.1 Gene therapy strategies for cancer treatment.....	11
2.1.2 Mechanisms of RNA-based therapeutics.....	12
2.1.3 RNA-based therapeutics.....	13
2.2 Apoptosis: A target for anticancer therapy.....	15
2.2.1 Role of apoptosis.....	15
2.2.2 Morphology features of apoptosis.....	15
2.2.3 Signaling transduction pathway of apoptosis.....	16
2.2.4 Apoptotic targeting in cancers.....	17
2.2.4.1 B-cell lymphoma-2 (Bcl-2) family.....	19
2.2.4.2 Inhibitors of apoptosis proteins (IAPs).....	20
2.2.5 Applications of siRNA targeting apoptosis in breast cancers.....	20

2.3 Challenge of siRNA delivery.....	21
2.3.1 Extracellular barriers	21
2.3.2 Intracellular barriers	22
2.3.2.1 Internalization of nanoparticles	22
2.3.2.1 Endosomal escape	24
2.4 siRNA delivery systems	25
2.4.1 Classification of gene delivery methods	25
2.4.2 Non-viral nanoparticles for siRNA delivery	27
2.4.2.1 Biological nanoparticles	27
2.4.2.2 Inorganic nanoparticles	28
2.4.2.3 Organic nanoparticles.....	28
2.4.2.3.1 Polymer-based delivery systems.....	28
2.4.2.3.2 Lipid-based delivery systems (LNPs).....	29
2.4.2.3.2.1 Solid lipid nanoparticles (SLNs)	29
2.4.2.3.2.2 Lipid nanovesicles: liposomes and niosomes.....	29
2.5 Niosomes: siRNA delivery	32
2.5.1 Surface modification of niosomes	32
2.5.1 Surface modification of niosomes	33
2.5.1.1 Cationic lipids.....	33
2.5.1.2 PEGylation	35
2.5.2 Applications of niosomes for siRNA delivery	35
CHAPTER 3	39
MATERIALS AND METHODS.....	39
3.1 Materials	39
3.2 Equipments	41
3.3 Methods	43
3.3.1 Preparation of plasmid DNA.....	43
3.3.2 Preparation of siRNA targeting green fluorescent protein and siRNA targeting apoptotic pathway	43

3.3.3 Cell culture	43
3.3.4 Preparation of plier-like cationic niosomes (PCN) and PEGylated plier-like cationic niosomes (PEG-PCN)	44
3.3.5 Preparation of cationic niosomes/nucleic acid complexes (nioplexes)	44
3.3.6 Characterization of niosomes and DNA or siRNA complexes	45
3.3.6.1 Size and zeta potential measurements	45
3.3.6.2 Agarose gel retardation assay	45
3.3.6.3 Transmission electron microscopy (TEM).....	45
3.3.6.4 Buffer capacity	46
3.3.7 Cytotoxicity test of cationic niosomes and nioplexes	46
3.3.9 Study of <i>in vitro</i> silencing efficiency of siRNA complexes in HeLa cells	47
3.3.10 Study of effect of serum on <i>in vitro</i> gene transfection in HeLa cells.....	48
3.3.11 Study of cellular uptake by flow cytometry	48
3.3.12 Confocal laser scanning microscope	48
3.3.13 Investigation of internalization pathways.....	49
3.3.14 Quantification of mRNA level by real-time PCR	49
3.3.15 Cell proliferation analysis	50
3.3.16 Double stain apoptosis detection by Hoechst 33342 and SYTOX™ Green staining.....	51
3.3.17 Physical stability study.....	51
3.3.18 Statistical analysis	51
CHAPTER 4	52
RESULTS AND DISCUSSION	52
4.1 Screening of plier-like cationic lipid-A (PCL-A) molar ratios.....	52
4.1.1 Particle sizes and zeta potential.....	52
4.1.2 Transfection and silencing efficiency study	54
4.1.3 Cytotoxicity of nioplexes	55
4.2 Effect of plier-like cationic lipids (PCLs)	56
4.2.1 Cationic niosomes for DNA delivery.....	56

4.2.1.1 Particle sizes and zeta potential of cationic niosome and nioplexes	56
4.2.1.2 Gel retardation assay	58
4.2.1.3 Transfection study for DNA delivery	58
4.2.1.4 Cytotoxicity of nioplexes	59
4.2.1.5 Internalization pathways of nioplexes for DNA delivery	60
4.2.2 Cationic niosomes for siRNA delivery	61
4.2.2.1 Particle sizes and zeta potential of cationic nioplexes.....	61
4.2.2.2 Gel retardation assay	62
4.2.2.3 Silencing study for siRNA delivery	63
4.2.2.4 Cytotoxicity of nioplexes	64
4.2.2.5 Cellular uptakes of nioplexes studied by using flow cytometry analysis and confocal laser scanning microscopic (CLSM)	65
4.2.3 Cytotoxicity of Plier-like cationic niosomes (PCNs).....	67
4.2.4 Internalization pathways of nioplexes for siRNA delivery	67
4.2.5 Morphology analysis	68
4.2.6 Buffering capacity	69
4.3 Effect PEGylation on plier-like cationic niosome-B (PCN-B).....	71
4.3.1 Particle sizes and zeta potential.....	71
4.3.2 Gel retardation assay	72
4.3.3 Cellular activity of nioplexes	73
4.3.4 Cytotoxicity of cationic niosomes and nioplexes.....	74
4.3.5 Effect of serum on transfection and silencing efficiency	75
4.3.6 Protein serum aggregation.....	76
4.3.7 Physical stability of PEGylated cationic niosomes	77
4.4 Apoptosis induction of Bcl-2, Mcl-1 and survivin targeted siRNA delivery in breast cancer cells.....	79
4.4.1 Cellular uptake of nioplexes studied by using flow cytometry analysis and CLSM	79
4.4.2 Expression level of mRNA target by real-time PCR	81

4.4.3 Cytotoxicity of cationic niosomes	84
4.4.4 Inhibition of cell proliferation	84
4.4.5 Double stain apoptosis detection: Hoechst 33342 and SYTOX™ Green	86
CHAPTER 5	89
CONCLUSION.....	89
5.1 Formulation of cationic niosomes (PCN) containing plier-like cationic lipids (PCLs) as non-viral gene carriers	89
5.1.1 The molar ratio of PCL in cationic niosomes.....	89
5.1.2 Weight ratio of carriers/DNA siRNA complexes.....	89
5.1.3 Structure of cationic lipids	90
5.1.4 PEGylation cationic niosomes.....	90
5.2 Cellular internalization mechanisms of PCNs.....	90
5.3 Apoptosis-related siRNA in breast cancer cells including MCF-7 and MDA- MB 231 cells by PCNs.....	91
REFERENCES	92
VITA.....	108



LIST OF TABLES

	Page
Table 1 Role of anti-apoptotic protein to Bcl-2 family members (94).....	19
Table 2 Chemical inhibitors of endocytosis and their putative mechanism of action (101).....	23
Table 3 Non-viral based for siRNA delivery for cancers in clinical trials (74, 100)..	26
Table 4 Advantages and disadvantages non-viral nanoparticles used in gene delivery (74).....	31
Table 5 Applications of cationic niosomes for siRNA delivery (58)	38
Table 6 The particle size, zeta potential and polydispersity index (PDI) of cationic niosomes with plier-like cationic lipid-A (PCN-A) at various molar ratios are presented as mean \pm SD	53
Table 7 The particle size, zeta potential and PDI of cationic niosomes (PCNs) formulated with different cationic lipids PCL-A, -B and -C at molar ratios of 2 The data were presented as the mean \pm SD of triplicates.	56
Table 8 IC ₅₀ of plier-like cationic niosomes (PCNs) in HeLa cells were presented as the mean \pm SD of triplicates.....	67
Table 9 The particle size and zeta potential and PDI of PCN-B, 2% PEG-PCN-B and 5% PEG-PCN-B are presented as mean \pm SD	71
Table 10 The IC ₅₀ of 0% PEG-PCN-B, 2% PEG-PCN-B and 5% PEG-PCN-B in HeLa cells were presented as the mean \pm SD of triplicates	74
Table 11 The IC ₅₀ of 0% PEG-PCN-B and 2% PEG-PCN-B in MCF-7 and MDA-MB 231 cells were presented as the mean \pm SD of triplicates.....	84

LIST OF FIGURES

	Page
Figure 1 gene therapeutic approaches (74)	10
Figure 2 gene therapy strategies for cancer therapy targeting TME and molecular strategies are presented in green and purple, respectively (74).	12
Figure 3 Intracellular processing of RNA-based therapeutics depending on the endogenous miRNA pathway (77).....	13
Figure 4 Signaling transduction pathway of apoptosis (6)	17
Figure 5 Endocytic mechanisms classification in mammalian cells.(103)	24
Figure 6 Non-viral nanoparticles used in gene delivery	27
Figure 7 Chemical structure of some of compounds used in the composition of niosomes (58).....	32
Figure 8 Examples of lipid-types and structures used for the delivery of siRNAs including monovalent and multivalent cationic lipids (119). Representative structure of cationic lipid DOTMA and linker bonds of cationic lipid (48).	34
Figure 9 The structures of PCLs: (a) PCL-A, (b) PCL-B and (c) PCL-C	39
Figure 10 The particle size (bars) and zeta potential (lines) of (a) PCN-A/DNA complexes at weight ratios of 0.1-20 and (b) PCN-A/siRNA complexes at weight ratios of 1-20.....	54
Figure 11 Cellular activities presented as (a) transfection efficiency and (b) silencing efficiency of PCN-A at various molar ratios of 1.5-2 mM. *The data significantly higher than Lipo2k at p value < 0.05.	55
Figure 12 Cell viability of PCN-A 1.5, PCN-A 2 and PCN-A 2.5 of (a) DNA complexes and (b) siRNA complexes in HeLa cells at various weight ratios	56
Figure 13 The particle size and zeta potential of various weight ratios of PCNs/DNA complexes from 0.1-20	57
Figure 14 The DNA complex formation ability of PCN-A, PCN-B and PCN-C by gel agarose electrophoresis	58
Figure 15 Transfection efficiency of PCN-A, PCN-B and PCN-C in HeLa cells at the weight ratio from 0.1-20. *The data was significantly higher than Lipo2k at p-value < 0.05.....	59

Figure 16 Cell viability of PCN-A, PCN-B and PCN-C/DNA complexes at the weight ratio of 0.5-20 in HeLa cells	60
Figure 17 Investigation of internalization pathways of PCN-A, PCN-B and PCN-C/DNA complexes evaluated with pretreatment of specific endocytosis inhibitors, (a) transfection efficiency of each PCNs and (b) scheme of possible internalization pathways. *The data was significantly different from the transfection without pretreatment at p-value < 0.05.	61
Figure 18 The particle size and zeta potential of various weight ratios of PCNs/siRNA complexes from 0.1-20.....	62
Figure 19 The siRNA complex formation ability of PCN-A, PCN-B and PCN-C by gel agarose electrophoresis	63
Figure 20 The silencing efficiency of PCN-A, -B and -C/siGFP complexes compared to siNT complexes. *The data was significantly higher than Lipo2k at p-value < 0.05. #The data was significantly different at p-value < 0.05.	64
Figure 21 Cell viability of PCN-A, PCN-B and PCN-C/siRNA complexes at the weight ratio of 0.5-20 in HeLa cells	65
Figure 22 Cellular uptake evaluated after 24 h transfection with siAF488 complexes in HeLa cells. (a) the percentage of cellular uptake, (b) MFI plot and fluorescence histogram and (c) CLSM images. *The data was significantly different from Lipo2k transfection at p-value < 0.05.	66
Figure 23 Investigation of internalization pathways of PCN-A, PCN-B and PCN-C/siGFP complexes evaluated with pretreatment of specific endocytosis inhibitors, (a) transfection efficiency of each PCNs and (b) scheme of possible internalization pathway. *The data was significant different form the transfection without pretreatment at p value < 0.05.....	68
Figure 24 (a) the particle size and shape of PCN-B (~87 nm), (b) nioplexes of PCN-B/DNA at a weight ratio of 2.5 (~167 nm) (c) nioplexes of PCN-B/siRNA at a weight ratio of 15 (~186 nm)	69
Figure 25 Titration curves of PCN-A, PCN-B and PCN-C were compared to PEI and deionized water applied as a control. The systems were adjusted to pH 11.5 with NaOH and titrated with 0.5 μ L aliquot of 1 M HCl.	70
Figure 26 The particle size (bar graph) and Zeta potential (line graph) of (a) DNA complexes at weight ratios of 0.1-20 and (b) siRNA complexes at weight ratios of 1-20.....	72
Figure 27 The complex formation ability of (a) DNA complexes and (b) siRNA complexes by Gel agarose electrophoresis	73

Figure 28 Effect of PEGylation on transfection efficiency and silencing efficiency of PCN-B and 2% PEG-PCN-B/DNA at weight ratios of 2.5 and 10, respectively. *The data was significantly different higher than Lipo2k transfection at p -value < 0.05. ...74

Figure 29 Cell viability of 0% PEG-PCN-B, 2% PEG-PCN-B and 5% PEG-PCN-B complexes; (a) DNA complexes and (b) siRNA complexes75

Figure 30 Silencing efficiency of siRNA complexes at weight ratios of 5-20; (a) Effect of serum on silencing efficiency of 0% PEG-PCN-B and (b) 2% PEG-PCN-B/siGFP at weight ratios of 5-20. *The data was significantly different from transfection without the presence of serum at p -value < 0.05.76

Figure 31 The variations in particle size of 0% PEG-PCN-B, 2% PEG-PCN-B and 5% PEG-PCN-B/ siRNA complexes in 10% FBS.....77

Figure 32 The particle size and zeta potential of 0% PEG-PCN-B, 2% PEG-PCN-B and 5% PEG-PCN-B after being kept at (a) 4 °C and (b) 25 °C for 4 months78

Figure 33 Cellular uptake evaluated after 24 h transfection with siAF488 complexes in MCF-7 cells, (a) the percentage of cellular uptake, (b) MFI plot and fluorescence histogram and (c) CLSM images. *The data was significantly different from Lipo2k transfection at p -value < 0.05.80

Figure 34 Cellular uptake evaluated after 24 h transfection with siAF488 complexes in MDA-MB 231 cells, (a) the percentage of cellular uptake, (b) MFI plot and fluorescence histogram and (c) CLSM images. *The data was significantly different from Lipo2k transfection at p -value < 0.05.81

Figure 35 The relative mRNA expression study evaluated using the $2^{-\Delta\Delta CT}$ method which presented as a percentage; (a) relative Mcl-1 mRNA expression and (b) relative survivin mRNA expression in MCF-7. ***The data was significantly different from siNT complexes transfection at p -value < 0.001. #The data was significantly different from Lipo2k transfection at p -value < 0.05.82

Figure 36 The relative mRNA expression study evaluated using the $2^{-\Delta\Delta CT}$ method which presented as a percentage; (a) relative Mcl-1 mRNA expression and (b) relative survivin mRNA expression in MDA-MB 231. ***The data was significantly different from siNT complexes transfection at p -value < 0.001. #The data was significantly different from Lipo2k transfection at p -value < 0.05.83

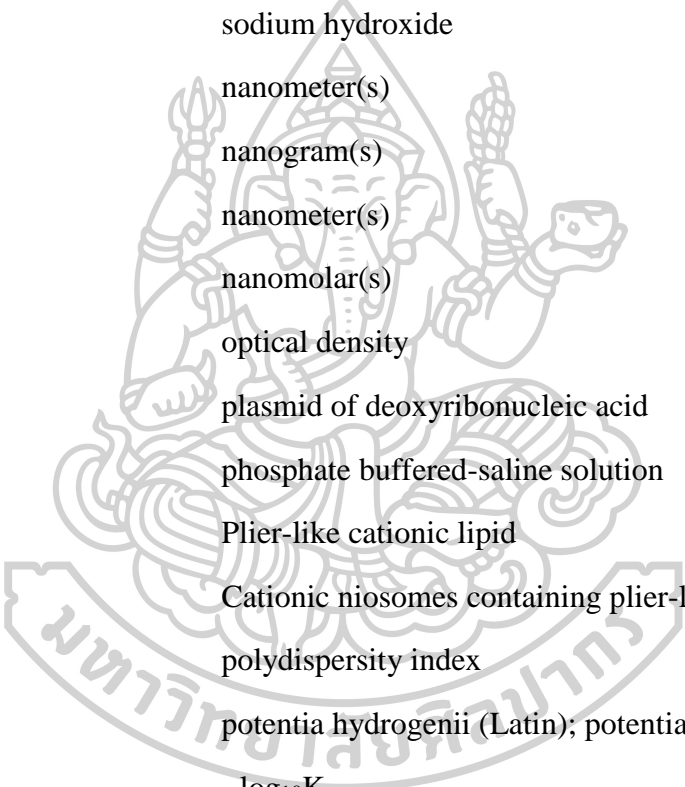
Figure 37 Cell viability of indicated siRNA targeting (Mcl-1, Bcl-2 and survivin) in (a) MCF-7 and (b) MDA-MB 231 cells. The percentage of induced cell death (c) was obtained from the comparison Mcl-1 siRNA complex with siNT complex treatment of each formulation in MCF-7 cells. *The data was significantly different from siNT complexes transfection at p -value < 0.05.86

Figure 38 Double stain apoptosis detection was observed under Inverted fluorescence microscope (100X) after 24h of treatments. Untreated cell control (a); PCN-B/siNT (b); 0.8 μ M of doxorubicin (c); Lipo2k/Mcl-1 siRNA (d); 0% PEG-PCN-B/Mcl-1 siRNA (e); 2% PEG-PCN-B/Mcl-1 siRNA (f).....88



LIST OF ABBREVIATIONS

AF488	Alexa fluor 488
ANOVA	analysis of variance
cm ⁻¹	wave number
CO ₂	carbon dioxide
CS	chitosan
DLS	dynamic light scattering
DNA	deoxyribonucleic acid
DMEM	Dulbecco's modified Eagle's medium
DMSO	dimethyl sulfoxide
Dox	doxorubicin
e.g.	exempli gratia (Latin); for example
et al.	and others
FBS	fetal bovine serum
FITC	fluorescein isothiocyanate
g	gram(s)
h	hour(s)
HCl	hydrochloride
IC ₅₀	half-maximal inhibitory concentration
i.e.	id est (Latin); that is
M	molarity
MEM	Minimum essential media
meq	milliequivalents
mg	milligram(s)
min	minute(s)
mL	milliliter(s)



mm	millimeter(s)
mm ³	cubic millimeter(s)
mmol	millimole
MTT	3-(4,5-Dimethylthiazol-2-yl)-2,5 diphenyltetrazolium bromide, a tetrazole
mV	millivolt(s)
MW	molecular weight
NaOH	sodium hydroxide
nm	nanometer(s)
ng	nanogram(s)
nm	nanometer(s)
nM	nanomolar(s)
OD	optical density
pDNA	plasmid of deoxyribonucleic acid
PBS	phosphate buffered-saline solution
PCL	Plier-like cationic lipid
PCN	Cationic niosomes containing plier-like cationic lipid
PDI	polydispersity index
pH	potentia hydrogenii (Latin); potential for hydrogen
pK _a	- log ₁₀ K _a
RH	relative humidity
RNA	ribonucleic acid
rpm	revolutions per minute
s	second(s)
siRNA	short interfering ribonucleic acid
SD	standard deviation
TEM	transmission electron microscopy
UV	ultraviolet (spectroscopy)

vs	versus
v/v	volume by volume
w/v	weight by volume
w/w	weight by weight
μg	microgram(s)
μL	microliter(s)
μm	micron; micrometer(s)
μM	micromolar(s)
%	percentage(s)
™	trademark
®	registered trademark
°C	degree Celsius
>	more than
<	less than
~	approximately
π	pi
θ	theta



CHAPTER 1

INTRODUCTION

1.1 Statement and significance of the research problem

Aberrant changes in genes controlling the way cells function and how they grow and divide are one of the causes of cancers (1). There are approximately 38.4% of the population may be detected with cancer at some point in the lifetimes (2). Currently, breast cancer is the leading cancer found in female patients and was the second cause of death in the US in 2020 (3). It has been linked to inherited gene mutations obtained from one's mother or father by 5-10%, whereas 85% of breast cancer is found in women who have no family history (4). Genetic mutation can occur during the aging process and general life more than obtaining from an inherited family (5).

Apoptosis or programmed cell death is a fundamental biological process regulating homeostasis. Deregulation of this pathway is important in the pathology of many diseases as well as cancer (6, 7). As early as the 1970's, Kerr et al. proposed that hypergenesis sometimes results from the loss of apoptosis rather than an increase in mitosis (8). The evasion of apoptosis is known as one of the hallmarks of cancer (9). The initiation of apoptosis is governed by the balance of pro and anti-apoptotic proteins. The anti-apoptotic proteins, i.e., the B-cell lymphoma-2 (Bcl-2) protein family, includes Bcl2-A1, Bcl-2, Bcl-xL, Bcl-w and Mcl-1 which are pro-survival mediators preventing apoptosis (10, 11). The up-regulation and hyperactivation of the Bcl-2 family have been described in cancers, which contributes to the survival of cancerous cells and the resistance to chemotherapy (10, 12). Bcl-2 is overexpressed in half of human malignancies and 50-70% of breast cancer patients (13-15). Bcl-2 exerts its oncogenic role by preventing cells from undergoing apoptosis (16). It is commonly associated with estrogen receptor (ER)-positive tumors. Bcl-2 can also be expressed in human epidermal growth factor receptor 2 (HER2) positive tumors (~50%), and basal-like (~19%) and triple-negative (TN) breast cancers (~41%), defined by absent or minimal ER, Progesterone Receptor (PR) and HER2 expression. Apart from breast cancer, Bcl-2 is overexpressed in approximately 75% of tumors (17). Mcl-1 is an anti-

apoptotic protein in the Bcl-2 family which plays an important role in apoptosis induction. Mcl-1 is also a vital protein regulating breast cancer cell survival (18). Overexpression of Mcl-1 is manifested in various human malignancies including breast cancer which contributes to cell survival and conventional therapeutic resistance (10, 19, 20). Mcl-1 is involved in many pathways including the phosphatidylinositol-3 kinase (PI3K) pathway, the mTOR pathway and the mitogen-activated protein kinase (MAPK) pathway. Mcl-1 overexpression was related to poor prognosis in many cancer types (21). Recent evidence from in vitro experiments suggests that Mcl-1 is an important role in breast cancer cell survival. Particularly in TN breast cancers, they lack the ER and the PR expression and do not have amplification of ERBB2, and they do not respond to current targeted therapies (22). The initiation of the apoptosis pathway eventually converges at the activation of the caspase cascade. However, the function of caspases can be blocked by a family of proteins through caspases binding termed inhibitor of apoptosis proteins (IAPs); e.g., NIAP, c-IAP1, XIAP and survivin (23, 24). Among these IAPs, survivin exhibits significant overexpression in many tumors, especially in breast and lung cancer. However, it is present at low levels or completely absent in healthy cells and tissues (25-28). Moreover, targeting survivin with siRNA or miRNA re-sensitizes drug-resistant breast cancer cell lines to chemotherapeutic agents including paclitaxel, taxol and Dox (29, 30). Despite the attractive attributes of siRNA in cancer precision therapy, the success of siRNA-based therapy relies on safe and effective siRNA delivery systems. The developments in novel therapeutic strategies for breast cancer are urgently needed to improve therapeutic outcomes and patients' quality of life.

It has been almost five decades of ongoing gene therapy study (31). The genetic therapeutic strategy may fulfill the gaps of unachievable treatments and preventions for several diseases, not only in hereditary diseases but also acquired diseases such as AIDs, cancers and infectious diseases (32-34). Gene delivery is the process of introducing foreign genetic material, such as DNA or RNA, into host cells (35). However, it challenges delivering the naked nucleic acids directly through plasma membrane due to their size and physicochemical properties (36, 37). Genetic materials must reach the desired target site of actin in host cells to provide gene expression or

alteration (38). The delivery systems are categorized as follows: viral and nonviral (39, 40). Although approximately two-thirds of the trials in viral vectors have been the desired approach, the primary limitations toward development are safety concerns and the relatively small capacity of viral vectors. In recent years, the use of nonviral vectors has been expanding and conducting to date in trials since its strengths such as ease of chemical characterization, simplicity and reproducibility of use, larger packaging capacity, and minimal serious concerns. Due to these reasons, the development of nonviral vectors has been expected that they could be potential candidates for gene delivery systems (41). Not only therapeutically suitable genes but also the specific RNA molecules can be used in gene therapy. The post-transcriptional gene silencing effect via the RNA interference (RNAi) mechanism has been widely investigated as a promising new approach for curing human diseases such as genetic disorders, inflammation and viral infection, etc (42, 43). The RNAi mechanism can be triggered by some effective molecules such as small interfering RNA (siRNA). siRNA are short double-stranded RNA segments with two nucleotide 3'-overhangs, usually composed of 21–23 nucleotides. Results from siRNA action, a specific mRNA are degraded and the protein synthesis is inhibited (44). siRNA is highly specific, easily synthesized and cost-effective. In addition, siRNA-mediated target gene silencing is significantly more potent (more than 100-fold difference in the half-maximal inhibitory concentration) and efficient than antisense oligonucleotides or ribozymes (45). Consequently, RNAi technology is concerned as a potential therapeutic agent for diseases of a genetic etiology (46).

Lipofection has been intensively investigated and applied in 4.5% of all gene delivery trials. Lipofection is known as lipid-based transfection, which is constructed as lipid bilayer vesicles behaving like a cell membrane and can carry both hydrophobic and hydrophilic molecules, including nucleic acids, into cells (41). Cationic liposomes have been widely used as potentially efficacious gene carriers due to their ability to form complexes with anionic DNA molecules supposed to deliver DNA into the cells via the endosomal pathway (47). Cationic liposome-mediated gene delivery is affected by numerous factors, and one of the major factors is the composition of the liposomes. Moreover, the altering type and amount of cationic lipid composed in the cationic

liposomes can enhance the transfection efficiency (48). Additionally, several studies have reported that another vesicular system, non-ionic surfactant vesicles (niosomes), can also be used as an alternative to liposomes for gene delivery (49).

Niosomes were invented to imitate the bilayer of liposomes. Niosomes are primarily composed of nonionic surfactants (i.e., Sorbitan monolaurate (Span) and Polysorbate (Tween) that are used instead of phospholipids in liposomes with the assistance of cholesterol (Chol) for bilayer rigidity (50, 51). Distinctive points of niosomes compared with liposomes are cost-effective and exhibit better chemical stability against both oxidation and temperature for introduction into pharmaceutical manufacturing (52-54). Cationic lipids are also incorporated into vesicles as charge inducers to allow the complex formation via electrostatic interaction. Paecharoenchai et al. successfully formulated non-ionic surfactant vesicles consisted of Span 20, Chol, and spermine derivative cationic lipids for pDNA delivery into HeLa cells. It not only exhibited similar physical properties but also efficiently transferred pDNA with low cytotoxicity and hemolytic activity as those of liposomes (53, 55).

Generally, the structure of cationic lipids is composed of 3 parts (cationic polar head, linker, and hydrophobic tail). It has been reported that the lipid used could affect the physicochemical properties and efficiencies of niosomes; for example, the particle size, charge, stability, serum protection, cellular internalization, nucleic acids binding ability, and condensation (56, 57). Many researchers synthesized cationic lipids as an alternative composition for gene carriers, but a few were successful in increasing the transfection efficiency of niosomes (58, 59). The commonly used cationic lipids can be classified by their chemical structure into: i) monovalent aliphatic lipids, e.g. N[1-(2,3-dioleyloxy) propyl]-N,N,N trimethylammonium chloride (DOTMA) and 1,2-dioleyl-3-trimethylammonium-propane (DOTAP), ii) multivalent aliphatic lipids, e.g. dioctadecylamidoglycylspermine (DOGS) and iii) cationic cholesterol derivatives, e.g. 3b-[N-(N0 ,N0-dimethylaminoethane)-carbamoyl]cholesterol (DC-Chol) (48). Multivalent aliphatic lipids exhibit higher performance than the monovalent ones; therefore, they have attracted more attention in the last decade (59-62). Modifications of the cationic lipid structure involve three components, cationic head, linker, and hydrophobic tail, which have been considerably investigated since relatively few

structural changes might affect their physicochemical properties and biological activity (63, 64). The hydrophobic tail is commonly a double alkyl chain or a cholesterol derivative. Extensive evidence regarding the double alkyl chain alteration indicates that generally 12–18 carbon units are essential for fusogenic characters and intermembrane mixing between delivery systems and cell membrane, including endosomal escape ability (63, 65). The ethylenediamine head had been reported to enhance the silencing efficiency of luciferase-targeted siRNA in the HT29 colon cancer cells and also improve the transfection efficiency in ARPE-19 cells and PECC cells (66-68). Nonetheless, positive charges on cationic niosomes cause non-specific interaction with plasma protein, leading to complex dissociation. The rapid clearance and high cytotoxicity of carrier/gene complexes also occur if the particles present a positive charge. Polyethylene glycol (PEG) is a hydrophilic polymer that has been widely used for steric stabilization of nanoparticulate delivery systems to prevent particle aggregation. On the contrary, PEGylation also perturbs gene condensation, cellular attachment and intracellular trafficking which could decline the biological activity of gene delivery systems (69). However, a number of articles have lightly studied PEGylated niosomes for gene delivery.

The aim of this study was to formulate the plier-like cationic niosomes (PCNs) containing novel synthesized cationic lipids with or without PEGylation. PCNs mediating gene/siRNA transfection was screened in HeLa and HeLa stably expressing cells (HeLa-GFP cells). PCNs was also applied to deliver apoptosis-related siRNA in breast cancer cells including MCF-7 and MDA-MB 231 cells. The influences of various factors, such as the chemical structure of cationic lipids, molar ratios of cationic lipids in formulation and weight ratios of the carrier to nucleic acids, on the transfection efficiency, silencing efficiency and cell viability of cationic niosomes were evaluated. Furthermore, cellular internalization pathways of niosomes/nucleic acid complexes were evaluated by using inhibitors specific to various endocytic pathways (70-72). Cellular uptake of cationic niosome/Alexa Fluor 488-labeled siRNA (siAF488) complexes was also evaluated by flow cytometry and confocal laser scanning microscope. The most effective formulation of PCN was selected to deliver siRNA related to apoptosis pathway siRNA targeting Bcl-2, Mcl-1 and survivin into breast

cancer cells including MCF-7 and MDA-MB 231 cells. The cellular uptake, cell proliferation analysis and double stain apoptosis detection (Hoechst 33342/ SYTOX™ Green) were also analyzed. Moreover, the physical stability of these cationic niosomes was evaluated by size and charge measurements.

1.2 Aims and objectives

1. To formulate cationic niosomes containing plier-like cationic lipids (PCLs) as non-viral gene carriers for *in vitro* study.
2. To investigate factors affecting *in vitro* transfection efficiency, silencing efficiency and cell viability of cationic niosomes i.e., chemical structure, the molar ratio of PCLs:surfactant:helper lipid, PEGylation, serum presence and the weight ratios of plier-like cationic niosomes (PCNs) to nucleic acids.
3. To investigate the possible cellular internalization mechanisms of PCNs which may involve their role as a gene carrier in HeLa cells.
4. To deliver apoptosis-related siRNAs and silence those mRNA expressions in breast cancer cells including MCF-7 and MDA-MB 231 cells by PCNs.

1.3 The research hypothesis

1. The molar ratios of Span 20: Chol: PCLs, PCNs/nucleic acid weight ratios, PEGylation, serum presence and different of hydrophobic tails on PCLs affect DNA or siRNA delivery.
2. PCNs are safe and can be potential carriers for DNA or siRNA delivery *in vitro*.
3. PCNs/nucleic acid complexes can be taken up by HeLa cells via clathrin-dependent endocytosis, clathrin-independent endocytosis or micropinocytosis pathway.
4. The PCNs can be applied for siRNA delivery, which involves apoptosis targeted genes in breast cancer cells (MCF-7 and MDA-MB 231 cells).

CHAPTER 2

LITERATURE REVIEWS

2.1 Introduction of gene therapy

Expression modulations are approached by introducing genetic material with exogenous versatile nucleic acids such as DNA (e.g., pDNA) or RNA-based therapeutics (e.g., miRNA, siRNA). Genetic modification can be achieved either through *ex vivo* or *in vivo* strategies for preventing or treating diseases. The *ex vivo* gene therapy, the target cells can be harvested from a patient, corrected, and transferred back into the patient, while *in vivo* genetic material can be directly conveyed through systemic administration to desired tissue or organ, as depicted in Figure 1. A defective specific gene can cause various genetic diseases, for instance, haemophilia due to mutations in genes encoding clotting factors which is able to be corrected by missing gene delivery (73). In the case of cancer therapy, genetic aberration often expresses in many stages in order to promote tumor cell survival. The overexpressed gene can be downregulated with RNA interference technology, e.g., siRNA, miRNA.

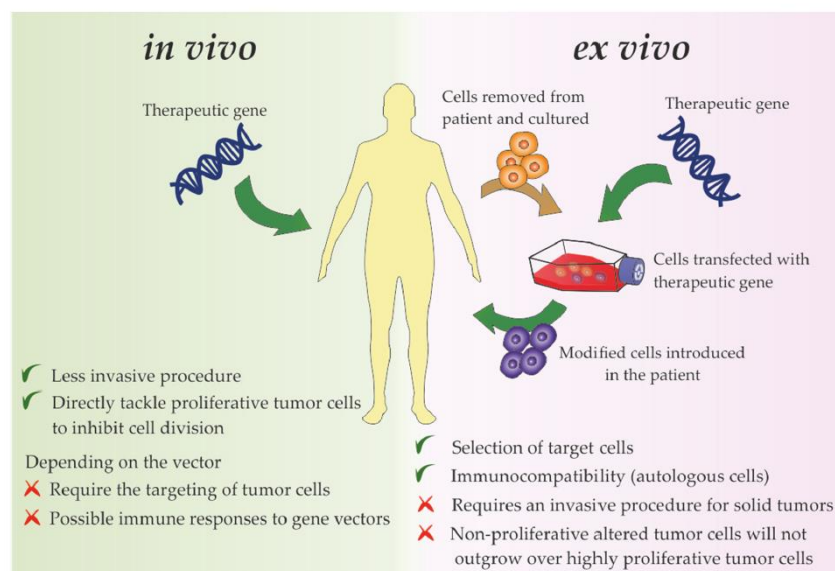


Figure 1 gene therapeutic approaches (74)

2.1.1 Gene therapy strategies for cancer treatment

Cancer is caused by aberrant changes to genes that control the way our cells function, especially they grow and divide (1). Approximately 38.4% of men and women will be diagnosed with cancer at some point during their lifetimes (based on 2013–2015 data) (2). Two crucial keys promoting tumor growth are pro-inflammatory environment and genomic instability. Complex signaling networks of TME promote not only tumor development but also metastasis (75). Nonetheless, the consequence of aberrant cell division and tumor suppression regulations frequently causes genomic instability supporting cell proliferation, evasion of tumor suppressors, and replicative immortality (76). For cancer treatment, gene therapy applications are divided into two major strategies (Figure 2): 1) therapies targeting complex tumor microenvironment (TME), i.e., immunization gene therapy (tumor vaccines, CAR-T cell therapy, cytokines genes), targeting angiogenesis, targeting cancer-associated fibroblasts, targeting tumor-derived exosomes and 2) molecular genetic modification, i.e., oncogene silencing, tumor gene replacement, miRNA targeted therapy, genome editing, suicide genes. Gene delivery to cancer cells has been allowed to treat cancer through the gene silencing strategies such as siRNA or miRNA involving oncogene such as cMYC or KRAS as well as genes related with multi-drug resistance 1 (MDR1). Gene replacement and editing strategies are exploited for cancer treatments via introducing gene expression such as tumor suppressor gene or correcting gene mutations. Gene therapy product was firstly used gencidine, a recombinant P53 adenovirus, in 2003 by delivering DNA for head and neck cancer treatment (74).

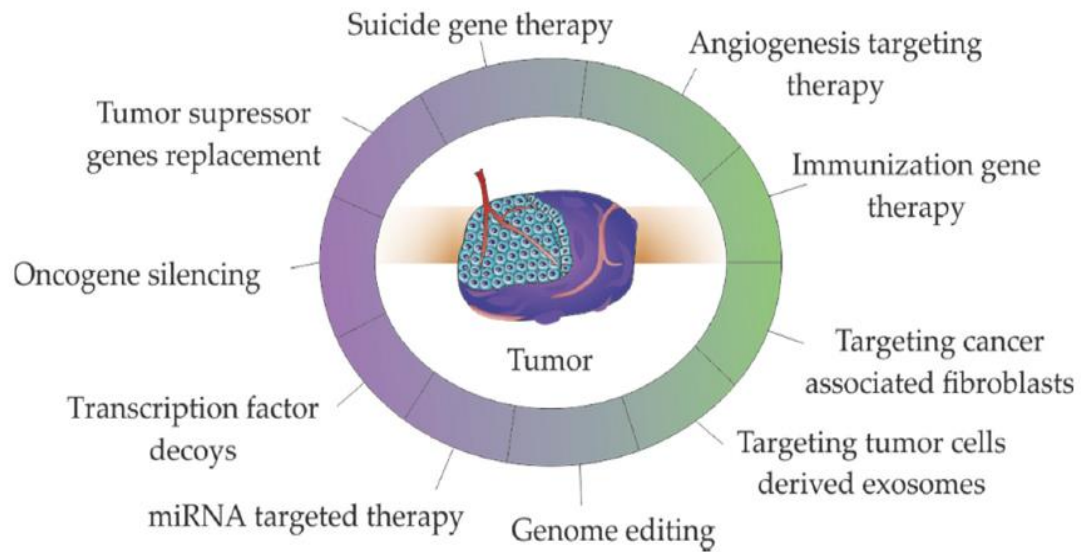


Figure 2 gene therapy strategies for cancer therapy targeting TME and molecular strategies are presented in green and purple, respectively (74).

2.1.2 Mechanisms of RNA-based therapeutics

RNAi, known as post-transcriptional silencing of the cellular biological mechanism, is essential for homeostasis. The gene silencing process can be triggered by exogenous dsRNA to defend against pathogen infection which is governed by RNA-induced silencing complex (RISC). Mature miRNA can also be produced from endogenous miRNA gene, which is transcribed to the double-stranded stem-loop structure of primary miRNA (Pri-miRNA) and then processed into pre-miRNA by Drosha-DGCR8 complex with loop structure duplex (70-100 nucleotides). It is transported by Exportin 5 from the nucleus to cytoplasm and is processed to mature miRNA by Dicer into 18-25 nucleotides. Short double-stranded RNA is called siRNA/shRNA. AGO2 in RISC unwinds and saves antisense/guide strand for mRNA target downregulation. The post-transcriptional silencing converges at RISC and is processed through several mechanisms, as presented in Figure 3.

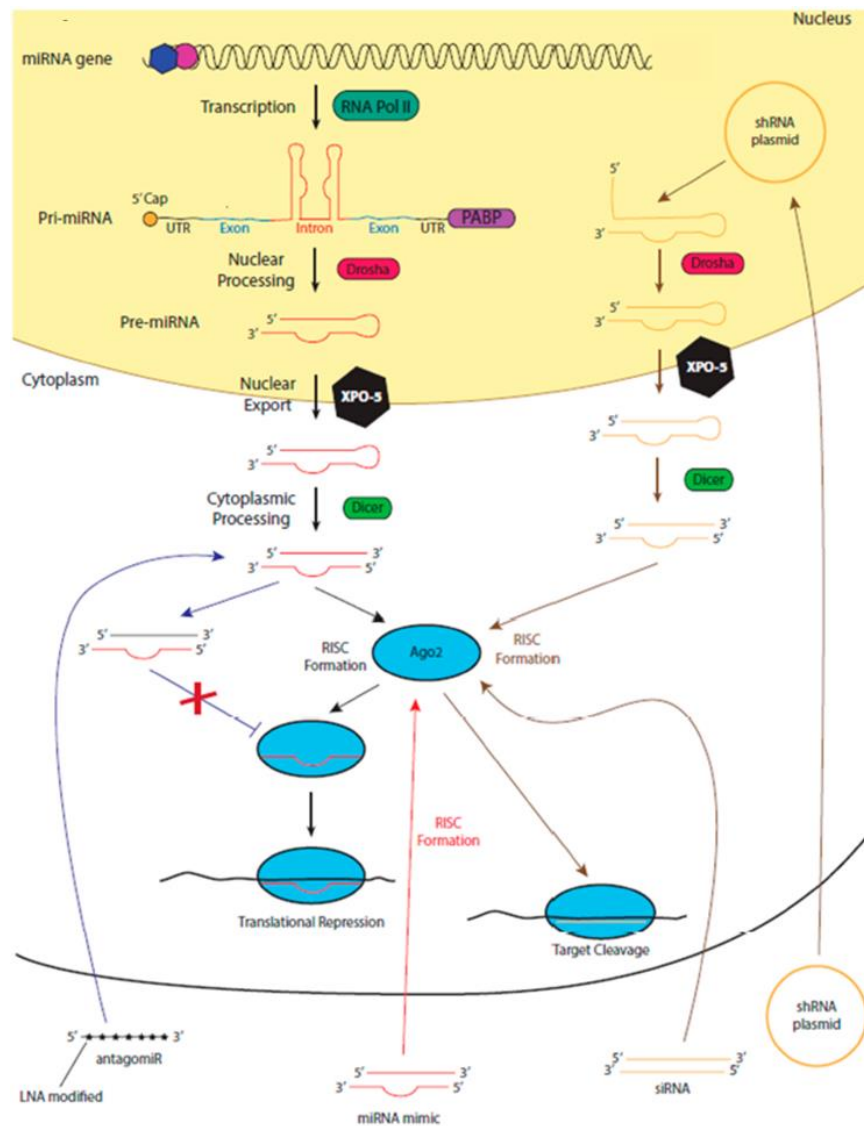


Figure 3 Intracellular processing of RNA-based therapeutics depending on the endogenous miRNA pathway (77)

2.1.3 RNA-based therapeutics

The RNAi study has been apparently increasing for a potential therapeutic candidate, an accurate and precise treatment strategy. Gene silencing therapy is usually implemented through RNA interference (RNAi) technology for downregulating target genes. Gene regulation through gene silencing in tumor cells is to retard tumor progression, control cell division, promote apoptosis, or suppress oncogenes. Common

RNA drugs recently have been developed are antisense oligonucleotide (ASO), siRNA, or microRNA (miRNA), which are further discussed.

Antisense oligonucleotides (ASO)

Antisense oligonucleotide (ASO) is synthetic single-stranded nucleic acids that can be RNA or DNA sequences. ASOs bind complementary with mRNA targets and introduce a range of outcomes, including alteration of splicing process, an obstacle of ribosomal activity, and downregulation of gene translation which is the consequence of RNase H recruitment to target transcript via ASOs binding (78).

Small interfering RNA (siRNA)

siRNA consists of 19-21 nucleotides with 3' overhang of 2 nucleotides which usually are TT or UU for RNAi machinery recognition. Passenger or sense strand is cleaved by Argonaute 2 (AGO2). Sense strand guides the RISC to mRNA target which is highly selective leading to mRNA degradation and translation inhibition. siRNA completely binds to complementary sites and further cleaves the target transcript resulting in translation inhibition. On the other hand, siRNA is applied for identification and validation in drug discovery and development models. Drug candidate for cancer therapy in pipelines are presented in Table 3.

microRNA (miRNA)

miRNA is produced for a post-transcriptional manner, contributing to critical roles in cellular maintenance and dynamic environmental response. The overexpression and downregulation of miRNA can be found in various cancers promoting tumor progression and bypassing inhibitory. Moreover, miRNA is essential to control the processes such as cell proliferations and apoptosis. The mature miRNA comprises 19-25 nucleotides which partially bind with mRNA targets requiring 2-8 complementary nucleotides. The distinctive characteristic of miRNAs potentially makes them being promising therapeutic candidates for inhibition of multiple mRNA targets at the same time. Moreover, the expression levels of miRNA can be an indicator of disease progressions. miRNAs utilize not only drug target therapeutic agents but also diagnostic and biomarker tools (77)

2.2 Apoptosis: A target for anticancer therapy

2.2.1 Role of apoptosis

Apoptosis or programmed cell death coined in 1972 by John Kerr is a fundamental process to develop and regulate tissue homeostasis and serve for the elimination of any unnecessary or unwanted cells. There are differential features of apoptosis from necrosis. Necrosis is considered an uncontrollable process triggered by environmental perturbation and release inflammatory mediators, cause accidental cell death and extensive tissue damage consequence. On the other hand, apoptosis is related to complicated signaling cascades accomplished by effector molecules called “cysteine-aspartic proteases or caspases”. Nomenclature Committee on Cell Death (NCCD) has been classified apoptosis as regulated cell death without leakage of the cell content into the surrounding environment (79).

2.2.2 Morphology features of apoptosis

Once abnormal cells are found, the activation of caspases initiates a cascade of apoptotic events resulting in morphological changes. In the early stage, cells experiencing apoptosis change to round shape, and water loss results in cell shrinkages. Typically, a lipid refers to as phosphatidylserine is only in an inner plasma membrane exposed on the apoptotic cell surface. The biological consequence of phosphatidylserine is useful for the recognition of phagocytes (80, 81). The nuclear chromatin condenses toward degradation nuclear envelope as a pyknosis and initiates DNA to nuclear fragmentation called karyorrhexis. Cell components and cytoplasm are closely packed into the individual plasma membrane sealing separated from the cell in terms of blebbing. The membrane-bound-vesicles containing cell organelles are called apoptotic bodies and promptly eliminated via phagocyte systems in *in vivo* without the consequence of inflammation from the releasing of intracellular components. In the event of *in vitro* apoptosis, there is a lack of the phagocyte resulting in apoptotic bodies eventually undergoing late apoptosis or secondary necrosis (82, 83).

2.2.3 Signaling transduction pathway of apoptosis

Signaling of apoptosis is initiated via varieties of conditions, for instance, DNA damage, uncontrolled proliferation and cell death from viral infection. It can be activated through two pathways, namely the extrinsic or intrinsic pathways differing in the origin of cascades (Figure 4). Finally, the activation of either pathway converges at the execution of mitochondrial caspases which are caspase-3, -6, and -7, as downstream effectors of apoptosis, leading to the programmed cell death termination by the enzymatic cleavages; proteases and nucleases (84).

The extrinsic pathway is triggered by the ligation of death receptors at the plasma membrane; thus, it is also called the receptor pathway. The receptors (for example, Fas, also known as CD95, tumor necrosis factor receptor, or TRAIL receptors) can be induced by death-inducing signals, mostly from immune response to infected or damaged cells. The consequences of stimulation result in oligomerization receptors, recruitment of adaptor proteins such as Fas-associated protein with death domain (FADD) and TNF receptor-associated protein with death domain (TRADD), including the formation of the death-inducing signaling complex (DISC), which in turn, change effector proteins to active forms, namely, caspase-8 and caspase-10 (85). Moreover, as the results of activated caspase-8 of the extrinsic pathway can alternatively turn on the intrinsic pathway via Bid cleavage to truncated Bid (tBid) but it is deferred and less effective stimulation (86, 87).

The intrinsic pathway is known as the mitochondrial pathway, where the pivotal events begin. Intrinsic signals, for instance, DNA damage, defective growth factor and metabolic stress, can induce mitochondrial permeability transition pore (MPT) formation and lead to pro-apoptotic factor release; cytochrome C and small mitochondria-derived activator of caspases (SMACs) subsequently stimulating executor caspases.

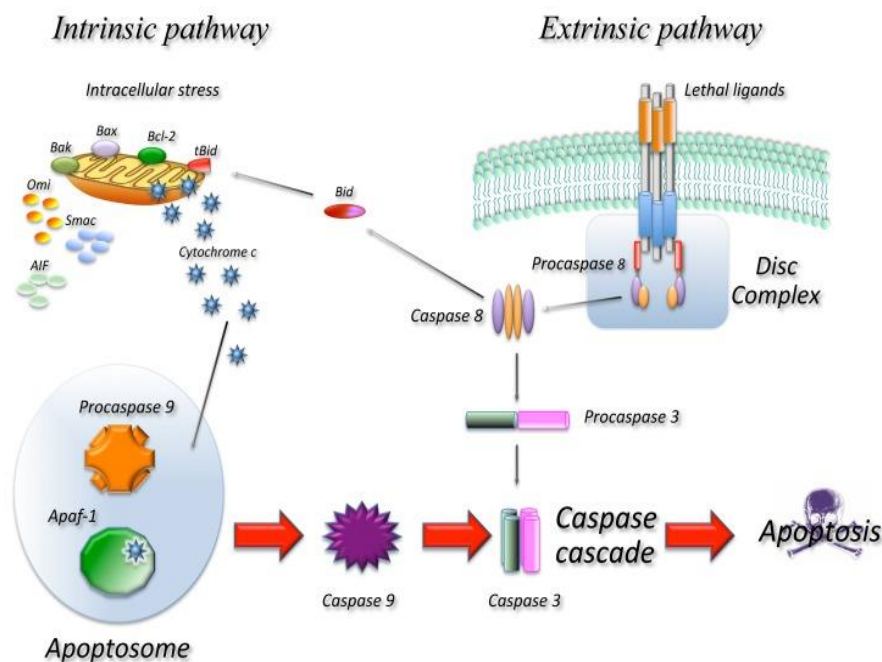


Figure 4 Signaling transduction pathway of apoptosis (6)

2.2.4 Apoptotic targeting in cancers

There are a number of variety diseases that are caused by apoptosis dysregulation. The abnormality of apoptosis can be excessive elimination or survival prolongation of cells. Since the definition of programmed cell death is a basic biological process to regulate homeostasis, thus the fundamental alteration has significant importance in the pathology of diseases such as degenerative diseases, immunodeficiency, autoimmunity and cancer (6). As early as the 1970's, Kerr et al. had considered that hypergenesis might sometimes result from loss of apoptosis rather than an increase of mitosis. Apoptosis has been related to the elimination of potentially cancerous cells, hypergenesis and progressive tumors. The fallacious cell cloning subjects increase of hormones and fail to be controlled by apoptosis (8).

Hallmarks of cancer have been constructed for understanding the logical framework of cancer biology in the year 2000 by Hanahan and Weinberg. The influential review consisted of the six common hallmarks: self-sufficiency in growth signals, insensitivity to anti-growth signals, apoptosis evasion, limitless replicative

potential, sustained angiogenesis, and tissue invasion/metastasis. Weinberg has updated in a decade later two more hallmarks: reprogramming energy metabolism and evading immune response in term of Hallmarks II (88).

Based on role of apoptosis, it is not surprising that alterations of apoptosis have become a crucial one of hallmarks and attractive therapeutic targets of cancer. The evasion of apoptosis in cancer may involve in both extrinsic and intrinsic pathways which are generally described into three mechanisms (7).

- 1) Disruption of the balance between pro-apoptotic and anti-apoptotic proteins
- 2) Reduction of caspase function
- 3) Impairment of death receptor signaling

Targeting apoptosis can be applied for many types of cancer by using cell fundamental mechanisms in order to terminate the uncontrollable growth of cancerous cells. Moreover, defective apoptosis is responsible for both conventional therapy and new therapeutic drug resistance (7). Many strategies have been developing new cancer therapies to increase death signaling and suppress apoptotic signaling inhibition (89).

Two common therapeutic targeting strategies are described as follows 1) stimulation of pro-apoptotic molecules and 2) inhibition of anti-apoptotic molecules (79). Tumor cells frequently escape the cellular response to programmed cell death. Typically, the intrinsic pathway is disabled in order to increase cell survival in tumor cells, such as upregulation of anti-apoptotic molecules (90).

Two classes of proteins have recently become more interesting for promising therapeutic interventions, namely Bcl-2 family and IAPs (91). The initiation of apoptosis is governed by the balance of pro and anti-apoptotic proteins. The anti-apoptotic proteins, i.e., the Bcl-2 protein family: Bcl2-A1, Bcl-2, Bcl-xL, Bcl-w and Mcl-1 are responsible pro-survival mediators preventing apoptosis (10, 11). Nevertheless, the initiation of the apoptosis pathway eventually converges at the activation of the caspase cascade. The function of caspases can also be controlled by a family of proteins through caspases binding termed IAPs; e.g., NIAP, c-IAP1, XIAP and survivin (23, 24).

2.2.4.1 B-cell lymphoma-2 (Bcl-2) family

The Bcl-2 family hyperactivation results in tumor cells being resistant to intrinsic apoptotic stimuli and anticancer activity (10, 12). The Bcl-2 protein overexpression is present in over half of all cancers, regardless of type (13-15). Mitochondrial outer membrane permeabilization (MOMP) is particularly regulated and mediated by the Bcl-2 protein family which is comprised of three functional protein groups summarized in Table 1 (92-94).

- (1) **BH3 proteins** are initiators responding to the stimuli signals. They can stimulate executioner proteins and neutralize anti-apoptotic members during apoptosis which act as a direct activators and sensitizers, respectively, e.g., BID, BIM, PUMA, tBID NOXA, BMF, BIK, HRK, and BAD etc.
- (2) **Executioner proteins or pro-apoptotic proteins**, Bax or Bak can be activated by BH3 Proteins and subsequently oligomerize which in turn, MOMP and the release of mitochondrial intermembrane space components to initiate effector caspases such as caspase-3.
- (3) **Anti-apoptotic proteins** function to restrain BH3 and executioner protein which maintains mitochondrial outer membrane integrity such as Bcl-2, Bcl-XL, Bcl-W, Mcl-1 and A1/BFL-1.

Table 1 Role of anti-apoptotic protein to Bcl-2 family members (94)

Anti-apoptotic protein	Anti-apoptotic protein binds to		
	Executioner proteins	BH3 proteins	
		Direct activator	Sensitizer
Bcl-2	Bax, Bid	Bim, Puma	Bmf, Bad
Bcl-XL	Bax, Bak, Bid	Bim, Puma	Bmf, Bad, Bik, Hrk
Bcl-w	Bax, Bak, Bid	Bim, Puma	Bmf, Bad, Bik, Hrk
Mcl-1	Bak, Bid	Bim, Puma	Noxa, Hrk
A1	Bak, Bid	Bim, Puma	Noxa, Bik, Hrk

2.2.4.2 Inhibitors of apoptosis proteins (IAPs)

The function of caspases can be blocked by the second class of proteins, resulting in cell death resistance at many stages following mitochondria involvement. Eight mammalian IAPs consist of at least one baculovirus inhibitor of apoptosis repeat domain (BIR) as protein recognition. Three IAPs are commonly expressed, including XIAP, c-IAP 1 and c-IAP 2 which can bind and thereby inhibit caspase activity. Survivin is the smallest IAP and structurally unique containing a single BIR. The current view suggests that only one IAPs called XIAP can efficiently inhibit caspases-3, -7 and -9. survivin cannot directly inhibit caspases but can decrease apoptosis by cooperative interaction with XIAP. The complexes of survivin-XIAP can improve its stability, enhance the activity of XIAP for caspase inhibition, promote tumor growth and participate in intracellular signaling pathways especially, NF- κ B activation (91).

2.2.5 Applications of siRNA targeting apoptosis in breast cancers

siRNA-based therapy has become an attractive therapeutic strategy due to its ability to interfere with desired mRNA targets specifically. Therefore, siRNA therapeutic is applied in various targets for apoptosis activation in cancers. Mcl-1 silencing led to loss of cell viability in Dox-resistant MDA-MB-435 cells overexpressing P-gp, BCRP, Mcl-1 and surviving. The result suggested that targeting Mcl-1 could serve as a treatment alternative for Dox-resistant cancer (95). Overexpression of Mcl-1 is manifested in various human malignancies including breast cancer which contributes cell survival and conventional therapeutic resistances (10, 19, 20). Moreover, Mcl-1 is also a vital protein regulating breast cancer cell survival (18). siRNA mediated downregulation of Mcl-1 confers beneficial therapeutic effects toward breast cancer management. The siRNA against Mcl-1 suppressed the cell viability of MDA-MB-435 cells (95). Additionally, the transient transfection of miR-193b downregulated Mcl-1 mRNA and protein expression noticeably increased Dox sensitivity in Dox-resistant MCF-7 cells (96). Among these IAPs, survivin exhibits significant overexpression in many tumors especially in breast and lung cancer, but it is present at low levels or completely absent in healthy cells and tissues (25-28). Moreover, targeting surviving with siRNA or miRNA re-sensitizes drug-resistant breast

cancer cell lines to chemotherapeutic agents including paclitaxel, taxol and Dox (29, 30).

2.3 Challenge of siRNA delivery

As the attractive RNAi mechanism, siRNA requires protein mediators such as AGO in the cytoplasm for post-transcriptional gene silencing. Various obstacles need to be circumvented depending on the route of administration. The delivery systems are essential for systemic exogenous siRNA administration to avoid elimination in the circulation systems, escape from the endosome/lysosome compartment and achieve desired target gene at the cytoplasm. The siRNA delivery barriers can be divided into extracellular barriers and intracellular barriers.

2.3.1 Extracellular barriers

Regarding the siRNA attributes, the length and diameter of siRNA are around 7-8 nm and 2-3 nm, respectively, rapidly filtrated through urine. Consequently, the particles with a smaller size than 8 nm can easily be eliminated by renal filtration. Nevertheless, the reticuloendothelial system (RES) consisting of phagocytes such as monocyte macrophages is responsible for eliminating exogenous particles as well as nanoparticulate systems. Phagocytic cells are usually accumulated to organs of RES including the liver and spleen. Opsonized particles covered with non-specific protein are generally recognized by phagocytic cells which are eventually removed from blood circulation. The force of non-specific protein binding depends on the surface of particles. The neutral charge has a slower opsonizing rate than highly charged particles. Modification of surface properties can reduce non-specific interaction and protect electrostatic or hydrophobic interaction against opsonization in the bloodstream by using grafted shielding materials such as polysaccharides (dextrans) and polyethylene glycols (PEGs) (97). Transportation of nanomedicine through vessel walls is limited by its pore sizes. A general capillary pore is between 2-6 nm limiting the extravasation of several hundred nanometers. The important feature of tumor microvessels is enhanced permeability and retention (EPR) effect which is found in the aberrant vascular architecture of tumors for supporting oxygen and nutrients. Tumors possess the pore

diameter of tumor microvessel ranges in 100-780 nm and lack lymphatic drainage. EPR is exploited in nanomedicine research for passive tumor delivery. As a consequence of EPR, nanoparticles tend to be highly accumulated and retained in tumor tissue (98, 99).

2.3.2 Intracellular barriers

There are only a few types of cells such as retinal ganglion cells and neurons, can take up naked siRNA. As the characteristic of genetic materials, high molecular weight and negative charge inhibit crossing through the cell membrane. Various carriers are exploited to facilitate the internalization of genetic materials into the target cells. The positive charge of lipids, polymers or cell-penetrating peptides becomes a choice in the first stage of cell membrane interaction increasing cellular uptake probability. Moreover, intracellular localization is one of the key assessments to obtain therapeutic action. Internalized particles are eventually entrapped in intracellular vesicles called endosomes. Delivery systems must finally escape from endosome/lysosome compartments and further convey genetic materials into the target site of action (100).

2.3.2.1 Internalization of nanoparticles

Cellular attachment can be driven by many ways including non-specific hydrophobic interaction, electrostatic interaction or specific recognition resulting in immobilization of nanoparticles on the cell surface. Hydrophobic nanoparticles are advantageous for intracellular drug delivery. Cellular membrane presents a negative surface charge at physiological pH, which consists of anionic glycosaminoglycans in proteoglycans, presenting a high density of carboxyl and sulfate groups. Anionic nanoparticles are usually recognized via scavenger receptor of macrophage. Noticeably, cationic nanoparticles have stronger adhesion leading to a higher rate of internalization (101). Chemical inhibitors of endocytic pathways are employed as a tool to study the mechanism of endocytosis, summarized in

Table 2.

Table 2 Chemical inhibitors of endocytosis and their putative mechanism of action (101)

Agent	Mechanism
Chlorpromazine	Dissociates clathrin and adapter proteins from the plasma membrane
Ammonium chloride	Increases pH of late endosomes and lysosomes
Cyclodextrin	Extracts cholesterol out of plasma membrane
Genistein	Inhibits tyrosine-phosphorylation of caveoline-1
Wortmannin	Blocks PI3-kinase; inhibits fusion of membrane protrusions
Nocodazole	Depolymerises microtubules
Filipin III	Binds cholesterol in plasma membrane

In general, immobilized nanoparticles on the cell surface are suggested internalizing through endocytosis. The routes of endocytosis are classified in Figure 5. Phagocytosis is an engulfment of foreign large particles as well as pathogens, bacteria or dead cells by professional phagocytes e.g. macrophage, neutrophils. Pinocytosis commonly refers to micropinocytosis, clathrin- and caveolin-mediated endocytosis and clathrin- and caveolin-independent endocytosis. Micropinocytosis initiates ruffle membrane formation and further ingests a large volume of fluids ranged 0.2-10 μm into endocytic vesicles. It is known as macropinosomes which easily leak when compared with other types of endocytic vesicles. For clathrin-mediated endocytosis, it typically takes up particles of 100-150 nm with the aid of dynamin. The pH of the vesicles is rapidly changed which is eventually followed by enzymatic degradation. With regard to caveolin-mediated endocytosis, the cellular membrane abundantly exists of cholesterol-rich microdomain called raft. Pathogens dependently utilize this route to avoid lysosomal degradation since it slowly takes up 60-80 nm particles in several cell types (102).

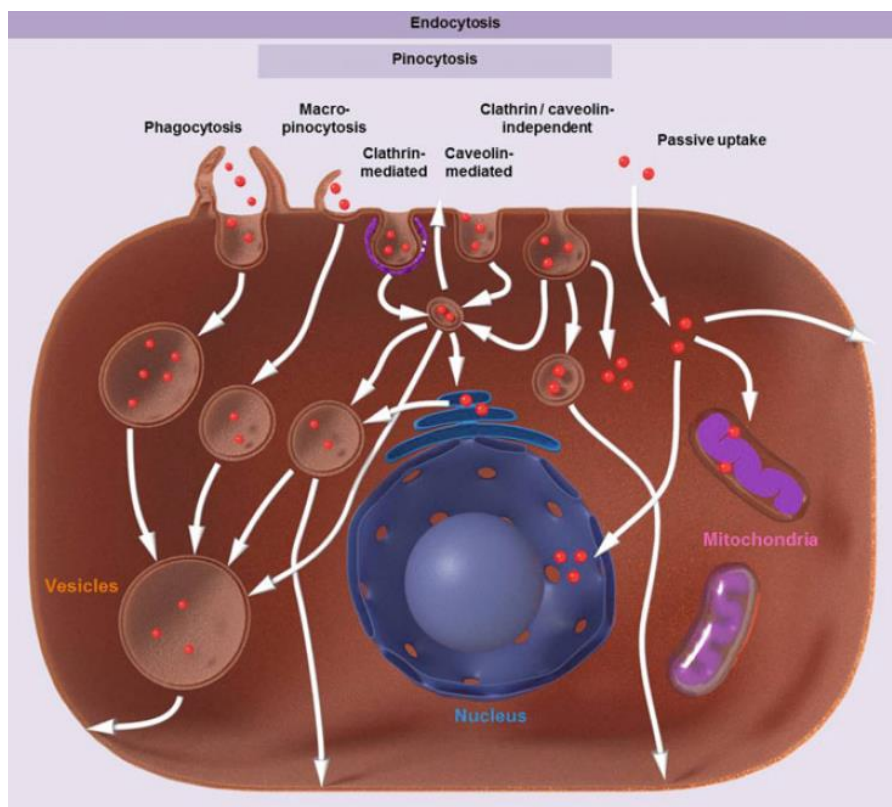


Figure 5 Endocytic mechanisms classification in mammalian cells.(103)

2.3.2.1 Endosomal escape

The nanoparticle/nucleic acid complexes inhabit in membrane-bound endosomes after internalization through endocytosis. There is no direct for endosomal release to the cytoplasm or nucleus (Figure 5). Normally, lysosomes pinch off from the Golgi-apparatus to fuse with endosomes. The contents are eventually degraded or recycle back to the cell surface. Therefore, endosomal escape is the essential step to overcome. The delivery strategies must be considered in order to the design of responsive systems to biological stimuli such as pH drop, enzymatic cleavage, or change of a redox potential: the use of ionizable lipids, lipids with a desired phase transition temperature (with melting temperature around body temperature), cleavable lipids, cis-trans isomerization, charge-switching lipids and free-radical-generating compound as photosensors. The consequences of designated responsive systems lead to destabilization, fusion or pore-formation of the membrane and further release before lysosomal compartmentalization (104).

2.4 siRNA delivery systems

2.4.1 Classification of gene delivery methods

The first gene therapy drug had been employed in 1998 for the treatment of cytomegalovirus retinitis. Recently, there are 22 gene therapy drugs have been approved till 2019 (100). There are several approaches to transferring genetic materials into desired targets which can be classified as follows: 1) Virus-Based Gene Delivery Systems, 2) Non-viral Vector-Based Gene Delivery and 3) Gene Delivery Using Physical Approaches (38). Although viral-vectors provide high transfection efficiency, there are several drawbacks that need to be obliterated, for instance, immunogenicity and low loading capacity. Therefore, non-viral vectors have been exponentially developed which are broadly used for gene delivery.

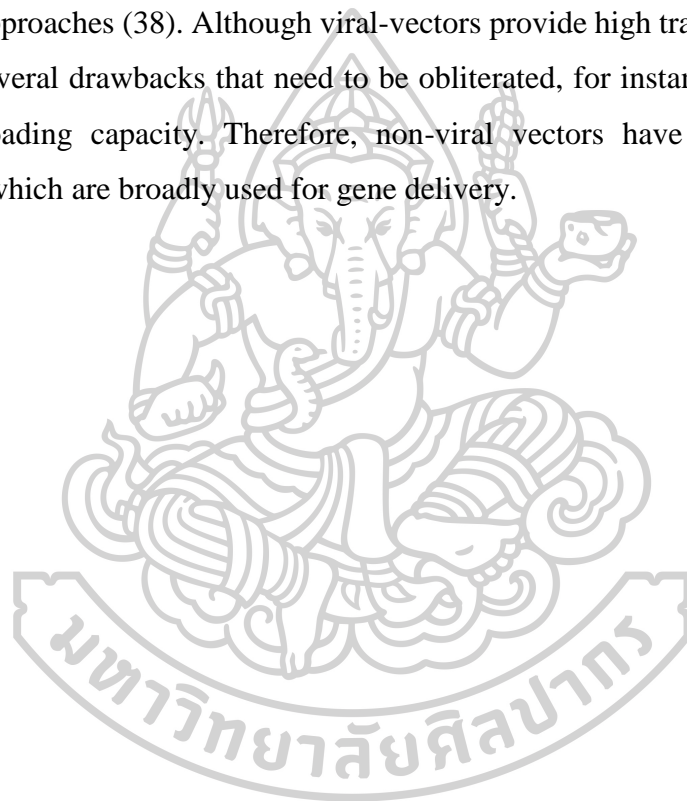


Table 3 Non-viral based for siRNA delivery for cancers in clinical trials (74, 100)

Delivery system	Therapeutic name	Target(s)	Condition(s)	Clinical trial phase	NCT ID
Exosome	Mesenchymal stromal cell-derived exosomes with KRAS-G12Dtargeting siRNA	Kras G12D Mutation	Pancreatic cancer	1	NCT03608631
Gold nanoparticle	NU-0129	BCL2L12	Glioma	1	NCT03020017
Ex vivo electroporated PBMCs	APN401 (siRNA transfected PBMCs)	Cbl-b/DC	Solid tumors that are metastatic or cannot be removed by surgery	1	NCT03087591 NCT02166255
Liposome	siRNA-EphA2-DOPC	EphA2	Advanced cancers	1	NCT01591356
Liposome (AtuPlex)	Atu027	PKN3	Pancreatic ductal carcinoma, advanced solid tumors	1/2	NCT01808638 NCT00938574
Solid lipid	TKM-080301	PLK1	liver cancer	1	NCT01437007
			Adrenocortical cancer	1/2	NCT01262235
Solid lipid	ALN-VSP02	VEGF-A 23 and KSP 24	hepatocellular carcinoma	1/2	NCT02191878
			Solid tumors	1	NCT01158079

2.4.2 Non-viral nanoparticles for siRNA delivery

Nanoparticles have emerged for gene delivery applications becoming more attractive since they ease for production and modification as well as serve minimal safety concerns. Non-viral nanoparticles can be categorized into 3 groups; biological nanoparticles, inorganic nanoparticles and organic nanoparticles (Figure 6) (74). They might be potential approaches of siRNA delivery systems in which are innumerable studies in clinical trials (Table 3). The advantages and limitations of Non-viral nanoparticles have been summarized in Table 4.

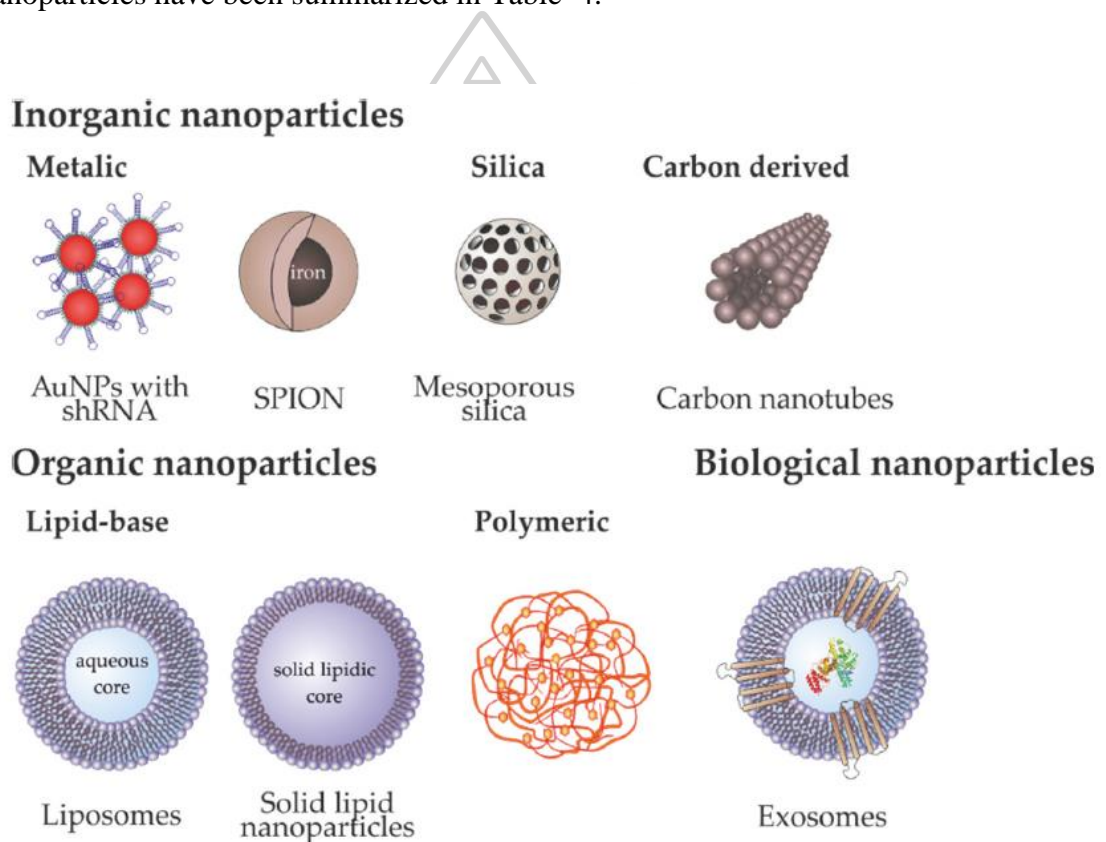


Figure 6 Non-viral nanoparticles used in gene delivery

2.4.2.1 Biological nanoparticles

Exosomes, the smallest natural bio-carriers are lipid bilayer vesicles having the size of 40-120 nm. They are found in extracellular fluids. It is the important process of cell-to-cell communication in which the series of protein and genetic materials are enclosed exosomes delivered and released from many cells. Exosomes also transfer

coding and non-coding RNA as well as miRNA to target cells for the transcriptional and translational processes. The modification of exosomes is still a challenge to overcome. The modifying can be approached by two different methods, including parent cell engineering for modified exosome production and direct modifying after exosome secretion. siRNA could be transferred in the exosomes by several methods, e.g., incubation, electroporation and lipofection. However, there still have some limitations to effective loading methodologies (105).

2.4.2.2 Inorganic nanoparticles

Gold nanoparticles (AuNPs) are the most often metals used in nanomedicines. Attractively, the surface of AuNPs is easily functionalized with various moieties such as chitosan or cationic lipids in order to allow ionic interaction with siRNA. Protection against RNases degradation is one of the advantages of AuNPs which probably prevent physical contact of enzyme catalytic site with siRNA by steric hindrance. Moreover, particle sizes can be controlled using distinct methodologies, making them a promising strategy for gene delivery. However, AuNPs still need several development stages for bringing to translational research in a clinical setting (106).

2.4.2.3 Organic nanoparticles

2.4.2.3.1 Polymer-based delivery systems

Linear or branched cationic polymers are used for nucleic acid condensation, known as polyplexes or nano-sized complexes. The prominent characteristic of polymeric nanoparticles is controlled release since the structural complexity makes polyplexes more stable than lipoplexes. Natural biopolymers have been widely used due to their biodegradable and biocompatible. Polymers can be functionalized to improve the delivery systems properties for purposed activity in gene delivery applications such as chitosan, PEI, PLGA or dendrimers (74).

2.4.2.3.2 Lipid-based delivery systems (LNPs)

The nanoparticles made of lipid-based systems have been applied for several drug delivery research due to amphiphilic characteristic cell membrane interaction and delivery of therapeutic agents efficiently into the cells (107).

2.4.2.3.2.1 Solid lipid nanoparticles (SLNs)

SLNs composed of solid lipid core at room temperature and body temperature are covered with a surfactant layer in the aqueous phase (107). The complex of siRNA and cationic lipids are formed by ionic interaction and then capped by a hydrophobic ion-pairing (HIP) approach into the electrically neutral hydrophobic core. Encapsulated siRNA in SLNs gradually releases siRNA for sustaining gene silencing in more than seven days *in vitro* and *in vivo* experiments (108). Despite the solid core of SLNs presenting high physical stability and biocompatibility, drug loading and siRNA loading methods are limited. Another strategy can be employed by cationic SLNs coated with siRNA via electrostatic interaction and loaded lipophilic drug in the inner core (109).

2.4.2.3.2.2 Lipid nanovesicles: liposomes and niosomes

Liposomes

Liposomes are spherical vesicular systems containing hydrophilic core and hydrophobic membrane. It is usually made up of phospholipids with the assistance of helper lipids to enhance lipid bilayer stability. The surface attributes of liposomes are typically incorporated with cationic lipids. The positive charge can contribute siRNA complex formation, cellular uptake as well as endosomal/lysosomal compartment escape. Cationic liposomes can spontaneously neutralize and further form multilamellar lipoplexes with anionic siRNA. It has been widely used for siRNA in clinical trials offering minimal toxicity, ease of preparation (74). Functionalization of liposomes with specific targeting such as monoclonal antibodies, aptamer, protein (transferrin), peptide (Arg-Gly-Asp, RGD), carbohydrates (sugar) or small molecules (folic acid) ligands may improve its liposome properties (110). Binding receptor-mediated on the cells tends to enhance cellular uptake of liposomes by endocytosis.

Moreover, the surface modification with specific ligands overexpressing on tumor cell surface was exploited in siRNA delivery into the specific target cells, called active targeting (111). For example, AS1411, an aptamer, was applied to activated PEGylated cationic liposomes which could provide a specific binding to nucleolin on A375 cells (human melanoma cell line) enhancing cellular uptake and silencing efficiency of siRNA delivery (112). Polycationic liposomes were modified with RGD-grafted distearoylphosphatidylethanolamine-polyethylene glycol 2000 (DSPE-PEG 2000) for active targeting αv integrins on in B16F10-luc2, murine melanoma cells which could double gene silencing outcome in B16F10-luc2 lung metastatic model mice (113).

Niosomes

The application of niosomes was firstly reported for the cosmetic industry. Since the feature of niosomes having structural like liposomes, they have been considerably used for drug transporting in the pharmaceutical field, providing stable particles and improving the stability of encapsulated drugs. Nonetheless, they are studied in numerous preclinical and clinical researches since they are biodegradable, biocompatible and less immunogenicity. Niosomes become alternative colloidal vesicles like liposomes that have been continuously developed in several routes and applications as well as gene therapeutic strategies. Hydrated non-ionic surfactants are incorporated with synthetic cationic lipids receiving a lot of attention for genetic materials delivery such as plasmid DNA, ASOs, siRNA (58, 114).

Table 4 Advantages and disadvantages non-viral nanoparticles used in gene delivery (74)

Delivery systems	Composition	Advantages	Disadvantages
Biological nanoparticles	Exosomes	<ul style="list-style-type: none"> - Less immune response - Protection of circulating genetic material - Possibility of cell targeting 	<ul style="list-style-type: none"> - Limited transfection efficiency
Inorganic Nanoparticles	Metallic (Gold, iron) Multiple forms (spherical, nanorods, triangles)	<ul style="list-style-type: none"> - Biocompatibility - Tunable size - Straightforward functionalization - More information about uptake, biocompatibility and low cytotoxicity 	<ul style="list-style-type: none"> - They are required for clinical translation
Organic nanoparticles	Polymeric nanoparticles	<ul style="list-style-type: none"> - Biodegradable properties - Good tissue penetration - Ease manipulation 	<ul style="list-style-type: none"> - Non-degradable polymers tend to accumulate in tissues - Promote allergic reactions - <i>In vivo</i> metabolism and elimination routes are not elucidated
	Lipid nanovesicles	<ul style="list-style-type: none"> - Low toxicity - Biodegradable - They can transport hydrophobic and hydrophilic molecules - Moderate loading capacity 	<ul style="list-style-type: none"> - They could crystallize after prolonged storage conditions

2.5 Niosomes: siRNA delivery

2.5.1 Surface modification of niosomes

Niosomes, the new generation of gene delivery systems, are prepared with non-ionic surfactants. It has emerged as a safe and viable delivery alternative of the conventional liposomes with key advantages in increased chemical stability and lower cost (115-117). The lipid layer of niosomes is usually incorporated with neutral helper lipids such as Chol or DOPE for membrane rigidity. Colloidal vesicle systems like liposomes consist of phospholipids which can be degraded by oxidation or phospholipase. Some of compounds used in the composition of niosomes have been studied for gene delivery systems are presented in Figure 7. Moreover, cationic charged molecules could lead to dose-dependent cytotoxicity and inflammatory response. To address this issue, non-ionic surfactant in niosomes might minimize cytotoxicity from cationic and anionic counterparts.

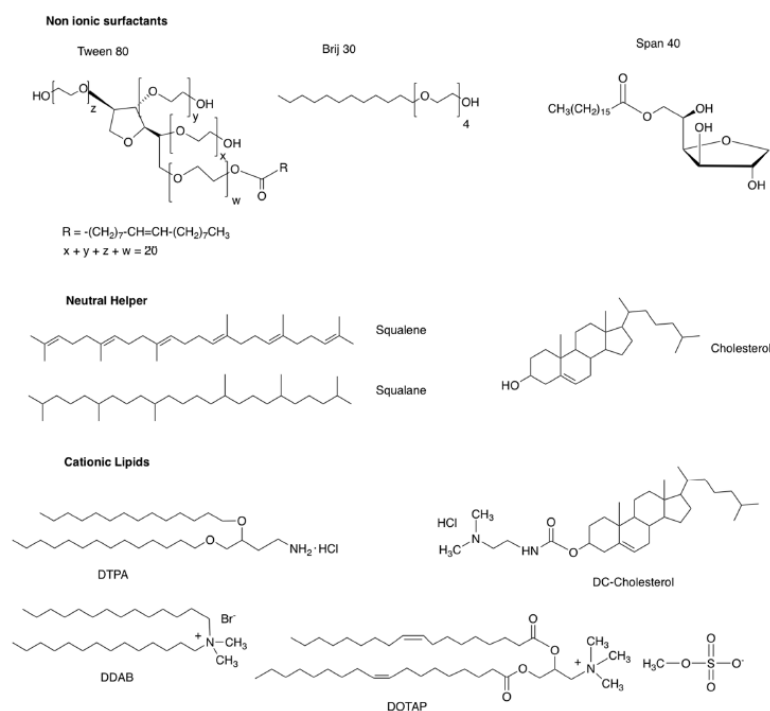


Figure 7 Chemical structure of some of compounds used in the composition of niosomes (58).

2.5.1 Surface modification of niosomes

2.5.1.1 Cationic lipids

Generally, negative charged nucleic acids can be loaded in LNPs via ion-interaction. Charge inducers have been exploited for given benefits to LNPs properties, for instance, colloidal stabilization, electrostatic interaction with genetic materials and cell membrane interaction (58, 114). The structure of cationic lipids has been modified for their property improvements, which proven 3 indicated parts as follows: positively charged head, hydrophobic tails and linker/spacer showing in Figure 8.

Monovalent cationic lipids such as DOTMA and DOTAP are mostly representative cationic lipids used in gene delivery (Figure 8). Multivalent cationic lipids with more than one amine groups may provide higher capacity for electrostatic interaction with genetic material and cellular membrane, such as the commercial transfection agent called Lipofectamine. The pH-sensitive lipids typically contain one protonable ternary amine group presenting a neutral charge at physiological pH. The ternary amine is protonated when the drop of pH from 7.4 to 5-6 before fused with lysosomes. The consequence of the protonable amine renders to endosomal membrane destabilization and release genetic materials (111).

Hydrophobic tails have been modified such as a decrease of the length, increase of branches or double bonds which are utilized for the increasing rate of intermembrane transfer, lipid mixing or hexagonal phase transition at lower temperatures (118).

Linkers have also been studied for gene delivery applications, e.g., ether, ester, amide, carbamate, disulfide, urea, acylhydrazone, phosphate linkers (Figure 8). The designs of cationic lipid linkers determine chemical stability and biodegradable transfection efficiency and cytotoxicity. Chemical stable and non-biodegradable bonds result in higher toxicity. For instance, the ether linker is more stable than the ester bond which associates with less toxicity. Amide liker can be found in peptides or proteins. It has been widely used for cationic lipid design having high transfection efficiency and no noticeable cytotoxicity. Carbamate linker is susceptible to degradation into small molecules in an acidic environment but stable in neutral pH. Intracellular glutathione

pool is utilized for disulfide-linker reduction improving the release of genetic material into the cytoplasm (48).

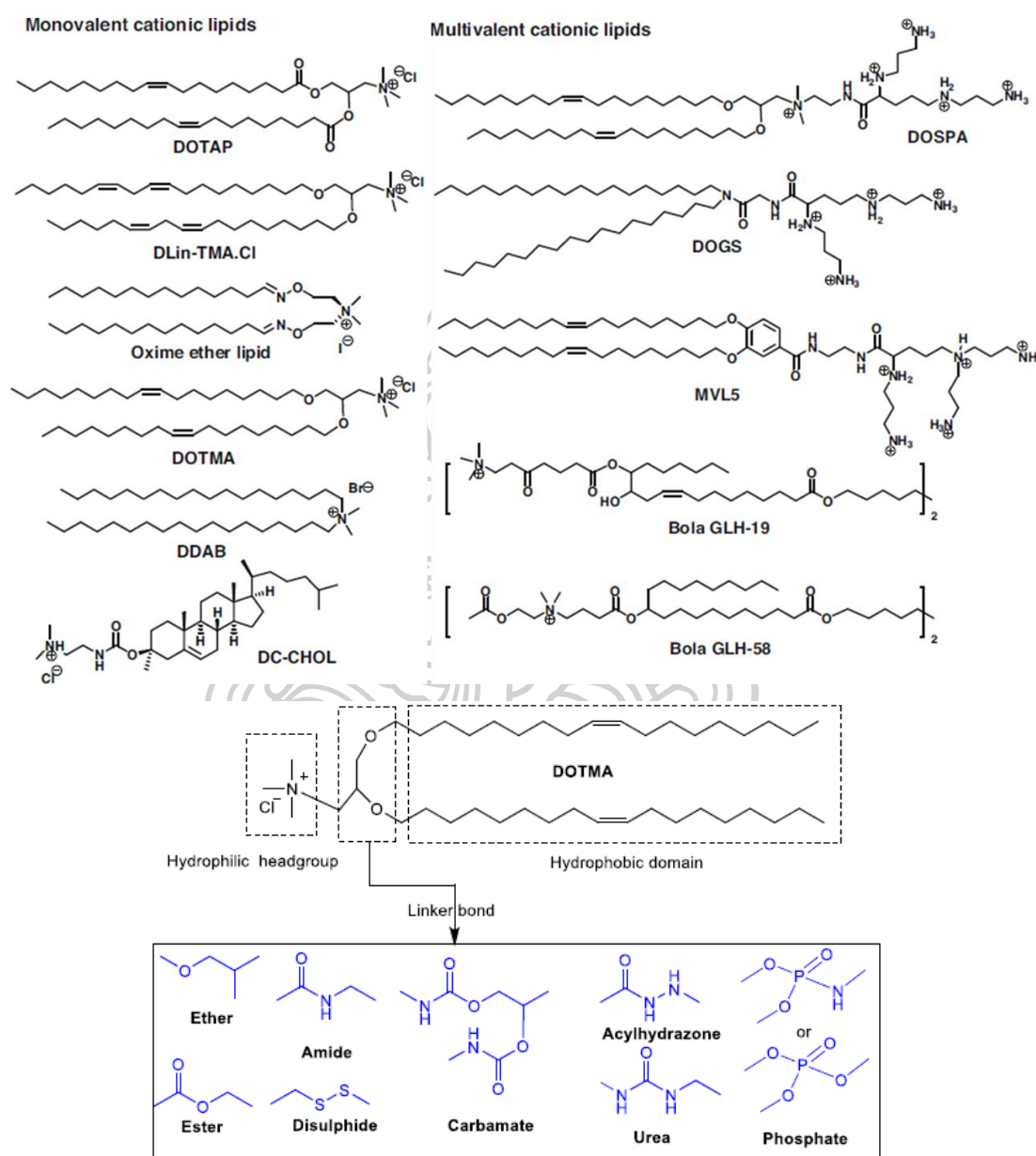


Figure 8 Examples of lipid-types and structures used for the delivery of siRNAs including monovalent and multivalent cationic lipids (119). Representative structure of cationic lipid DOTMA and linker bonds of cationic lipid (48).

2.5.1.2 PEGylation

Some circumstances in *in vivo* experiment, nanoparticles have been reported that host-immune systems recognized foreign particles that are eliminated via RES. The nanoparticles are designated for desired purposes, such as having surface electrostatic charges for drug delivery and efficacy improvement. Polyethylene glycol (PEG) is a non-toxic and non-ionic hydrophilic polymer that can enhance the stability, blood compatibility and prolong the blood circulation time of LNPs (120). Collectively, the advantages of PEGylation are thereby considered for LNP modification to circumvent immune recognition. PEGylated LNPs increase surface hydrophilicity and prevent LNPs/macrophage interaction by steric barriers. Nevertheless, PEGylation hinders LNPs from non-specific protein adsorption called opsonization resulting in inhibition of premature phagocytic uptake and providing longer time in bloodstream. Despite hindering PEGylation, they also have a double-edged sword called PEG dilemma, which may reduce interaction of LNPs with the cell membrane and endosomal membrane fusion in target cells and further diminish therapeutic efficacy. The length of PEG more than 5000 markedly affects cellular uptake and endosomal escape, whereas short PEG is insufficient for the LNP surface improvement. The medium length of PEG at 2000 has been widely applied 1-10% depending on PEGylation methods (111, 121).

2.5.2 Applications of niosomes for siRNA delivery

Several niosome-based formulations aimed at transporting genetic materials, presented in Table 5. It may be a useful approach to promising genetic delivery systems to the market (58, 114).

SPANosomes were formulated from Span 80 and DOTAP with or without D-tocopheryl PEG 1000 succinate. siLuc was used for the model of silencing efficiency showing 66–77% of silencing efficiency compared to standard transfection liposomes. Nevertheless, the intracellular trafficking experiment presented that the complexes of niosomes were able to escape from endosomes and were further located in the cytoplasm. In contrast, standard liposome complexes were abundant in endosomes (122).

Microfluidic method was exploited to prepare siRNA targeting green fluorescent protein loaded in cationic niosomes which presented small particles, good stability and low toxicity. The cationic niosomes were composed of non-ionic surfactants (monopalmitin glycerol (MPG) or Tween 85) mixed with cholesterol and Dimethyldidodecylammonium bromide (DDAB). Only the cationic niosomes formulated with Tween 85 manifested high transfection efficiency at 70%, thereby were further selected for *in vivo* mice model evaluation (123, 124).

The combining therapeutic strategies were also studied with the aid of cationic niosomes delivery. Doxorubicin was encapsulated in cationic niosomes composing of Span 80, DOTAP and 5% of tocopherol-PEG 1000 succinate (TGPS). The doxorubicin-loaded niosomes were further combined with two siRNAs targeting ATP-binding cassette transporter (ABCG2) and anti-apoptotic protein Bcl-2 by complexation [86]. The combination of doxorubicin along with the two siRNAs was delivered in cancer stem cells (CSCs). The silencing of ABCG2 and Bcl-2 genes could increase cytotoxicity and apoptosis in this study (125).

Another study has applied cationic niosomes for siRNA and thymoquinone (TQ) delivery. TQ obtained from natural black seed oil having antineoplastic activity. Gold nanoparticles were functionalized with the positive charge of octadecylamine (ODA) in order to provide an electrostatic interaction with the negative charge of siRNA targeting serine-threonine protein kinase Akt gene. The gold-loaded niosomes were prepared with ODA-coated gold nanoparticles, Tween 80 and PEG. TQ was loaded within the hydrophobic core of the niosomes and further applied with siRNA for complex formation. The ODA-coated gold nanoparticles/siRNA complexes were stable in neutral pH, while siRNA was dissociated and located in tumor and endosomes at acidic conditions. The Akt gene was efficiently knockdown with the niosome/siRNA complexes which led to sensitizing TQ and improving apoptosis against tamoxifen-resistant and Akt-overexpressing MCF-7 breast cancer cells. Nonetheless, tumor size was reduced in MCF-7/TAM human breast carcinoma xenografts on mice (126).

PEGylated cationic niosomes contained Tween 60, cholesterol, Dipalmitoylphosphatidylcholine (DPPC), DOTAP and 5% of DSPE-PEG2000 were

utilized as a delivery system for a triple combination of doxorubicin, chemosensitizer quercetin and siRNA targeting CDC20 mRNA. Doxorubicin and quercetin were contained in the aqueous compartment and lipid layer, respectively. The siRNA was incubated with the PEGylated cationic niosomes to form siRNA complexes. The results showed that the combination provided high toxicity and synergistic effects in 3 cell lines as follows: The cell lines of human gastric cancer (AGS), prostate cancer (PC3) and breast cancer (MCF-7) (127).

Theranostic platform was developed for both therapeutic and tracking systems in human mesenchymal stem cells (hMSCs) *in vitro* and *in vivo*. Indocyanine green (ICG) was loaded in cationic niosomes containing Span 80, DOTAP and TPGS which was prepared through the ethanol injection method for OFF/ON activatable near-infrared fluorescence called iSPN. The anti-miR-138 was conveyed by iSPN via electrostatic interaction for osteogenic differentiation improvement of hMSCs. The signal was activated by decomplexation of ICG from iSPN which was useful for dynamic tracking of hMSCs *in vivo* (117).



Table 5 Applications of cationic niosomes for siRNA delivery (58)

Non-ionic surfactant	Helper lipid	Cationic Lipid	Niosome Preparation	Cargo	Therapy	Testing Conditions
Span 80 and Tocofersolan	-	DOTAP	Ethanol injection	siLuc	-	<i>In vitro</i> (122)
Tween 85 or monopalmitin glycerol	cholesterol	DDAB	Microfluidic	siRNA GFP	Chemotherapy	<i>In vitro</i> and <i>In vivo</i> (123, 124)
Span 80 and tocofersolan	-	DOTAP	Ethanol injection	siRNAs	Chemotherapy	<i>In vivo</i> (125)
Tween 80	-	Gold niosomes (Nio-Au)	Ethanol evaporation	siRNA	Chemotherapy	<i>In vivo</i> (126)
Tween 60 and DSPE-PEG2000	cholesterol	DPPC and DOTAP	Thin-film	siRNA	Chemotherapy	<i>In vitro</i> (127)
Span 80 and tocofersolan	-	DOTAP	Ethanol injection	siRNA and miRNA	Chemotherapy	<i>In vitro</i> and <i>In vivo</i> (117)

CHAPTER 3

MATERIALS AND METHODS

3.1 Materials

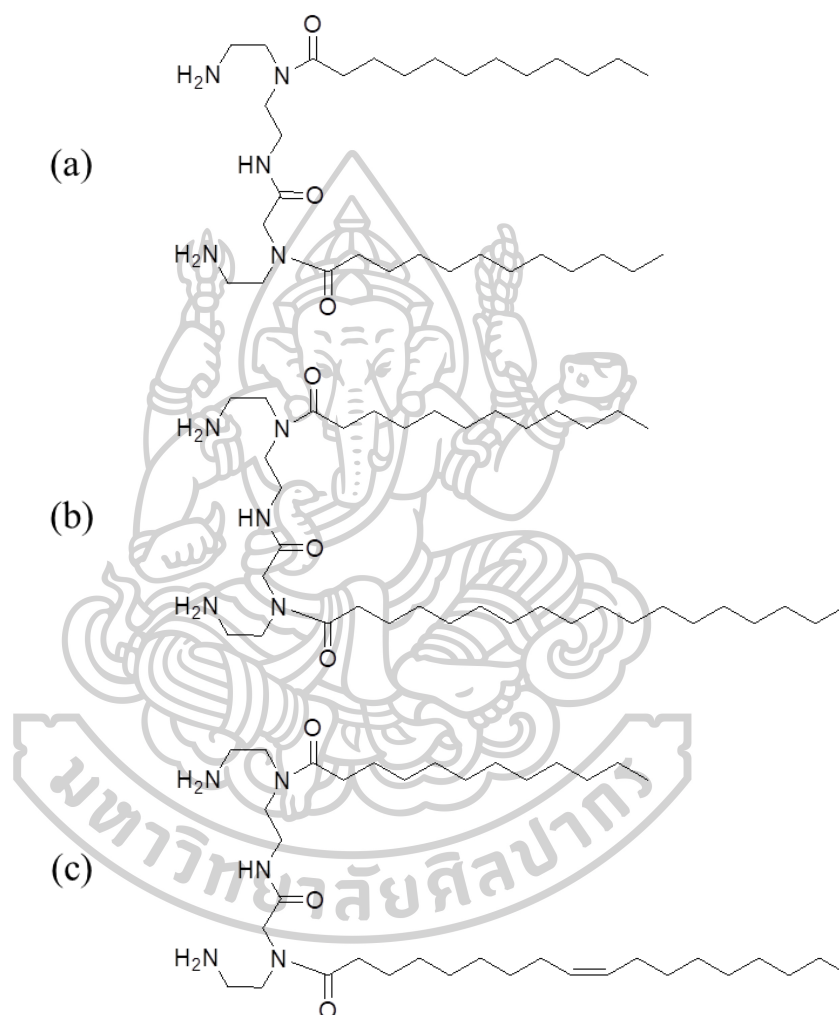


Figure 9 The structures of PCLs: (a) PCL-A, (b) PCL-B and (c) PCL-C

- plier-like cationic lipids (PCLs) illustrated in Figure 9 were obtained from the Faculty of Sciences, Ramkhamhaeng University.
- Cholesterol (Chol) (Carlo Erba Reagenti, MI, Italy)
- Sorbitan monolaurate (Span 20) (Sigma-Aldrich[®], MO, USA)
- Modified eagle medium (MEM) (GIBCO[™], Grand Island, NY, USA)

- Dulbecco's modified eagle medium (DMEM) (GIBCO™ , Grand Island, NY, USA)
- Fetal bovine serum (FBS) (GIBCO™ , Grand Island, NY, USA)
- L-glutamine (GIBCO™ , Grand Island, NY, USA)
- Non-essential amino acid (GIBCO™ , Grand Island, NY, USA)
- Inhibitors of endocytic pathways
 - Filipin complex, from Streptomyces filipinensis (Sigma-Aldrich ®, St Louis, MO, USA)
 - Chlopromazine (Sigma-Aldrich®, St Louis, MO, USA)
 - Genistein (Sigma-Aldrich®, St Louis, MO, USA)
 - Methyl-β-cyclodextrin (Sigma-Aldrich®, St Louis, MO, USA)
 - Nocodazole (Sigma-Aldrich®, St Louis, MO, USA)
 - Wortmannin (Sigma-Aldrich®, St Louis, MO, USA)
 - Ammonium chloride (Sigma-Aldrich®, St Louis, MO, USA)
 - Geneticin® selective antibiotic (G418 Sulfate) 50mg/ml solution (GIBCO™ , Grand Island, NY, USA)
- Gene Pure LE Agarose (ISC BioExpress®, USA)
- Ethanol (Merck, Germany)
- Chloroform (VWR International Ltd. England analytical reagent grade)
- Methanol (Merck, Germany)
- Tris(hydroxymethyl) aminomethane, Pacific Science, Thailand, molecular biology grade)
- 3-(4,5-dimethylthiazol-2-yl)-2,5-diphenyl-tetrazolium bromide (MTT) (Sigma-Aldrich®, St Louis, MO, USA)
- Dimethyl sulphoxide (DMSO) (Fisher Scientific; analytical reagent grade)
- Water for irrigation (General Hospital Products Public Co., Ltd.)
- ProLong™ Diamond Antifade Mountant (Invitrogen, NY, USA)
- Wheat Germ Agglutinin, Tetramethylrhodamine Conjugate (WGA-TC) (Invitrogen, NY, USA)
- Hoechst 33342 (Invitrogen, NY, USA)
- SYTOX™ Green Nucleic Acid Stain - 5 mM Solution in DMSO (Invitrogen, NY, USA)

- siRNA AF488 (siAF488) (Qiagen Santa Clarita, California, USA).
- Primer for real-time PCR (Bio Basic Inc., Markham, Canada)
- Apoptosis related siRNA (Ambion, Austin, TX, USA)
 - Bcl-2 siRNA:
 - BCL-2 Silencer Select Pre-designed siRNA (ID: s1915)
 - Mcl-1 siRNA:
 - MCL-1 Silencer Select Validated siRNA (ID: s8583)
 - Survivin siRNA:
 - BIRC5 Silencer Select Validated siRNA (ID: s1459)
- Doxorubicin (Sigma-Aldrich[®], St Louis, MO, USA)
- SuperPrep[®] Cell Lysis & RT Kit for qPCR (Toyobo, Japan)
- THUNDERBIRD[®] SYBR[®] qPCR Master Mix (Toyobo, Japan)
- QIAGEN Plasmid Midi Kits (Qiagen, Santa Clarita, CA, USA)
- Silencer[™] siRNA Construction Kit (Ambion, USA)
- Lipofectamine[™] 2000 (Invitrogen, NY, USA)

3.2 Equipments

- 1.5 ml, 2 ml Eppendorf[®] tubes (Eppendorf, Corning Incorporated, NY, USA)
- 10 ml test tube
- 15 mL, 50 mL centrifuge tubes-sterile (Biologic research company)
- 48-well tissue culture test plates (TPP[®]; Switzerland)
- 25 cm² and 75 cm² cell culture flask (SPL Cell Culture Plate, Korea)
- 24 and 96-well cell culture cluster (Costar[®]; Corning Incorporated)
- N² gas in laminar hood
- Analytical balance (Satorius CP224S, Scientific promotion Co., Ltd.)
- Desiccator
- Bath sonicator, Transonic series 890/H (Elma Hans Schmidbauer GmbH, Germany)
- Probe sonicator (Sonics Vibra Cell[™])
- Centrifuge (Sorvall[®] Biofuge Stratos)
- Automatic autoclave (Model: LS-2D; Scientific promotion CO., Ltd.)
- Bacterial incubator (Contherm; Lab Focus CO., Ltd)

- Cellulose acetate filter 0.2 μm (Sartorius AG. 37070 Goettingen, Germany)
- Centrifuge (Hermle Z300K; Labnet[®]; Lab Focus CO., Ltd.)
- CO₂ incubator (HERA Cell 240 Heraeus)
- Thermo Scientific™ NanoDrop™ OneC Spectrophotometer (Waltham, MA, USA).
- Fluorescence microscope (Model: GFP-B, wavelengths: excitation filter 480/40 and emission filter 535/50)
- VICTOR Nivo Multimode Microplate Reader (PerkinElmer Inc., USA)
- Fusion universal microplate analyzer (Model No: AOPUS01 and A153601; A Packard bioscience company)
- Fluoroskan ascent series microplate readers (Thermo fisher scientific, USA)
- Gel electrophoresis apparatus (MyRUN intelligent electrophoresis unit, Cosmobio CO., Ltd., Japan)
- GelDoc system (Multi Genus Bio- imaging system, Syngene™), Akkiance Q9 advanced chemiluminescence imager (Uvitec, Cambridge, UK)
- Inverted microscope (Eclipse TE 2000-U; Model: T-DH Nikon[®] Japan)
- BD FACSCanto™ Flow cytometer (BD Bioscience; Becton, Dickinson and Company)
- FV10i confocal laser scanning microscope (Olympus, Japan)
- LightCycler[®] 480 Instrument II (Roche, Switzerland)
- Laminar air flow (BIO-II-A)
- Magnetic stirrer and magnetic bar
- Micropipette 0.1-2 μL , 2-20 μL , 10-100 μL , 20-100 μL , 100-1000 μL (Eppendorf, Corning Incorporated, NY, USA) and micropipette tip
- pH meter (HORIBA compact pH meter B-212)
- Protein and nucleic acid electrophoresis (MyRUN intelligent electrophoresis unit; Cosmobio CO., Ltd.)
- Sartorius[®] filter set (Sartorius BORO 3.3 Goettingen, Germany)
- Shaking incubator (GFL 3031)
- Water bath (Hetofrig CB60; Heto High Technology)
- Vortex mixer

- Zetasizer Nano ZS (Malvern instruments Ltd., Malvern, UK)
- Transmission electron microscope (Philip Model TECNAI 20).

3.3 Methods

3.3.1 Preparation of plasmid DNA

pEGFP-C2 plasmid DNA (4.7 kbp) was propagated in *Escherichia coli* DH5- α and purified by using the Qiagen endotoxin-free plasmid purification kit (Qiagen, Santa Clarita, CA, USA). The DNA concentration and purity were quantified by measuring the absorbance at 260-280 nm using a Thermo Scientific™ NanoDrop™ OneC spectrophotometer (Waltham, MA, USA).

3.3.2 Preparation of siRNA targeting green fluorescent protein and siRNA targeting apoptotic pathway

The sequences of siGFP and noncoding siRNA (siNC) were designed as follows: sense strand: 5'-GCUGACCCUGAAGUUCAUCUU-3', antisense strand: 5'-GAUGAACUUCAG GGUCAGCUU-3', and sense strand: 5'-GCACCGCUUACGUGAUACUUU-3', antisense strand: 5'-AGUAUCACGUAAGCGGUGCUU-3', respectively. Silencer siRNA Construction Kit (Ambion, USA) was used to synthesize the siRNA for targeting the enhanced green fluorescent protein (EGFP) at the position of the open reading frame (124–144). The Silencer® Select siRNAs targeting at apoptosis pathway including Mcl-1, Bcl-2 and Survivin siRNA were purchased from Invitrogen (Carlsbad, California, USA).

3.3.3 Cell culture

The human cervical carcinoma cells (HeLa cells) were used as a model for the transfection and cytotoxicity study of DNA. Whereas HeLa Cells Stably Expressing Green Fluorescent Protein (HeLa-GFP cells) were used as a model for the transfection and cytotoxicity study of siRNA. HeLa and HeLa-GFP cells were grown in complete MEM (MEM containing 1% of nonessential amino acid solution, 100 mg/mL of streptomycin, 100 U/mL of penicillin, 1% of L-glutamine and 10% of FBS) under the condition of 37 °C with 5% CO₂. HeLa-GFP cells were treated with 0.1 mg/mL G418 every 3 weeks for maintaining EGFP expression. MCF-7 and MDA-MB 231 were

cultured in a completed medium containing 10% fetal bovine serum and 1% Penicillin-streptomycin in Dulbecco's Modified Eagle Medium (DMEM), GIBCO (San Diego, California, USA). The cells were trypsinized when they reached at 70-80% cell confluence and further incubated in controlled 37 °C and 5% CO₂ incubators.

3.3.4 Preparation of plier-like cationic niosomes (PCN) and PEGylated plier-like cationic niosomes (PEG-PCN)

Cationic niosomes and cationic PEGylated niosomes were prepared by the thin film hydration with sonication method. Briefly, non-ionic surfactants (Span 20) and Chol were dissolved in the mixture of ethanol: chloroform (1:1 v/v) to obtain Span 20: Chol at 2.5:2.5 solution. The various amounts of cationic lipids (PCL-A, PCL-B and PCL-C) dissolved in the same mixture solvent were then added to the solution of Span 20 and Chol to achieve the Span 20: chol: PCLs molar ratio of 2.5:2.5:0.5, 2.5:2.5:1, 2.5:2.5:1.5 and 2.5:2.5:2. For PEGylation, DSPE-PEG 2000 was dissolved in the mixture solvent which was further incorporated into the most effective PCN formulation by 0.14, 0.35 mM. Then, the solvents were evaporated under N₂ gas flow to generate a thin film. The thin film was left in a desiccator overnight to remove the remaining organic solvents. Thin film hydration was performed using a Tris-buffer (20 mM Tris and 150 mM NaCl, pH 7.4). After hydration, the dispersion was done by sonication using a bath sonicator for 30 min followed by a probe sonicator (Vibra-Cell™ Ultrasonic Processor) for 30 min two cycles.

3.3.5 Preparation of cationic niosomes/nucleic acid complexes (nioplexes)

Cationic niosomes/nucleic acid complexes were prepared at variable weight ratios of carrier to a constant weight of nucleic acids. Before complexation step, DNA or siRNA solution and cationic niosomes solution were diluted with Tris-EDTA buffer (TE), diethylpyrocarbonate (DEPC)-treated water and Tris-buffer, respectively. The complexes were prepared by adding the diluted carrier solution to the diluted nucleic acid solution. The mixture was gently mixed by pipetting up and down for 3-5 sec to initiate complex formation. Then, the mixture was left at room temperature for 30 min to complete the complex formation.

3.3.6 Characterization of niosomes and DNA or siRNA complexes

3.3.6.1 Size and zeta potential measurements

The particle size and surface charge of cationic niosomes and cationic niosomes/nucleic acid complexes were determined by photon correlation spectroscopy using a Zetasizer Nano ZS (Malvern Instruments Ltd, Malvern, UK). Cationic niosomes and various weight ratios of cationic niosomes /DNA complexes were diluted 1:100 with distilled water to obtain a volume of 1 ml. All samples were measured in triplicate at room temperature.

3.3.6.2 Agarose gel retardation assay

Agarose gel electrophoresis was performed to confirm the formation of complexes. For DNA, the mixture of the complexes comprising of 0.25 μg DNA was loaded per well on 0.8% agarose gel (0.8 g agarose in 100 ml Tris acetate-EDTA (TAE) buffer) which was sunk in TAE buffer pH 7.4 as a running buffer. The electrophoresis was carried out for 45 min at 100 V. For the siRNA complexes, the amount of siRNA was fixed at 7.5 pmol or 0.105 μg . Complex formation was assured by agarose gel electrophoresis using 1% agarose gels (1 g agarose in 100 ml Tris borate-EDTA (TBE) buffer). The electrophoresis was carried out for 20 min at 100 V in TBE running buffer pH 8.3. Agarose gel was stained with ethidium bromide for 5 min and then de-stained in sterile water for 15 min. The remaining DNA or siRNA bands were visualized under a UV transilluminator using a GelDoc system.

3.3.6.3 Transmission electron microscopy (TEM)

The morphology of cationic niosomes and cationic niosomes/DNA or siRNA complexes was analyzed by a transmission electron microscope (TEM) (Philip Model TECNAI 20). Before the observation at an accelerating voltage of 80 kV, cationic niosomes and the complexes were stained with 1% uranyl acetate solution and dropped onto a formvar-coated copper grid.

3.3.6.4 Buffer capacity

pH titration of cationic niosomes was performed to evaluate the buffer capacity of the niosomes using the modified procedure from [60]. The cationic niosomes were diluted to obtain 1 mg/mL of total lipids. Twenty-five kDa polyethyleneimine (PEI) (1 mg/mL) was used as a positive control. The pH of the niosomes and PEI (1 mL) was adjusted to 11.5 by adding 1 N sodium hydroxide. The solutions were then titrated dropwise with 1 N hydrochloric acid (titrant). The pH of solution was measured using a pH meter (LAQUAtwin pH-22, Irvine, CA, USA). Afterwards, the titration curve between pH and volume of the added titrant was plotted. The lower steepness of slope indicated the higher buffer capacity.

3.3.7 Cytotoxicity test of cationic niosomes and nioplexes

The cell viability was investigated by the MTT assay. HeLa, MCF-7, MDA-MB 231 cells were seeded into a 96-well plate at a density of 1×10^4 cells/well in 100 μ l of complete medium and were incubated at 37 °C and 5 % CO₂ overnight. On the day of cytotoxicity test, the medium was replaced with variable concentrations of cationic niosomes or cationic niosome/nucleic acids complexes at various weight ratios in the same concentrations as *in vitro* gene transfection experiments and the cells were incubated at 37 °C and 5 % CO₂ for 24 h. The day after treatment, the cells were rinsed with phosphate saline buffer (PBS) pH 7.4 and incubated in 100 μ l MTT-containing medium (at the final concentration of 1 mg/ml) for 3 h. The formazan crystals formed in living cells were dissolved in 100 μ l dimethyl sulfoxide (DMSO) per well. Relative cell viability (%) was calculated based on the absorbance observed at 550 nm using a microplate reader (Universal Microplate Analyzer, Models AOPUS01 and AI53601, Packard BioScience, CT, USA) and compared with non-treated cells. The viability of non-treated cells was defined as 100 %.

3.3.8 Study of *in vitro* transfection efficiency of DNA complexes in HeLa cells

The day before transfection, HeLa cells were seeded into 48-well plates at a seeding density of 1×10^4 cells/well in 0.25 ml growth medium and were cultured at 37 °C in a humidified atmosphere of 5% CO₂ for 24 h. At the day of transfection, the cells

were incubated with the cationic niosomes/DNA complexes in serum-free medium at various weight ratios for 24 h at 37°C under 5% CO₂. After that, the cells were cleansed with PBS and further incubated in growth medium. Finally, the transfected cells were observed under fluorescent microscope (Model: GFP-B, wavelengths: emission filter 535/50 and excitation filter 480/40) followed by analysis using the ImageJ software after 48 h of transfection. Non-treated cells and cells transfected with naked DNA and the complex of lipofectamine® 2000 (Lipo2k) with DNA at weight ratio of 2 were used as control, negative control and positive control, respectively. The amount of DNA was fixed at 0.5 µg/well. All transfection experiments were performed in triplicate. The calculation of % transfection efficiency was computed using equation as follows:

$$\begin{aligned} \text{\% Relativeransfection efficiency} \\ = \frac{\text{Transfected cells}_{\text{nioplexes}} - \text{Transfected cells}_{\text{negative control}}}{\text{Transfected cells}_{\text{Lipo2k}} - \text{Transfected cells}_{\text{negative control}}} \times 100 \end{aligned}$$

3.3.9 Study of *in vitro* silencing efficiency of siRNA complexes in HeLa cells

The gene silencing efficiency of GFP was examined in HeLa-EGFP cells that were seeded in a 96-well black clear-bottom plate at a density of 9000 cells/well and incubated under normal conditions for 24 h. The medium was changed as serum-free, and the fluorescence intensity is analyzed at day 0 by Fluoroskan™ Microplate Fluorometer. The cells were treated with the complexes of niosomes/siGFP or Lipo2k/siGFP (at the weight ratio of 2.5), which presented 10 pmol/well (0.14 µg/well) of siRNA for 24 h. siNC was also transfected by the transfection agent for calculating the gene silencing efficiency as described previously (128). The percentages of silencing efficiency were calculated using equation as follows:

$$\text{\% silencing efficiency} = \frac{I_{\text{siNT}} - I_{\text{siGFP}}}{-I_{\text{siNT}}} \times 100$$

I_{siGFP} was the fluorescence intensity of siGFP transfection

I_{siNC} was the fluorescence intensity of siNC transfection

3.3.10 Study of effect of serum on *in vitro* gene transfection in HeLa cells

The effect of serum on the transfection efficiency was investigated. The experiment was similar to *in vitro* transfection study, except that 2 types of culture medium were used. The first one was MEM containing 10% FBS and the other was serum-free MEM medium. After transfection day, the medium was replaced with the complete medium. The cells were incubated at 37°C under 5% CO₂ for 48-72 h.

3.3.11 Study of cellular uptake by flow cytometry

HeLa, MCF-7, MDA-MB 231 cells were seeded into a 24-well plate at a density of 3×10^4 cells/well in complete MEM on a day before transfection and incubated under normal conditions. The serum-free medium containing the niosome complexes or Lipo2k/siAF488 complex was transferred to the cells and incubated for 24 h. The cells were cleansed twice with PBS and detached using trypsin. Then, 4% formaldehyde in PBS was added and rapidly mixed with the cell suspension and then preserved at 4°C until analysis. The cells were analyzed by Flow Cytometer (BD FACSCanto™, Becton and Dickinson Bioscience Company) to obtain % cellular uptake and %relative mean fluorescence intensity (MFI) of siAF488 complexes which was calculated equation as follows:

$$\%MFI = \frac{MFI_{niosomes} - MFI_{control}}{MFI_{Lipo2k} - MFI_{control}} \times 100$$

3.3.12 Confocal laser scanning microscope

Sterilized coverslips were placed at the bottom of a 24-well plate. HeLa, MCF-7, MDA-MB 231 cells were seeded at a density of 30,000 cells/well for 24 h. The optimal weight ratios of cationic niosome/siAF488, in which siAF488 was fixed at 30 pmol/well (0.42 µg/well) were incubated to the cells for 24 h. The cells were cleansed three times with PBS. Then, 5 µg/mL of Wheat Germ Agglutinin, tetramethyl rhodamine conjugate (WGA-TMR) and 5 µg/ mL of Hoechst 33342 were mixed together. Next, 200 µL/well of the mixture was applied to the cells for staining the plasma membrane and the nucleus for 15 min. The cells were cleansed three times with PBS before fixing with 4% formaldehyde in PBS for 15 min. The coverslips were taken

out of the well and air-dried before mounting on a glass slide by ProLong™ Diamond Antifade Mountant. Cell imaging was conducted using 60x oil immersion objective in FV10i confocal laser scanning microscope, Olympus.

3.3.13 Investigation of internalization pathways

The nioplexes of DNA and siRNA internalization pathways were investigated in HeLa cells. Specific endocytosis inhibitors were applied to the cells for 30 min before transfection that was further performed through the same processes as the in vitro transfection experiments (gene transfection and gene silencing). The mechanism of nioplexes was delineated using 0.05 μM of wortmannin (PI3-kinase inhibition of macropinocytosis), 1000 μM of methyl- β -cyclodextrin (Chol depletion of cell membrane), 5 μM of chlorpromazine (specific inhibition of clathrin-mediated endocytosis by dissociation of clathrin lattice), 10 μM of genistein (tyrosine-phosphorylation inhibition of caveolae-mediated endocytosis), 10 μM of filipin (specific inhibition of caveolae-mediated endocytosis by Chol binding), 0.010 μM nacodazol (inhibition of microtubule depolymerization) and 20,000 μM of ammonium chloride (pH increase of late endosomes and lysosomes). Before investigating the cellular uptake pathway of the complexes, the optimal concentration of inhibitors which did not affect cell viability was determined in HeLa cells by MTT assay.

3.3.14 Quantification of mRNA level by real-time PCR

MCF-7 and MDA-MB 231 were seeded in 96-well plate at 10^4 cells/well and incubated at 37 °C. At the day after, the cells were treated with designated samples. To evaluate gene expression level after 48 h of treatments, mRNA was extracted from cultured cells in 96-well plate and then converted to cDNA by using SuperPrep™ II Cell Lysis & RT Kit for qPCR (Toyobo, Japan). RT thermal cyclers were established followed the instruction. The obtained cDNA was amplified using Thunderbird™ SYBR® qPCR Mix (Toyobo, Japan), LightCycler® 480 Instrument II (Roche, Switzerland). The cycling conditions were as follows: 95 °C for 30 sec, followed by 40 cycles of 95 °C for 5 sec, 59 °C for 15 sec and 72 °C for 30 sec in 20 μL of total volume per reaction containing 0.3 mM of each primer. PCR reaction specificity was confirmed by DNA melting curve analysis of product. PCR efficiency of each specific gene was

performed with serial dilutions of cDNA template for each target. Specific primers spanning exons GAPDH, Mcl-1 and survivin were designed from NM_001357943.2, NM_021960.5 and NM_001168.3, respectively. The primer pairs were checked a specificity with the target genes by the Basic Local Alignment Search Tool (BLAST, <https://blast.ncbi.nlm.nih.gov/Blast.cgi>). The relative mRNA levels were computed using delta-delta CT method ($\Delta\Delta$ CT method).

The primer pair sequences were designed following:

GAPDH F: 3'-TTTTGCGTCGCCAGCCG-5'
 R: 3'-CGCCCAATACGACCAAATCC-5'
 (product length 84 bp).

Mcl-1 F: 3'-GGAGACCTTACGACGGGTT-5'
 R: 3'-AGTTTCCGAAGCATGCCTTG-5'
 (product length 75 bp).

survivin F: 3'-CCAGATGACGACCCCATAGAG-5'
 R: 3'-CCAAGGGTTAATTCTTCAAACACTGC-5'
 (product length 92 bp).

3.3.15 Cell proliferation analysis

MCF-7 and MDA-MB 231 cells were seeded in 96-well plate with cell density of 10,000 cells/well and further incubated for 24 h. the cells were transfected with the cationic niosome/siRNA complexes including Bcl-2, Mcl-1 and survivin targeted siRNA. Cell proliferation was evaluated after 48 h of transfection by MTT assay which was previously described in cytotoxicity test.

3.3.16 Double stain apoptosis detection by Hoechst 33342 and SYTOX™ Green staining

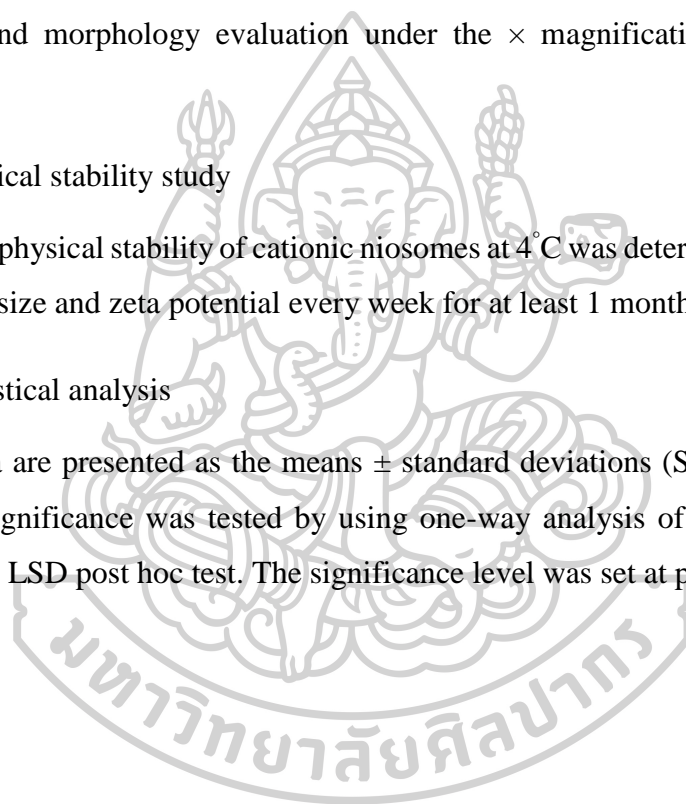
The apoptotic and nuclear morphology of cells were investigated in MCF-7 cell line. The cells were cultured in 96-well plate by 1×10^4 cells/well on the day before transfection. The cells were treated with cationic niosomes/siRNA complexes for 24 h. The half maximal inhibitory concentration of doxorubicin was used as a positive control. After that, the cells were stained in dark with 5 $\mu\text{g/ml}$ of Hoechst 33342 and 5 $\mu\text{g/ml}$ of SYTOX™ for 15 min. Inverted fluorescence microscope was used for cell apoptosis and morphology evaluation under the \times magnification within 1 h after staining.

3.3.17 Physical stability study

The physical stability of cationic niosomes at 4°C was determined by monitoring the particle size and zeta potential every week for at least 1 month.

3.3.18 Statistical analysis

Data are presented as the means \pm standard deviations (SD) of triplicate. The statistical significance was tested by using one-way analysis of variance (ANOVA) followed by LSD post hoc test. The significance level was set at $p < 0.05$.



CHAPTER 4

RESULTS AND DISCUSSION

4.1 Screening of plier-like cationic lipid-A (PCL-A) molar ratios

The influence of cationic lipid molar ratios in the plier-like cationic niosomes (PCNs) and the weight ratios of complexes between PCNs and nucleic acids are also important factors affecting their properties which were investigated.

4.1.1 Particle sizes and zeta potential

The molar ratio of Span20: Chol was assigned at 2.5: 2.5 which was optimized by Paecharoenchai et al. in the previous study (128). The particle size and zeta potential of niosomes without cationic lipids were about 200 nm and -22 mV, respectively. PCLs were added into the niosomes in order to introduce a positive charge to the systems. The molar ratios of PCL-A were varied at 0.25, 0.5, 1, 1.5, 2, and 2.5 mM. The particle size and zeta potential were measured as presented in Table 6. Surface charge was influenced by increasing the molar ratios of cationic lipids. Increasing the molar ratios of cationic lipid resulted in an increase of zeta potential. The zeta potentials were slightly different and appear highly positive charge of about 60 mV when the molar ratios of PCL-A were increased over than 0.5. The result showed that PCL-A could be inserted into the particles and generated a positive charge for the systems event at a low molar ratio of 0.5. The positive charge was purposed for electrostatic interaction with the negative charge of both nucleic acids and cellular membrane. The particle size of PCN-A was also changed by varying the molar ratios of PCL-A. The particle sizes were declined when increasing the molar ratios from 0.5-2, and PCN-A at a molar ratio of 2 showed the smallest particle size. However, when increasing the molar ratios up to 2.5, the particle size was slightly increased (Table 6). Incorporation of PCL-A at the optimal concentration range might provide stable particles of cationic niosomes. However, particle size also affects the complex formation as well as the transfection efficiency. The suitable particle size for nucleic acids delivery should be in the nano-sized range. Small particle size may be useful for cellular internalization; in contrast, large-sized particles could be tough and slowly captured (129, 130). PCN-A at a molar ratio of 0.5

mM represented unsuitable niosome vesicles that had large particle size and a wide range of size distribution. Therefore, the formulations of the niosomes with PCL-A lipid at the molar ratio of 1, 1.5, 2 and 2.5 mM were chosen for nucleic acid delivery.

Table 6 The particle size, zeta potential and polydispersity index (PDI) of cationic niosomes with plier-like cationic lipid-A (PCN-A) at various molar ratios are presented as mean \pm SD

Formulation	PCL-A (mM)	Particle size (nm)	Zeta potential (mV)	PDI
PCN-A 0.25	0.25	381.7 \pm 10.86	-1.89 \pm 0.23	0.34 \pm 0.02
PCN-A 0.5	0.5	1743 \pm 252.28	59.07 \pm 0.27	0.96 \pm 0.01
PCN-A 1	1	287.33 \pm 4.95	60.67 \pm 0.74	0.26 \pm 0.03
PCN-A 1.5	1.5	190.33 \pm 0.67	56.17 \pm 1.91	0.14 \pm 0.03
PCN-A 2	2	159.6 \pm 0.89	60.5 \pm 0.70	0.22 \pm 0.01
PCN-A 2.5	2.5	281.7 \pm 4.37	62.2 \pm 0.36	0.39 \pm 0.01

Cationic niosomes; PCN-A 1, PCN-A 1.5, PCN-A 2 and PCN-A 2.5 were incubated with DNA at various weight ratios of PCN-A/DNA from 0.1-20 to form nioplexes (Figure 10a). In overall, the particle sizes of the weight ratio ranged from 0.1 to 5 slightly dropped as the weight ratio increased, and they dramatically increased when the weight ratios were above 10. The zeta potential of nioplexes at the weight ratio between 0.1-5 was a negative charge. The negative charge of DNA was entirely neutralized by PCN-A 1, PCN-A 1.5, PCN-A 2 and PCN-A 2.5 at the weight ratio above 15, 15, 10 and 10, respectively. The characteristic of siRNA complex formation is shown in Figure 10b. The particle size and zeta potential increased when the weight ratio was increased. PCN-A 1.5, PCN-A 2 and PCN-A 2.5 could completely neutralize siRNA and convert the charge of those complexes into a positive charge at the weight ratio above 15, 10, and 10, respectively. The zeta potential of PCN-A 1 was unable to change the overall charge of siRNA complexes from negative charge to positive charge, even the increasing weight ratio to 20. PCN-A 1 might not be suitable for siRNA complexes formation. This result indicated that PCN-A 1.5, PCN-A 2, and PCN-A 2.5 were able to form complexes with both of DNA and siRNA.

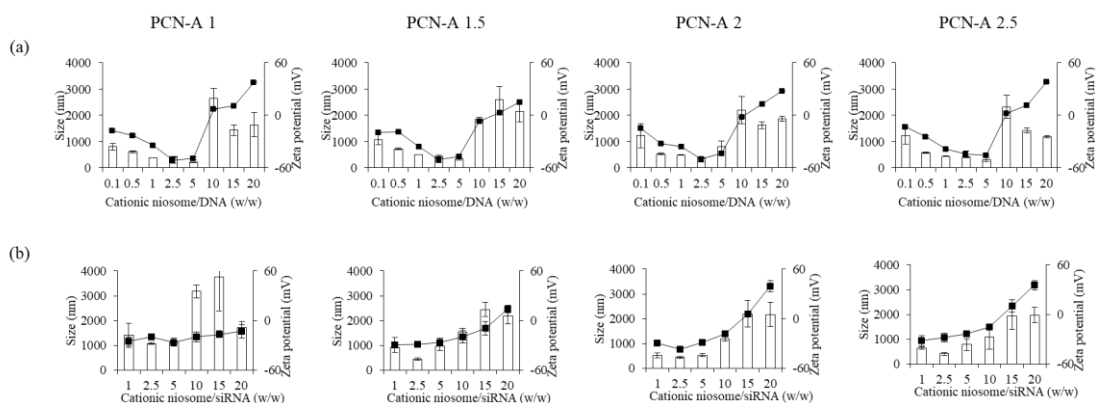


Figure 10 The particle size (bars) and zeta potential (lines) of (a) PCN-A/DNA complexes at weight ratios of 0.1-20 and (b) PCN-A/siRNA complexes at weight ratios of 1-20

4.1.2 Transfection and silencing efficiency study

The effect of PCL-A molar ratios on transfection and silencing efficiency was studied in HeLa cells (Figure 11). The pEGFP-C2 encoding to green fluorescent protein was applied for DNA delivery model to find the optimal molar ratio of PCL-A. As shown in Figure 11a, the nioplexes were formed at various weight ratios from 0.1-20 of PCN-A/constant amount of DNA (0.5 μ g). The transfection efficiency was calculated compared with Lipo2k at a weight ratio of 2 as a positive control (100 % transfection efficiency). The high percentage of transfection efficiency of PCN-A 1.5, PCN-A 2 and PCN-A 2.5 at weight ratio of 1 was $96.95 \pm 10.73\%$, $90.37 \pm 5.56\%$, and $83.98 \pm 8.38\%$, respectively. The PCN-A 1.5 and PCN-A 2 at the weight ratio of 1 presented high transfection efficiency as Lipo2k. The influence of various molar ratios of PCL-A for siRNA delivery was also evaluated in HeLa-EGFP cells. The result of siGFP delivery was measured as green fluorescence intensity by microplate reader to evaluate the silencing efficiency of each formulation as shown in Figure 11b. The finding revealed that the weight ratio at 5 of PCN-A 1.5, PCN-A 2 and PCN-A 2.5 presented the silencing efficiency at $19.60 \pm 0.85 \%$, $25.47 \pm 1.05\%$ and $19.8 \pm 3.20\%$, respectively. Further increase of weight ratio did not increase the silencing efficiency of siGFP delivery. PCN-A 2 at the weight ratio of 5 provided a significantly higher silencing

efficiency compare to Lipo2k. Therefore, the cationic lipid at 2 mM was used into PCN-A and PCN-C formulation for further studies.

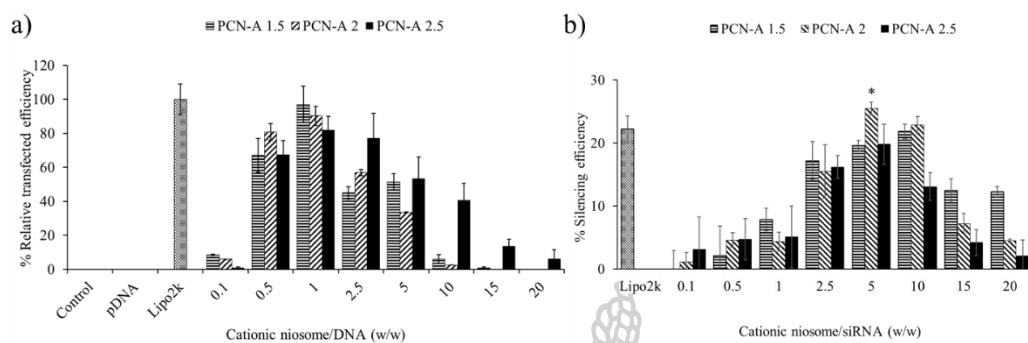


Figure 11 Cellular activities presented as (a) transfection efficiency and (b) silencing efficiency of PCN-A at various molar ratios of 1.5-2 mM. *The data significantly higher than Lipo2k at p value < 0.05.

4.1.3 Cytotoxicity of nioplexes

In vitro cytotoxicity of nioplexes was observed as the percentage of cell viability comparing to cell control in HeLa cells (Figure 12). The increasing weight ratio of PCN-A/ DNA and siRNA complexes resulted in the decrease of cell viability. The increase of cationic molar ratio influenced cytotoxicity which the cell viability was lower than 80 % at the weight ratio above 5 for DNA complexes. In contrast, the cell viability lower than 80 % of siRNA complexes was observed at the weight ratio above 15, 15 and 5 for PCN-A 1.5, PCN-A 2 and PCN-A 2.5, respectively. The guideline from ISO 10993-5 typically recommends that a decrease of cell viability by 30% (cell viability over than 70%) is considered as non-cytotoxicity. Since, the effective weight ratios of 1 for DNA delivery and 5 for siRNA delivery showed cell viability of more than 90 %, theses weight ratios therefore were considered non-cytotoxicity in HeLa cells (131).

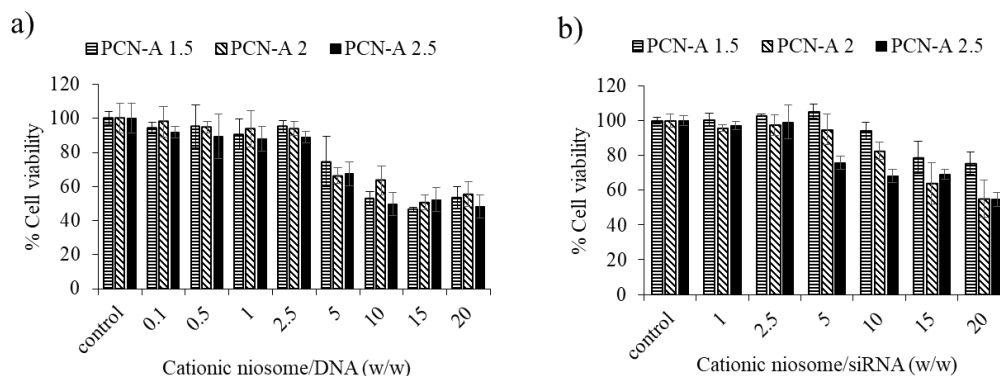


Figure 12 Cell viability of PCN-A 1.5, PCN-A 2 and PCN-A 2.5 of (a) DNA complexes and (b) siRNA complexes in HeLa cells at various weight ratios

4.2 Effect of plier-like cationic lipids (PCLs)

Three different hydrophobic tails of plier-like cationic lipids (PCLs) have been used in this study which was hypothesized that the structure of cationic lipids could affect physicochemical properties and cellular activities.

4.2.1 Cationic niosomes for DNA delivery

4.2.1.1 Particle sizes and zeta potential of cationic niosome and nioplexes

PCN-A, -B and -C were formulated with PCLs at molar ratios of 2 to observe the effect of different PCLs. The result revealed that the different hydrophobic tails of PLNs did not affect the zeta potential (Table 7). The particle sizes of all formulations were about 150 nm, and the zeta potentials were about (+) 55 mV.

Table 7 The particle size, zeta potential and PDI of cationic niosomes (PCNs) formulated with different cationic lipids PCL-A, -B and -C at molar ratios of 2 The data were presented as the mean \pm SD of triplicates.

Cationic niosomes	Particle size (nm)	Zeta potential (mV)	PDI
PCN-A	155.1 \pm 1.2	56.7 \pm 2.5	0.20 \pm 0.02
PCN-B	141.3 \pm 7.5	54.8 \pm 0.2	0.23 \pm 0.03
PCN-C	144.4 \pm 3.2	54.9 \pm 2.2	0.23 \pm 0.01

The purposed interaction of complex formation is the electrostatic interaction between positive and negative charges called nioplexes. Varying weight ratios between cationic niosomes and nucleic acids also affected the alignment of complexes described by changing particle sizes and zeta potentials. Phenomenal of complex formation was described by (132, 133). The electrostatically characteristic of complex formation had three different characteristic zones. Firstly, the complexes formed at a low weight ratio. Negatively charged nucleic acids were absorbed on cationic carriers which presented overall negative charge and small particle size. Secondly, the weight ratio gradually increased to form unstable colloidal complexes which the particle size dramatically increased while the zeta potential was nearly neutral. Lastly, the complexes became positively charged and small-sized complexes at a high weight ratio which has a proven excessive amount of cationic carriers. A similar result was observed in previous studies (134, 135). The result showed that increasing weight ratios of cationic niosomes tended to raising the zeta potential and changing the particle size of the complexes. As in Figure 13, the particle sizes of complexes at the weight ratios of 0.5–5 slightly dropped from 464 to 193 nm, however, the zeta potential was negative. Secondly, the particle size of DNA nioplexes dramatically rose to more than 3000 nm. The zeta potential was nearly neutral or transformed into a slightly positive charge when the weight ratio was increased to 10. At a weight ratio of 20, the particle size became smaller complexes and exhibited more positive charges than those at lower ratios. This experiment also confirmed that the addition of cationic niosomes can interact with negatively charged nucleic acids and generate nioplexes.

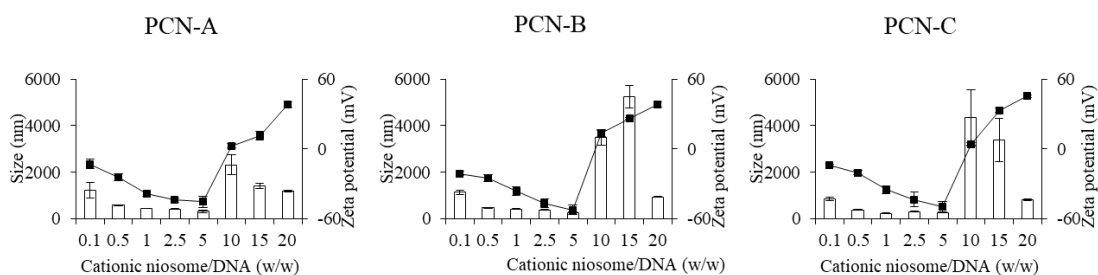


Figure 13 The particle size and zeta potential of various weight ratios of PCNs/DNA complexes from 0.1-20

4.2.1.2 Gel retardation assay

Gel agarose electrophoresis was used for the observation of complex formation. Nucleic acids can move through the porosity of agarose toward positive electrode gel under constant current. The gel was stained and then presented the band of remaining nucleic acids from incomplete complexes. However, the band of complete complex formation was invisible in the gel. Increasing weight ratios can increase the complex formation ability. Complexes formation ability of all PCNs depicts in Figure 14. The result exhibited that PCN-A, PCN-B, PCN-C entirely formed nioplexes at the weight ratio of 10, 10 and 15, respectively.

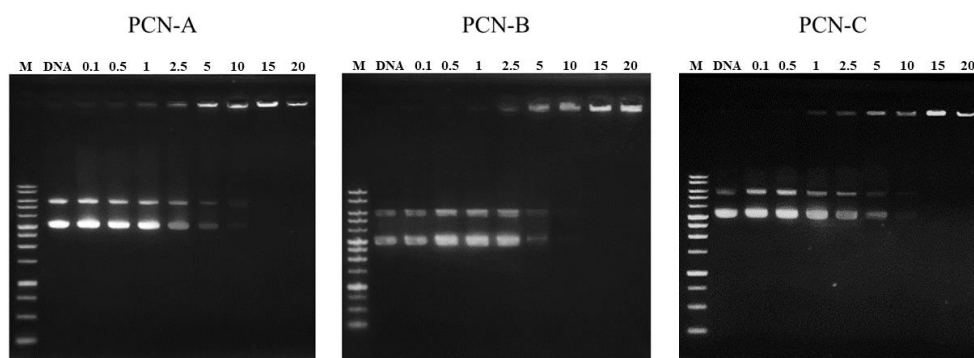


Figure 14 The DNA complex formation ability of PCN-A, PCN-B and PCN-C by gel agarose electrophoresis

4.2.1.3 Transfection study for DNA delivery

The transfection efficiency of different structure of PCNs was evaluated and the result is shown in Figure 15. The weight ratio of all formulation was optimized from 0.1 to 20 to obtain the effective activity. The optimal weight ratios of PCN-A, PCN-B, and PCN-C were 1, 2.5 and 1 presenting $91.2\% \pm 5.7\%$, $108.7\% \pm 6.5\%$ and $98.4\% \pm 7.8\%$ of transfection efficiency, respectively. The transfection efficiency of PCNs was comparable with Lipo2k, and PCN-B gave the greatest efficiency among PCNs.

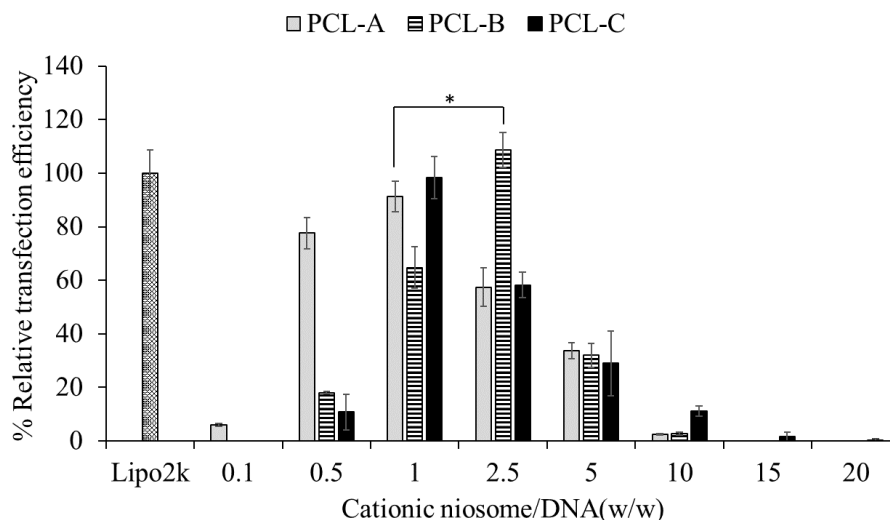


Figure 15 Transfection efficiency of PCN-A, PCN-B and PCN-C in HeLa cells at the weight ratio from 0.1-20. *The data was significantly higher than Lipo2k at p-value < 0.05.

4.2.1.4 Cytotoxicity of nioplexes

The cytotoxicity of PCNs/DNA complexes of PCNs was assessed cytotoxicity in HeLa cells (Figure 16). The cell viability was lower through the increasing of weight ratio of cationic content. The cytotoxicity of PCN-A and PCN-C/DNA complexes was noticed at the weight ratio above 5, while that of PCN-B/DNA complexes was observed at the weight ratio above 10. The outcomes exhibited negligible cytotoxicity of the most effective transfection efficiency of PCN-A, PCN-B and PCN-C that were the weight ratios of 1, 2.5 and 1, respectively. PCNs were considered to be safe and potential transfection agents for DNA delivery.

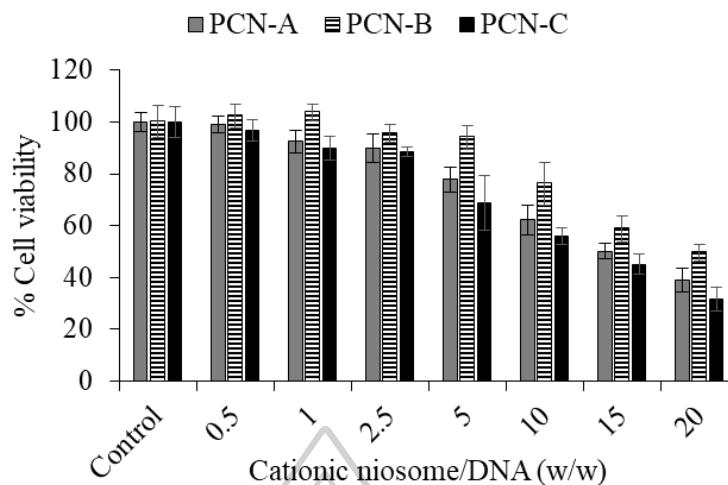


Figure 16 Cell viability of PCN-A, PCN-B and PCN-C/DNA complexes at the weight ratio of 0.5-20 in HeLa cells

4.2.1.5 Internalization pathways of nioplexes for DNA delivery

Nanocarriers are generally taken up by endocytosis as the major route across the plasma membrane (136, 137). After entry into cells as intracellular vesicles or endosomes, they would finally incorporate with lysosomes and be degraded if the carrier is not able to release nucleic acids to their target site. The cells were pretreated with specific endocytosis inhibitors to evaluate the predominant internalization pathway. The nioplexes at the effective weight ratio of each PCN in the previous experiment were then applied to the cell. The possible internalization pathways were identified by comparing their activity between cells pretreated with specific endocytosis inhibitors and cells untreated with inhibitors. The results in Figure 17 indicated that the transfection efficiency of PCN systems was decreased by pretreatment with ammonium chloride (inhibited endosome acidification). Therefore, it could be concluded that endosomal-lysosomal acidification was required for PCN escape. It was found that wortmannin, methyl- β -cyclodextrin, and chlorpromazine significantly ($p < 0.05$) affected the transfection efficiency of all nioplexes. PCN-A delivered pEGFP-C2 through micropinocytosis as a major internalization pathway. Whereas clathrin- and caveolae-mediated endocytosis was used as minor pathways. Although macropinosome has been mentioned that it is easy to escape from the vesicle, the delivery system could

be partially degraded by the lysosomal incorporation (138). DNA delivery of PCN-B and PCN-C was almost similar. PCN-B used clathrin-mediated endocytosis as a predominant internalization pathway, followed by caveolae-mediated endocytosis and micropinocytosis, respectively. Meanwhile, PCN-C did not significantly involve caveolae-mediated endocytosis.

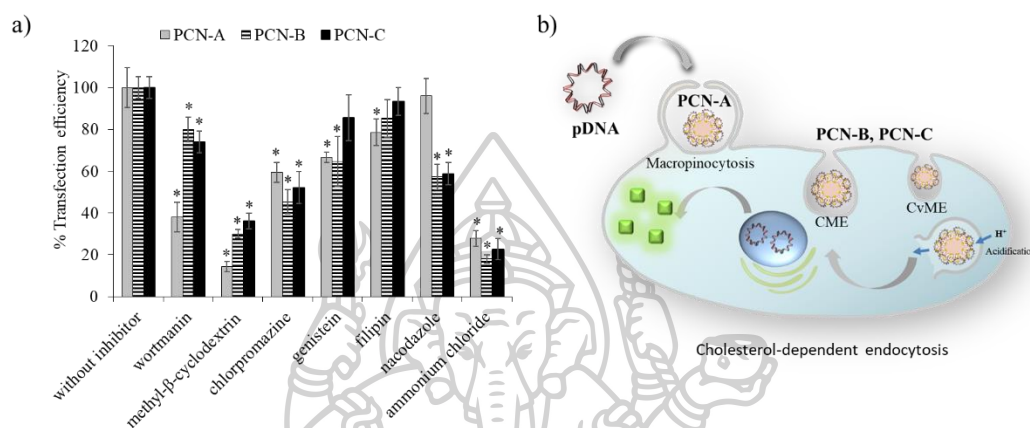


Figure 17 Investigation of internalization pathways of PCN-A, PCN-B and PCN-C/DNA complexes evaluated with pretreatment of specific endocytosis inhibitors, (a) transfection efficiency of each PCNs and (b) scheme of possible internalization pathways. *The data was significantly different from the transfection without pretreatment at p-value < 0.05.

4.2.2 Cationic niosomes for siRNA delivery

4.2.2.1 Particle sizes and zeta potential of cationic nioplexes

The properties of PCNs to form nioplexes with siRNA corresponded to DNA complexes formation. The zeta potential went up to a positive charge when the amount of cationic niosomes increased. The neutralizing ability of PCN-A, PCN-B and PCN-C to siRNA was at the weight ratios above 15. As in Figure 18, the overall particle size of siRNA complexes suggested that PCN-B could condense siRNA to compact size better than PCN-A and PCN-C. Interestingly, the neutralization of siRNA required a higher weight ratio of cationic niosomes than the DNA complex formation. The weight ratio of PCN-B completely formed complexes was above 15 and 10, for siRNA and

DNA complexes, respectively. The chemical structure of both DNA and siRNA was phosphodiester backbones but siRNA was shorter than abundant nucleotides of DNA. The strength of electrostatic interaction increases along with high molecular weight. Therefore, increasing cationic niosomes concentration is essential for overcoming the siRNA free energy and obtaining a stable complex. This manner was also described by Han Chang Kang et al. The structure of siRNA is more rigid and less flexible than the DNA resulting in steric repulsion; thus, the attribute of siRNA could interrupt the formation of complexes (139). siRNA frequently results in more loosely condensed and larger complex particles than that seen under similar complexing conditions when used for pDNA polyplexes of 100–200 nm in size (139, 140).

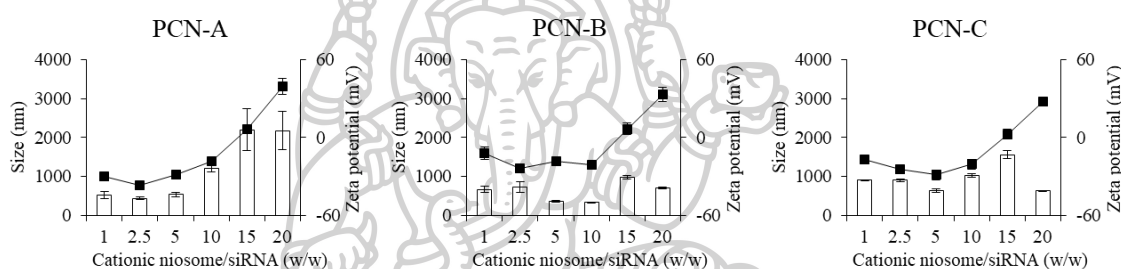


Figure 18 The particle size and zeta potential of various weight ratios of PCNs/siRNA complexes from 0.1-20

4.2.2.2 Gel retardation assay

Meanwhile, entire siRNA complex formation was above 10. These results showed that the different hydrophobic tails of PCNs did not affect the complex formation ability. Even if the core structure of DNA and siRNA is polymer nucleotides which are composed of a nitrogenous base, a sugar, and a phosphate group, the degree of PCNs to complex formation was not the same (Figure 19). The size of pEGFP-C2 is approximately 4.7 kb, whereas that of siRNA or small RNA is about 20 bp. As a result of siRNA structure, a short double-stranded RNA has more rigid structures which cause them more rotation and translation degree of freedom. Therefore, the weight ratio of PCNs for complete complex formation in siRNA was higher than DNA complex formation (141-143).

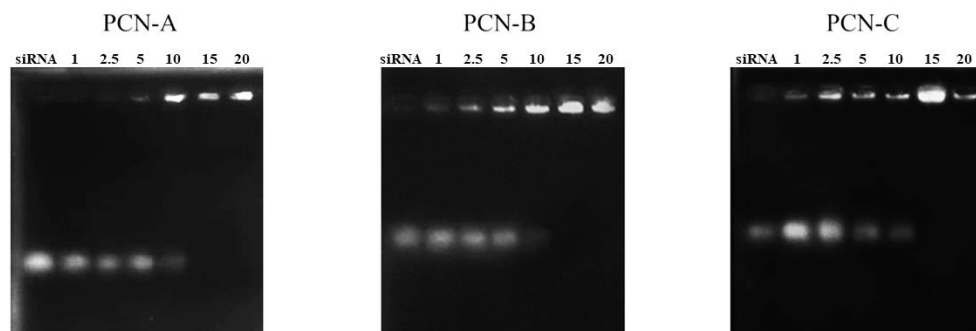


Figure 19 The siRNA complex formation ability of PCN-A, PCN-B and PCN-C by gel agarose electrophoresis

4.2.2.3 Silencing study for siRNA delivery

The results showed that asymmetric alkyl chains of cationic lipids (PCN-B and PCN-C) possessed more efficiency than the symmetry alkyl chains (PCN-A) (Figure 20). One of the keys to successful transfection is endosomal membrane perturbations for releasing nucleic acids into the environment. The asymmetric hydrocarbon chains could facilitate fusogenicity (63). Besides, a lower nucleic acid disassembly rate is obtained with symmetry (144). We hypothesized that a hydrocarbon chain with double bond might enhance the transfection efficiency by increasing the fluidity of the membrane bilayer through intermembrane mixing (63, 144, 145). However, our study found that the presence of hydrocarbon chain with a double bond did not improve the efficiency of the asymmetric novel synthesized PCLs. This might be caused from that lipid arrangement of the arch lipid (double bond area) was highly difficult for packing with other compositions, which could be the cause of the unstable bilayer. The saturated asymmetric hydrocarbon chain of cationic lipids remained overhanging on the hydrophobic tail to connect between both sides of the bilayer through Van der Waals forces which caused the aligned area (146, 147). The saturated asymmetric could increase the membrane integrity of the cationic niosomes and protect the early breakdown of the vesicles (148). Therefore, a balance between fluidity and rigidity of the bilayer system is required for cationic lipid designs.

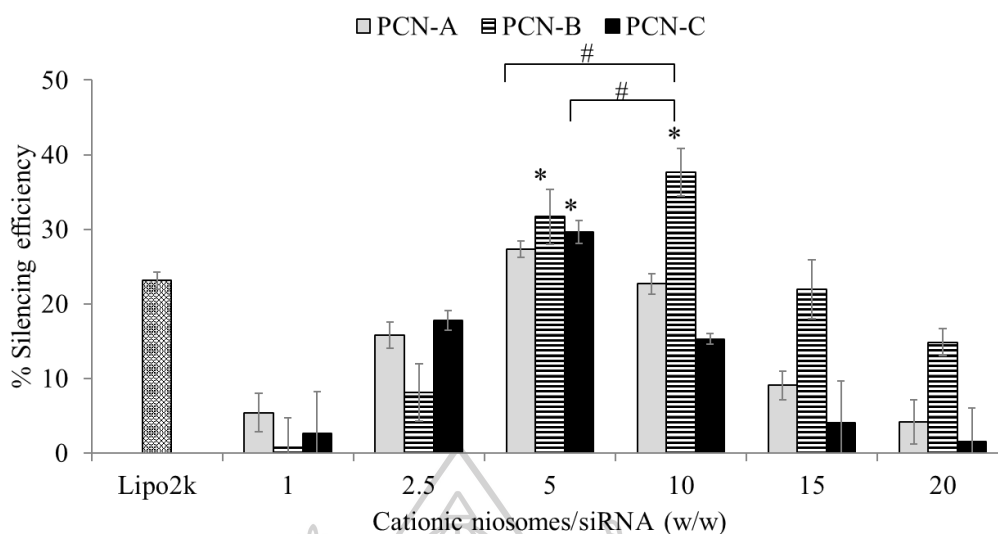


Figure 20 The silencing efficiency of PCN-A, -B and -C/siGFP complexes compared to siNT complexes. *The data was significantly higher than Lipo2k at p-value < 0.05. #The data was significantly different at p-value < 0.05.

4.2.2.4 Cytotoxicity of nioplexes

As shown in Figure 21, the cells were able to tolerate the toxicity of PCN-A and PCN-C at the weight ratio <10 and that of PCN-B at the weight ratio <20, wherein the cell viability was >80%. The increase in cationic lipids could lead to cytotoxicity. However, the most effective weight ratios of all formulations, PCN-A/siRNA (5:1), PCN-B/siRNA (10:1) and PCN-C/siRNA (5:1), exhibited negligible cytotoxicity, thereby they could be safe and potential transfection agents.

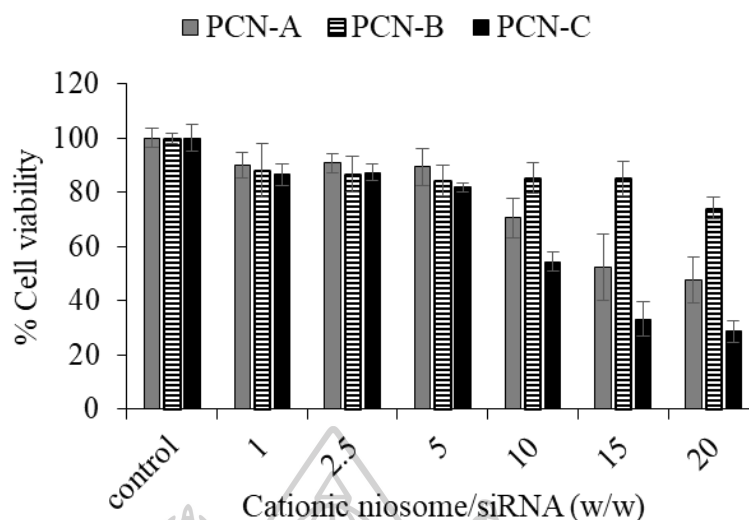


Figure 21 Cell viability of PCN-A, PCN-B and PCN-C/siRNA complexes at the weight ratio of 0.5-20 in HeLa cells

4.2.2.5 Cellular uptakes of nioplexes studied by using flow cytometry analysis and confocal laser scanning microscopic (CLSM)

Cellular uptake analysis was performed, and the CLSM images are shown in Figure 22c. Primarily, both Lipo2k and cationic niosomes could deliver siRNA into the cytoplasm, where it is the typical area for siRNA to regulate the mRNA level by interrupting the translation process. Furthermore, the PCN-B delivery system was considerably taken up by HeLa cells, which can be observed from the amount of green fluorescence complex of siAF488. The results from CLSM were consistent with flow cytometry interpretation. The results in Figure 22a and b depicted that the cellular internalization of Lipo2k, PCN-A, PCN-B, and PCN-C was almost 100% with no significant difference. The MFI of Lipo2k was two and three times higher than that of PCN-A and PCN-C, respectively, at the weight ratio of 5. Although Lipo2k could carry more siRNA to the cells than PCN, the silencing efficiency was lower. It has been reported that SPANosomes showed a superior rate of siRNA release into cytosol than Lipo2k (149). PCN-B at the weight ratio of 10 exhibited the highest MFI, which could deliver siAF488 into the cell by more than three times compared with Lipo2k and approximately seven times compared with PCN-A PCN-C at the weight ratio of 5. This

result suggested that the cellular uptake ability of PCN-B was not limited by the cytotoxicity at a higher weight ratio. Therefore, PCN-B could carry more siRNA into the cells and subsequently exhibited an effective activity.

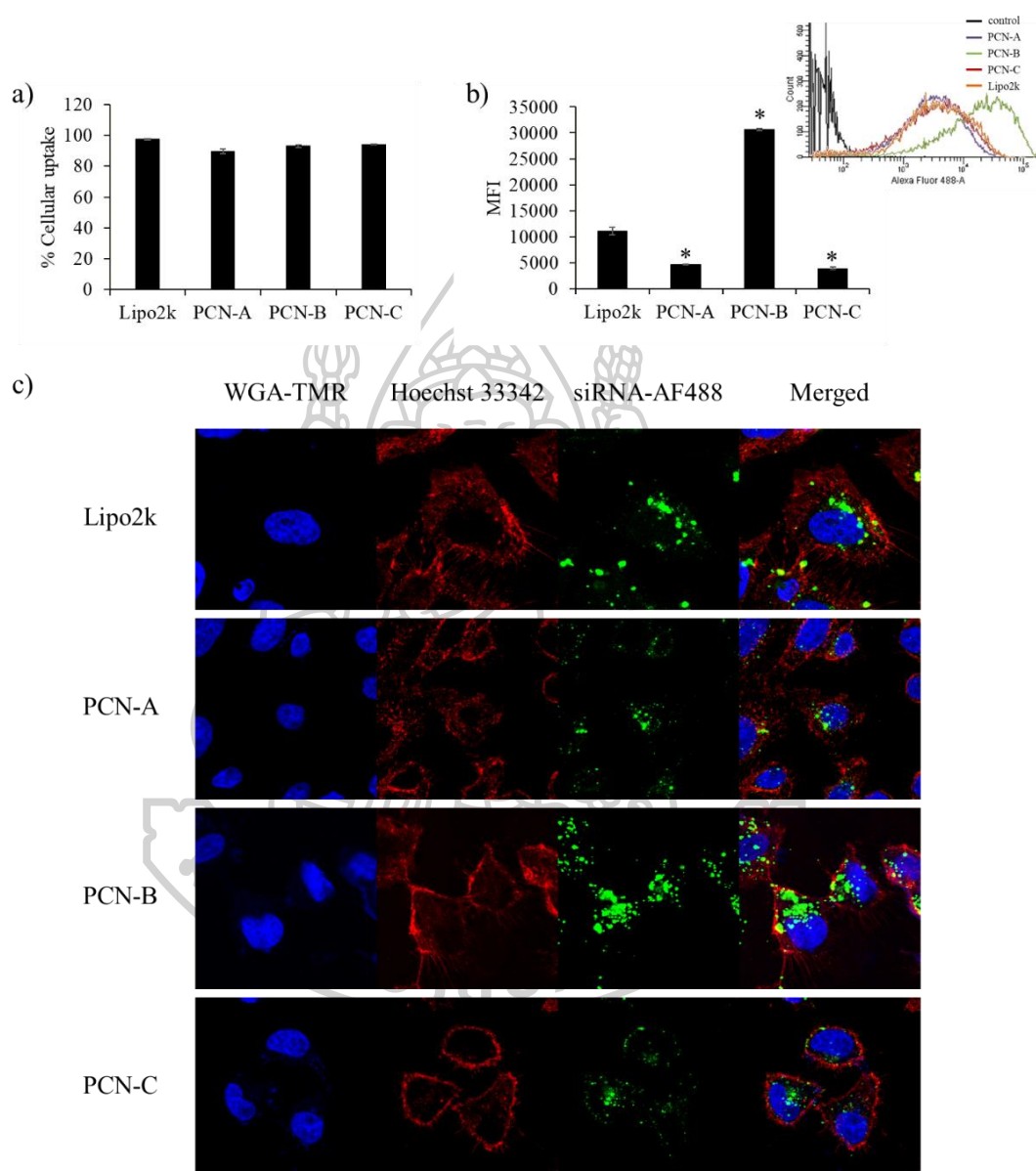


Figure 22 Cellular uptake evaluated after 24 h transfection with siAF488 complexes in HeLa cells. (a) the percentage of cellular uptake, (b) MFI plot and fluorescence histogram and (c) CLSM images. *The data was significantly different from Lipo2k transfection at p-value < 0.05.

4.2.3 Cytotoxicity of Plier-like cationic niosomes (PCNs)

The 50% inhibitory concentration (IC_{50}) of PCNs was evaluated by the MTT assay. The IC_{50} values are presented in Table 8 which was found to be in the following order: PCN-B, PCN-A and PCN-C. These results revealed that the shorter chain lipids are associated with toxicity (145). The saturated asymmetric hydrocarbon chains provided minimal cytotoxicity compared with the unsaturated chains. The cytotoxicity of the unsaturated hydrocarbon chains might be one of the reasons to diminish its efficiency.

Table 8 IC_{50} of plier-like cationic niosomes (PCNs) in HeLa cells were presented as the mean \pm SD of triplicates.

Cationic niosomes	IC_{50} ($\mu\text{g/mL}$)
PCN-A	29.13 ± 0.19
PCN-B	36.16 ± 0.98
PCN-C	28.93 ± 0.55

4.2.4 Internalization pathways of nioplexes for siRNA delivery

The internalization pathways of all siRNA complexes were associated with micropinocytosis and clathrin- and caveolae-mediated endocytosis Figure 23. The internalization pathway of siRNA delivery was depicted almost the same as DNA delivery. The major internalization pathways of asymmetric niosomes were clathrin- and caveolae-mediated endocytosis, while micropinocytosis was a minor pathway. Remarkably, pretreatment with methyl- β -cyclodextrin, which depleted chol from the cell membrane showed the most inhibitory effect on DNA and siRNA delivery. Chol is important for cell membrane ruffle formation which is involved in the endocytosis of extracellular macromolecules, including micropinocytosis and caveolae- and clathrin-mediated endocytosis (150-154). Furthermore, nioplexes with asymmetric hydrocarbon chains were different from niosomes with symmetry chains because their activities were inhibited by nocodazole. The intracellular pathway and the intracellular trafficking of the asymmetric hydrocarbon chains depended the polymerization of microtubules, which is essential for vesicle transport and machinery recycling. Thus, the travel of nioplexes with asymmetric chains might be obstructed before reaching the target site,

and machinery recycling was inhibited when pretreated with nocodazole. On the other hand, they might be interrupted during passive transportation of mitosis-cell division (155, 156). However, investigation of the exact internalization pathway has been laborious to date.

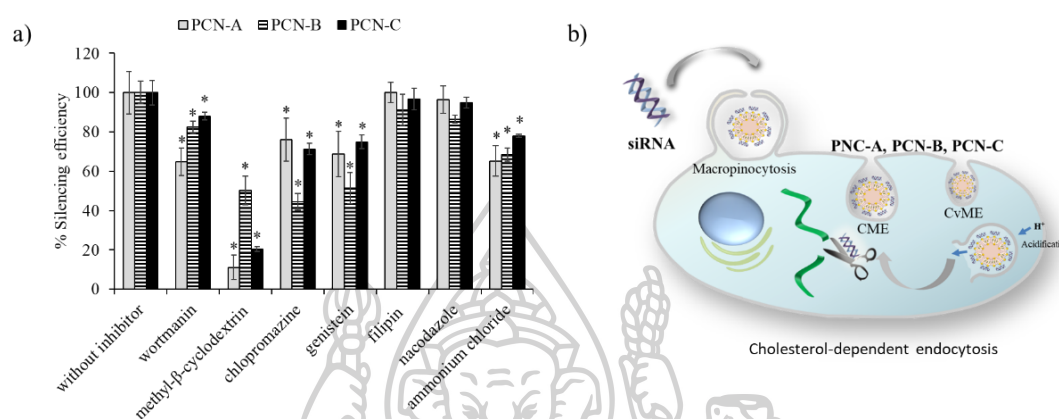


Figure 23 Investigation of internalization pathways of PCN-A, PCN-B and PCN-C/siGFP complexes evaluated with pretreatment of specific endocytosis inhibitors, (a) transfection efficiency of each PCNs and (b) scheme of possible internalization pathway. *The data was significant different form the transfection without pretreatment at p value < 0.05.

4.2.5 Morphology analysis

The morphological characteristic of cationic niosomes and nioplexes was observed via TEM. Niosomes and nioplexes were dried on formvar-carbon film and stained with 1% Uranyl acetate. The particle sizes from Zetasizer nano depicted relatively bigger sizes than the TEM image results, which are presented in Figure 24. The particles obtaining from the TEM image were in the range of 87 to 186 nm which was in the dried state and consequently smaller particle sizes, while the bigger particles obtaining from Zetasizer nano were in the water-containing state. PCNs had a unilamellar spherical shape and smooth border. Uranyl acetate is a negative staining reagent at the acid condition. Subsequently, they produced high electron density and image contrast which they cannot interact with positively charged niosomes thus niosomes were depicted as bright particles in dark background. Positively charged of

uranyl ion can interact with negatively charged material including phosphate group of nucleic acid which might be shown in darker area around the border of nioplexes.

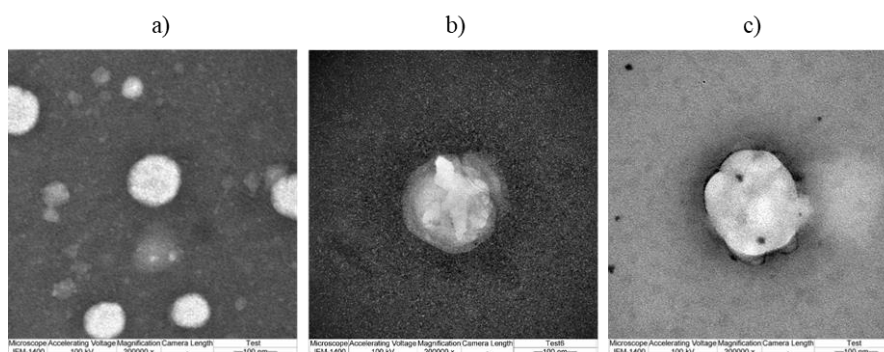


Figure 24 (a) the particle size and shape of PCN-B (~ 87 nm), (b) nioplexes of PCN-B/DNA at a weight ratio of 2.5 (~ 167 nm) (c) nioplexes of PCN-B/siRNA at a weight ratio of 15 (~ 186 nm)

4.2.6 Buffering capacity

Typically, lipid-base nanoparticles were endocytosed into cells as an endosome. The important point is that endosome escape ability and then release to the area of therapeutic effect which is the nucleus for pDNA and the cytoplasm for siRNA, are one of the critical steps. To simulate the pH change of endosome and lysosome, PCNs were observed pH resistance ability by using acidic titration. Regarding the proton sponge hypothesis, the buffer capacity is important for endosomal escape ability. PEI is a well-known polymer having proton sponge effect (157, 158). The pKa value of PEI is between neutral and endosomal pH which can buffer acidification of endosomal vesicles. The balancing of ion was controlled by counter ion influx (chloride) when a nitrogen atom was further protonated in the endosome. This event caused endosomal swelling and bursting followed by the release of the complexes to the environment. The pH-sensitive cationic lipids have been widely used, YSK05 has been presented pKa of 6.4-6.4 which had a tertiary amine attributing pH-sensitive properties and endosomal escape by promoting membrane fusion and destabilization (159). The mutual chemical structures of pH-sensitive cationic lipids have been studied such as DLinDMA, DLinKC2-DMA and YSK05 lipid containing one protonable ternary amine group (111). We hypothesized PCNs might have pH-sensitive property at lower pH. Therefore, the

buffer capacity of PCNs was evaluated by the slope of acidic titration curve over the pH range of endosome, which was depicted in Figure 25. The PCNs demonstrated buffer capacity indicated by a gradual slope in the endosomal pH range. The flattest slope between pH 5 to 7.4 indicated the greatest endosomal buffer capacity. The result revealed that PCN-C exhibited the highest buffer capacity with a slope of 1.42 μL (of 1 N HCl/pH unit) followed by PCN-B and PEI which the slope over the pH range was 0.87 μL and 0.80 μL , respectively. In contrast, PCN-A provided the lowest buffer capacity with a slope of about 0.74 μL over the pH range. However, the transfection efficiency was not increased as the buffer capacity increased. Gabrielson and Pack found that the increase in the degree of acetylation of PEI resulted in a declined buffer capacity. However, no change in the transfection efficiency was observed as the degree of acetylation of PEI increased. This is because acetylation appears to enhance the dissociation of polyplexes and release DNA to the target site (158). Although a buffer capacity has a benefit for the proton sponge effect, there are still other factors involved with nucleic acid delivery of the PCNs; for instance, lipid bilayer the integrity and intermembrane mixing of niosomes. These results exhibited that PCNs presented pH-sensitive properties which could contribute to intracellular endosomal escape for gene delivery application (160).

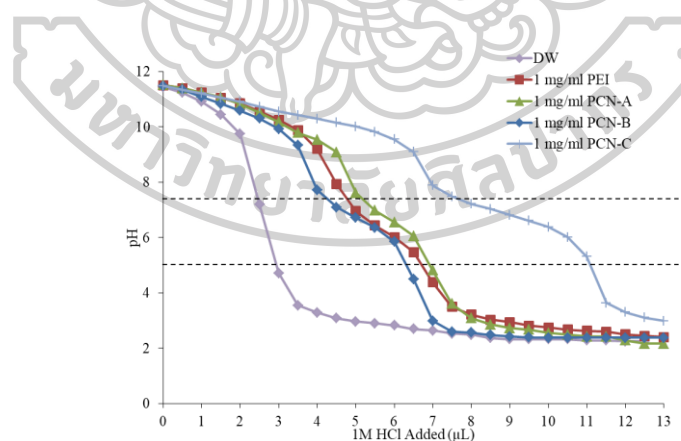


Figure 25 Titration curves of PCN-A, PCN-B and PCN-C were compared to PEI and deionized water applied as a control. The systems were adjusted to pH 11.5 with NaOH and titrated with 0.5 μL aliquot of 1 M HCl.

4.3 Effect PEGylation on plier-like cationic niosome-B (PCN-B)

The surface properties of cationic liposomes are usually modified by PEGylation. Both charge density and charge polarity play an important role that can affect systemic stability as well as cytotoxicity. PEGylation is widely used in both *in vitro* and *in vivo* applications to overcome barriers. It has been applied in many nanocarriers, not only increasing the stability in blood circulation but also avoiding clearance by recognition of phagocytic cells. In this study, PEGylation was applied by incorporation of DSPE-PEG2000 into PCN-B. To avoid PEG dilemma, PEG concentration was therefore varied at 2% and 5% mM of total lipids.

4.3.1 Particle sizes and zeta potential

The particle size and zeta potential were also evaluated which are presented in Table 9. The result showed that PEGylation of PCN-B slightly affected the particle size while the zeta potential was decreased. However, the PEGylated cationic niosomes exhibited a positive surface charge.

Table 9 The particle size and zeta potential and PDI of PCN-B, 2% PEG-PCN-B and 5% PEG-PCN-B are presented as mean \pm SD

Cationic niosomes	Size (nm)	Zeta potential (mV)	PDI
0% PEG-PCN-B	141.3 \pm 7.5	54.8 \pm 0.2	0.23 \pm 0.03
2% PEG-PCN-B	190.3 \pm 3.6	18.4 \pm 1.6	0.47 \pm 0.01
5% PEG-PCN-B	166.3 \pm 0.6	23.8 \pm 3.2	0.45 \pm 0.01

The ability of complex formation was further evaluated by particle size and zeta potential measurement (Figure 26). All cationic niosomes could condense DNA and siRNA to nanosized particles with different weight ratios. The DNA complexes of 0% PEG-PCN-B, 2% PEG-PCN-B and 5% PEG-PCN-B expressed a positive charge at the weight ratio of 10, 15 and 15, respectively (Figure 26a). The siRNA complexes of 0% PEG-PCN-B showed a positive charge at the weight ratio of 10, whereas 2% PEG-PCN-B and 5% PEG-PCN-B exhibited almost a neutral charge (Figure 26b). The result revealed that PEGylation of cationic niosomes in complex formation could protect particle aggregation, whereas the particle size of 0% PEG-PCN-B complexes

significantly increased, especially when the zeta potential of complexes reaching to neutral charge. On the other hand, PEGylation could reduce the ability of complex formation by its steric barrier properties requiring higher weight ratios than using 0% PEG-PCN-B.

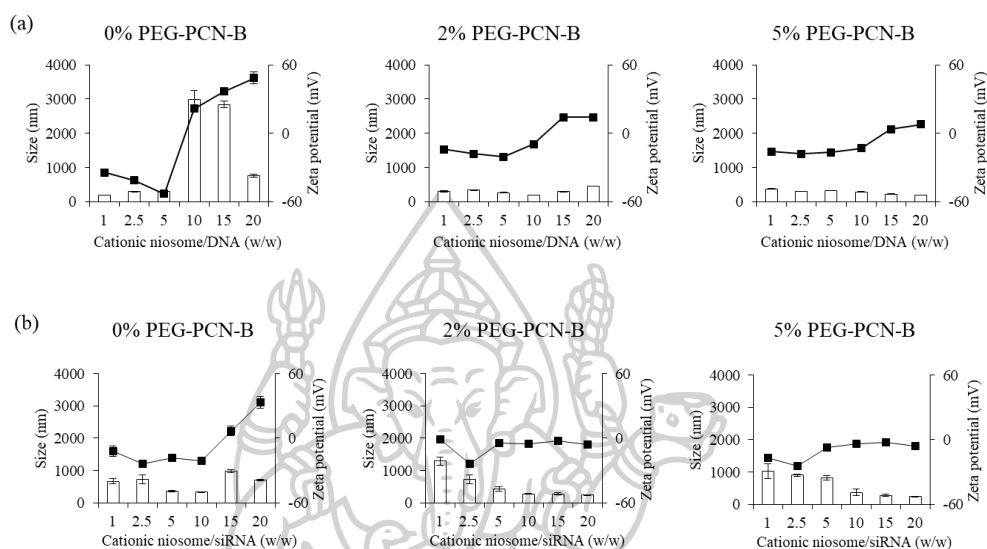


Figure 26 The particle size (bar graph) and Zeta potential (line graph) of (a) DNA complexes at weight ratios of 0.1-20 and (b) siRNA complexes at weight ratios of 1-20

4.3.2 Gel retardation assay

The complex formation was also confirmed by gel retardation assay. The DNA complex formations of 0% PEG-PCN-B, 2% PEG-PCN-B and 5% PEG-PCN-B were completed at the weight ratio of 10, 15 and 20, respectively (Figure 27a). The siRNA complex formations of 0% PEG-PCN-B, 2% PEG-PCN-B and 5% PEG-PCN-B were completed at the weight ratio over 10, 10 and 15, respectively (Figure 27b).

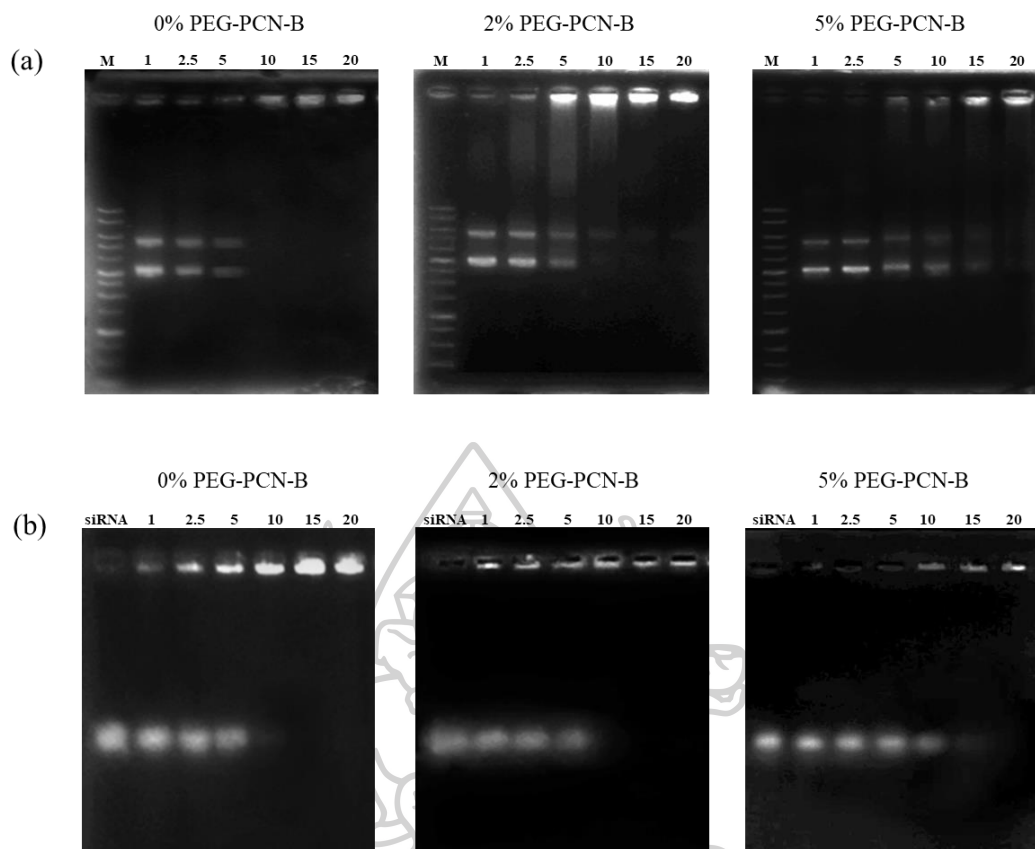


Figure 27 The complex formation ability of (a) DNA complexes and (b) siRNA complexes by Gel agarose electrophoresis

4.3.3 Cellular activity of nioplexes

Transfection and silencing efficiency were evaluated in HeLa and HeLa-EGFP cells, respectively. The data exhibited that PEGylation of PCN-B could improve the efficiency of PCN-B delivery system by using 2% of DSPE-PEG 2000 (Figure 28). Although the PEGylation at 5% significantly declined the transfection efficiency, it did not affect the silencing efficiency at the weight ratio of 15 and 10, respectively, compared to the weight ratio of PCN-B at the highest efficiency. The data of the experiment was also consistent with the zeta potential and gel retardation assay. The complex formation of PEGylation PCN-B required amount of carriers more than PCN-B to achieve complete formation and high efficiency.

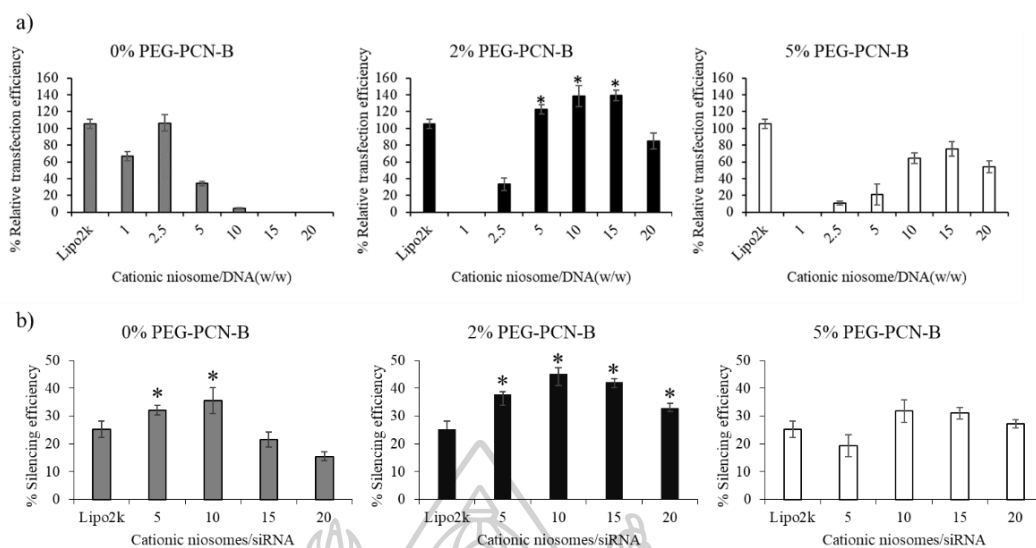


Figure 28 Effect of PEGylation on transfection efficiency and silencing efficiency of PCN-B and 2% PEG-PCN-B/DNA at weight ratios of 2.5 and 10, respectively. *The data was significantly different higher than Lipo2k transfection at p -value < 0.05.

4.3.4 Cytotoxicity of cationic niosomes and nioplexes

IC₅₀ of PEGylated cationic niosomes was evaluated in HeLa cells. As the IC₅₀ presented in Table 10, PEGylation at 2% was able to decline the cytotoxicity in HeLa cells as the consequence of a shielding effect of the positive surface charge on the systems. However, PEGylation can display effects on both cellular uptake and cytotoxicity depending on cell types such as the marked decrease in membrane damage, lipid peroxidation, and oxidative stress observed in nonphagocytic neuroblastoma cells (161). Therefore, to avoid PEGylation dilemma, cellular experiments have to be further investigated in other cell types.

Table 10 The IC₅₀ of 0% PEG-PCN-B, 2% PEG-PCN-B and 5% PEG-PCN-B in HeLa cells were presented as the mean ± SD of triplicates

Cationic niosomes	IC ₅₀ (µg/mL)
0% PEG-PCN-B	36.16 ± 0.98
2% PEG-PCN-B	83.05 ± 1.95
5% PEG-PCN-B	84.04 ± 2.19

The cytotoxicity of DNA and siRNA complexes of PEGylated formulations was also investigated which is depicted in Figure 29. Increasing the weight ratios affected cytotoxicity, especially in 0% PEG-PCN-B, which was considered toxicity to the cells at the weight ratio of 20 for DNA and siRNA complexes. However, the effective weight ratios of all formulations were safe for HeLa cell transfection which the cell viability was not less than 80%. The PEGylation could reduce the cytotoxicity even at the high weight ratios. Therefore, PEG could diminish the detrimental effect of surface charge on the cationic niosomes which increased IC50 and decreased the cytotoxicity in HeLa cells.

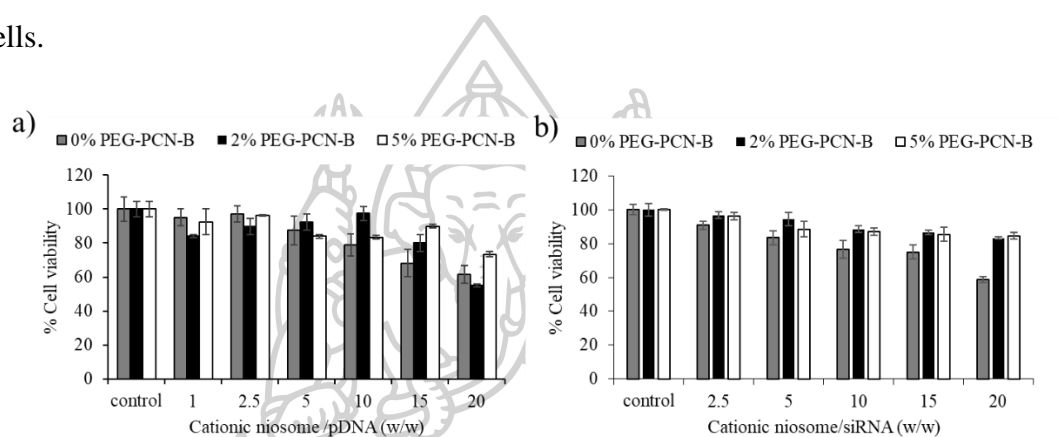


Figure 29 Cell viability of 0% PEG-PCN-B, 2% PEG-PCN-B and 5% PEG-PCN-B complexes; (a) DNA complexes and (b) siRNA complexes

4.3.5 Effect of serum on transfection and silencing efficiency

The effect of serum on silencing efficiency was also observed at the weight ratios from 5 to 20. As shown in Figure 30, the silencing efficiency of 0% PEG-PCN-B and 2% PEG-PCN-B was affected by presenting 10% serum at the lower weight ratios of 5 and 10. In contrast, the silencing efficiency of both formulations was not significantly different at the higher weight ratios of 15 and 20. However, the complexes of 2% PEG-PCN-B showed higher silencing efficiency than 0% PEG-PCN-B at a weight ratio of 15. This might be because the outer PEG layer could shield cationic groups which decreased cytotoxicity and increased the difference of mocked and treated GFP silencing.

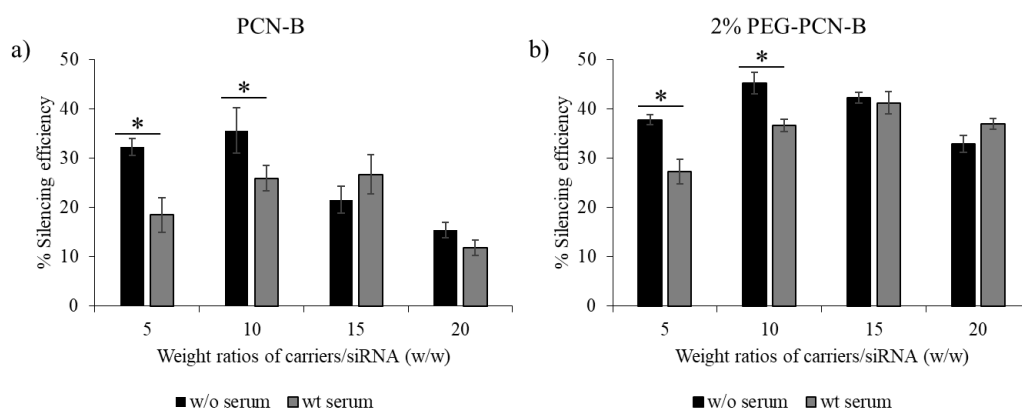


Figure 30 Silencing efficiency of siRNA complexes at weight ratios of 5-20; (a) Effect of serum on silencing efficiency of 0% PEG-PCN-B and (b) 2% PEG-PCN-B/siGFP at weight ratios of 5-20. *The data was significantly different from transfection without the presence of serum at p -value < 0.05 .

4.3.6 Protein serum aggregation

The changes in mean particle size of nioplexes in the presence of 10% serum were evaluated as a function of time. As in the data from Figure 31, the nioplexes of 2% PEG-PCN-B and 5% PEG-PCN-B manifested almost unchanged particle size around 200 nm when the time had passed. In the serum presence, the particle size of 0% PEG-PCN-B increased after 2 h from about 400 nm to 700 nm, and as time prolonged. The size continuously increased and peaked at about 900 nm after 6 h. This experiment demonstrated that PEGylation could improve the stability of nioplexes underwent serum mimicking conditions by reducing aggregation with negative charge on protein serum by electrostatic repulsion and steric barrier effect (162).

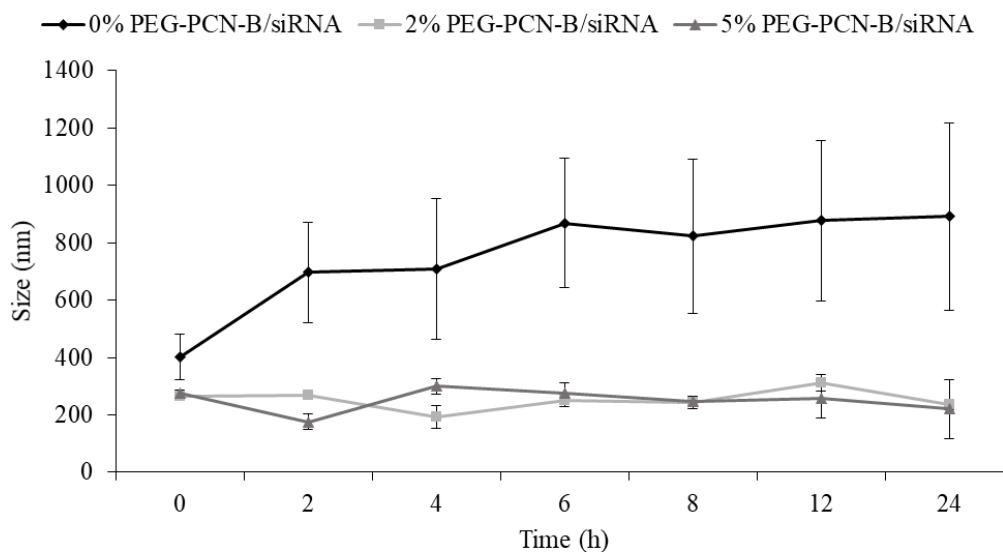


Figure 31 The variations in particle size of 0% PEG-PCN-B, 2% PEG-PCN-B and 5% PEG-PCN-B/ siRNA complexes in 10% FBS

4.3.7 Physical stability of PEGylated cationic niosomes

The particle size of non-PEGylated cationic niosomes stored at 25 °C obviously increased compared after the 2nd week, whereas gradually changed in the 4 °C storage condition of first 4 weeks and markedly increased at the 5th week. The PEGylated cationic niosomes could prevent particle aggregation for 16 weeks. The zeta potential of 0% PEG-PCN-B stored at 25 °C decreased markedly after be stored for 8 weeks, whereas no alteration was noticed in the PEGylated cationic niosomes (Figure 32). Meanwhile, insignificant change changes in zeta potential was observed at 4 °C for any formulation. The temperature and storage time are the important factors affecting the physical stability of cationic niosomes. Therefore, it is important to be concerned since the surface properties of vesicles should be optimized to prevent aggregation such as incorporation with charge inducers as well as PEGylation applications to provide suitable electrostatic or steric repulsion (163). This finding suggested that the stability of cationic niosomes is primarily influenced by the change of temperature. The alterations in the crystalline structure of lipids can be induced by temperature which is correlated with energy input. This finding agreed with a previous report that the decrease in the zeta potential of the SLNs associated with the rapid growth of solid lipid

nanoparticles (SLNs) stored at 50 °C. Moreover, high temperatures can induce the destabilization due to the changes in zeta potential (164). PEGylation significantly increased storage stability compared to non-PEGylated particles which could provide a steric barrier and prevent particle aggregation (165, 166). Therefore, the recommended storage condition of 0% PEG-PCN-B was 4 °C for 1 month, whereas 2% PEG-PCN-B and 5% PEG-PCN-B could be kept at both 4 °C or 25 °C for 16 weeks.

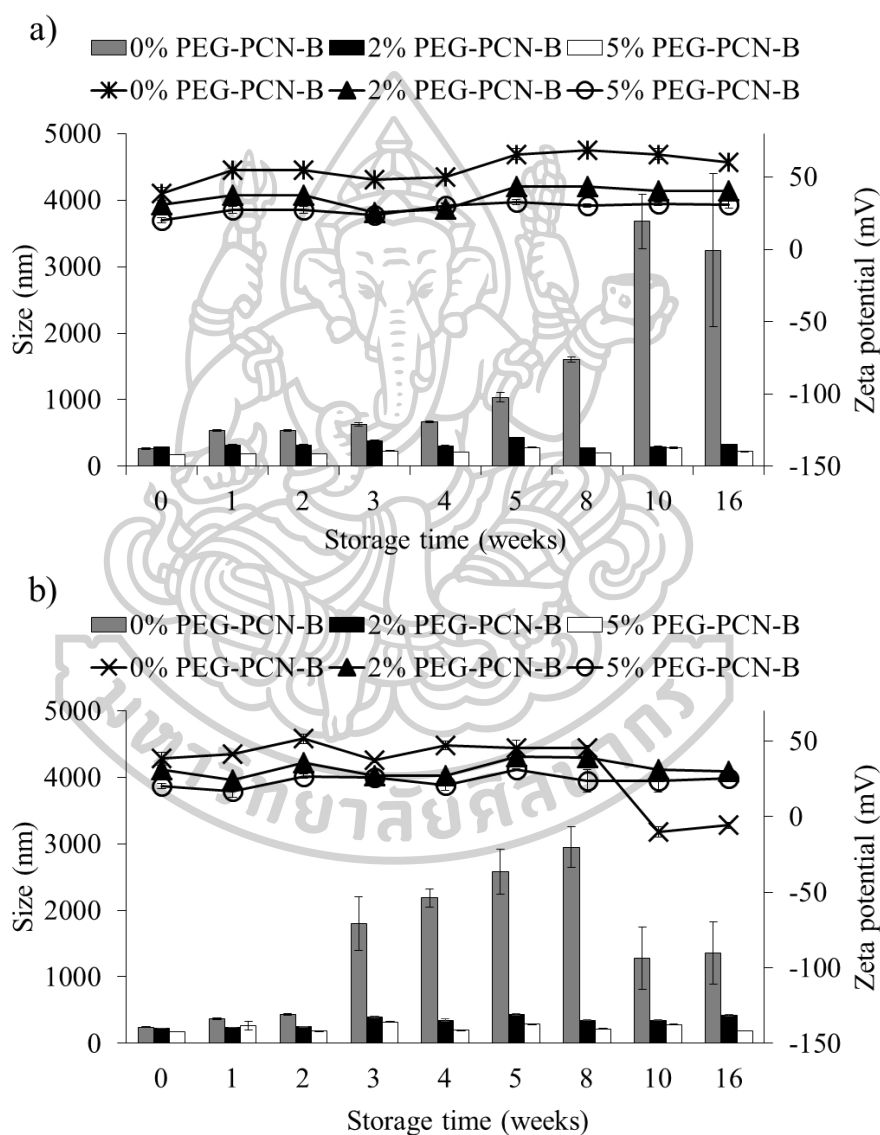


Figure 32 The particle size and zeta potential of 0% PEG-PCN-B, 2% PEG-PCN-B and 5% PEG-PCN-B after being kept at (a) 4 °C and (b) 25 °C for 4 months

4.4 Apoptosis induction of Bcl-2, Mcl-1 and survivin targeted siRNA delivery in breast cancer cells

4.4.1 Cellular uptake of nioplexes studied by using flow cytometry analysis and CLSM

Cellular uptake was performed to ensure that the complexes of siRNA could be taken up into MCF-7 and MDA-MB-231 cells. The data was obtained from flow cytometry analysis by using siAF488 for green fluorescence detection. The weight ratios of each sample presenting high silencing efficiency in the previous experiment were employed which were 2.5, 15 and 15 for Lipo2k, PCN-B and 2% PEG-PCN-B, respectively. The transfection of complexes was examined under in the presence of serum 10% serum. The result showed that all formulations presented high % cellular uptake in both cell lines which was more than 95% except that of lipo2k transfection in MCF-7 which was 84% (Figure 33a and Figure 34a). As presented in Figure 33b and Figure 34b, 2% PEG-PCN-B provided comparable MFI with Lipo2k. Meanwhile, MFI of 0% PEG-PCN-B was significantly higher than the others, which the complexes of 0% PEG-PCN-B/siAF488 were highly accumulated in both cell lines. This result suggested that 0% PEG-PCN-B might be a potential cationic lipid providing a high capacity to convey siRNA for breast cancer cells. Although PEGylation provides stability and the blood circulation time of liposomes, it may reduce siRNA loading on cationic niosomes by its steric effect which results in a decline in the MFI and cellular uptake (166). The result was also assured by CLSM that the delivery systems could deliver siAF488 into the desired target site. 0% PEG-PCN-B manifested as the most complexes accumulation in the cells. The results were consistent with flow cytometry data (Figure 33c and Figure 34c).

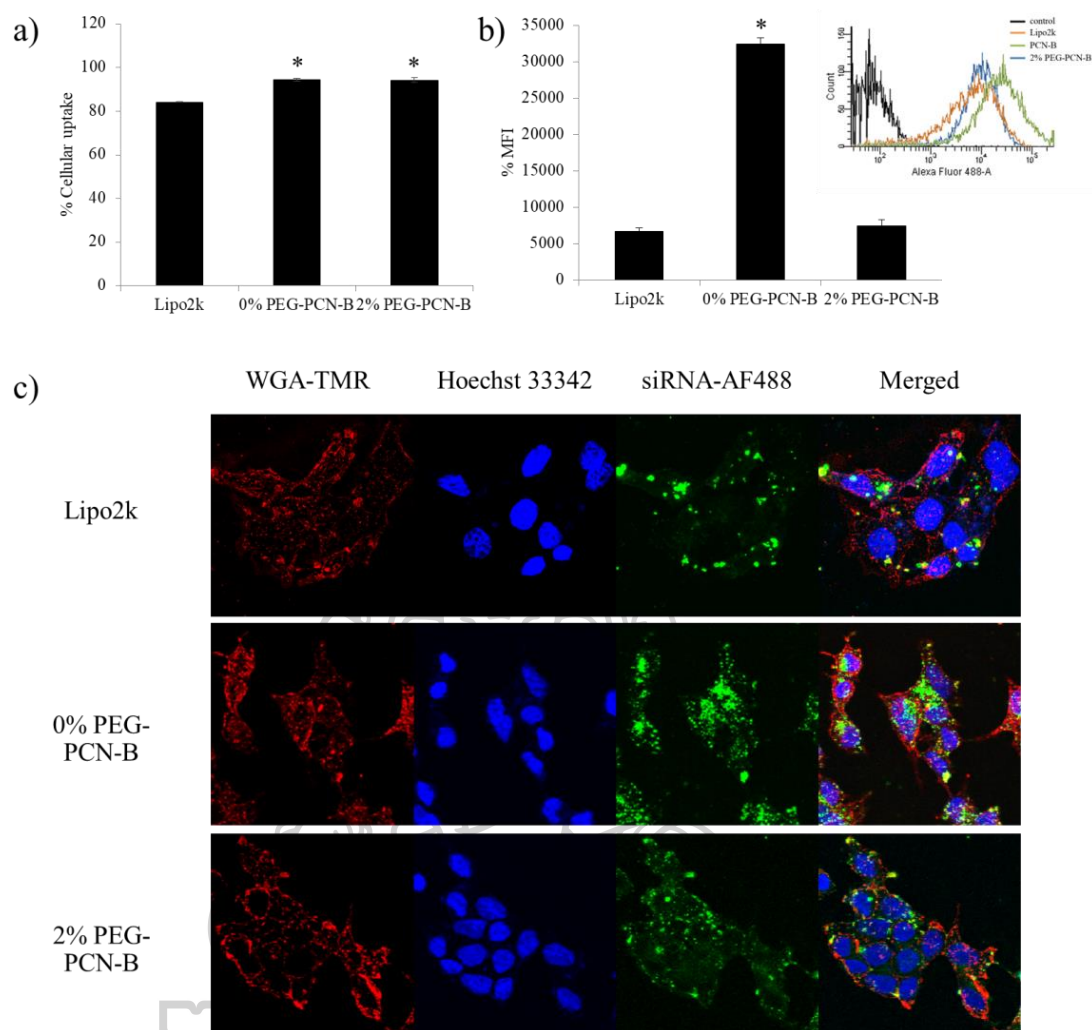


Figure 33 Cellular uptake evaluated after 24 h transfection with siAF488 complexes in MCF-7 cells, (a) the percentage of cellular uptake, (b) MFI plot and fluorescence histogram and (c) CLSM images. *The data was significantly different from Lipo2k transfection at p-value < 0.05.

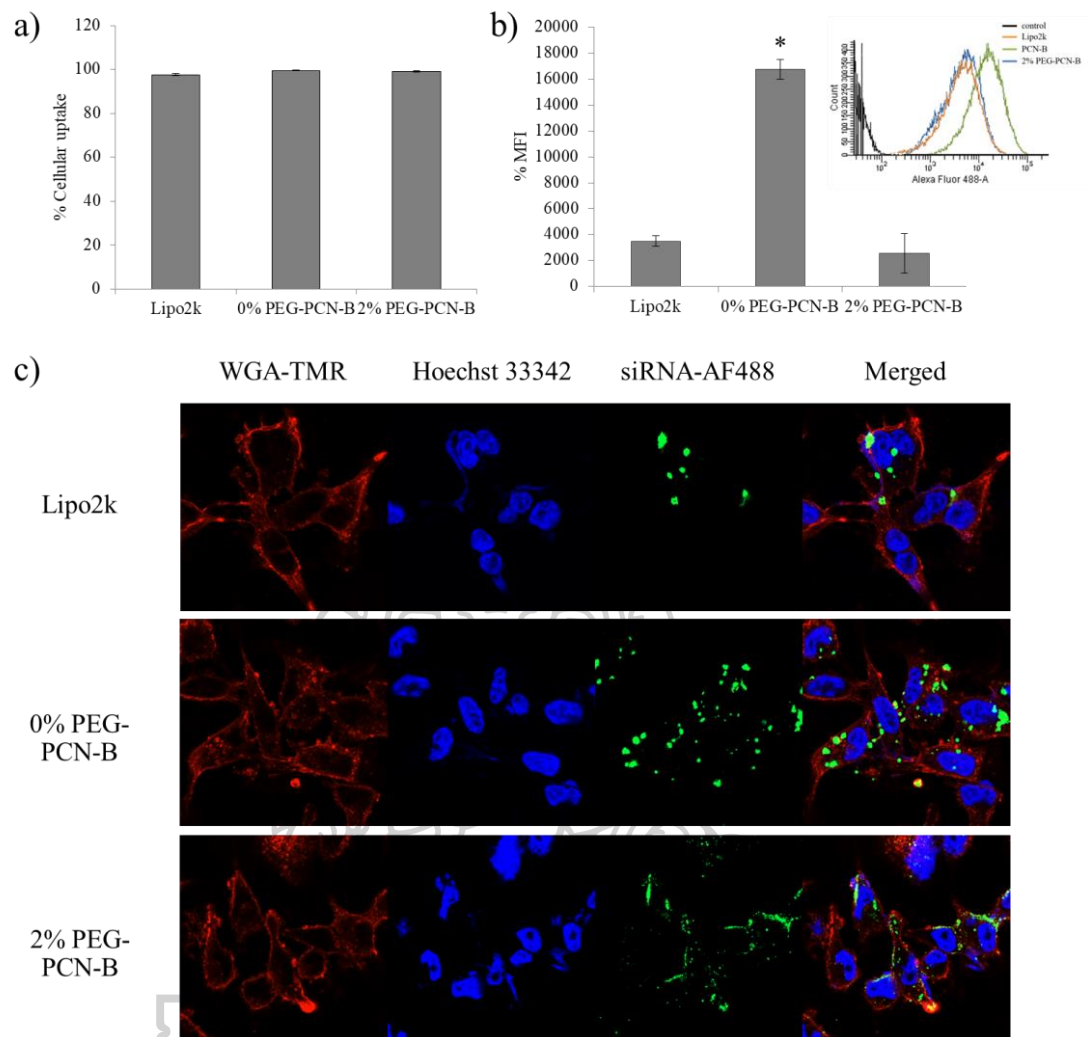


Figure 34 Cellular uptake evaluated after 24 h transfection with siAF488 complexes in MDA-MB 231 cells, (a) the percentage of cellular uptake, (b) MFI plot and fluorescence histogram and (c) CLSM images. *The data was significantly different from Lipo2k transfection at p-value < 0.05.

4.4.2 Expression level of mRNA target by real-time PCR

The mRNA expression of anti-apoptosis targets including Mcl-1 and survivin was determined by using real-time PCR. The relative mRNA expression was calculated by the $2^{-\Delta\Delta CT}$ method to assure the specific gene silencing effect of siRNA delivery systems. The determination of the mRNA levels was performed in breast cancer cells including MFC-7 and MDA-MB-231. The siNT complexes were employed as mock-

treated cells of each formulation. The indicated mRNA expression level was compared with the mRNA level of untreated cell control as % relative mRNA expression. Approximately 60% and 40% reduction of Mcl-1 and Survivin mRNA, respectively, were significantly observed in MCF-7 (Figure 35).

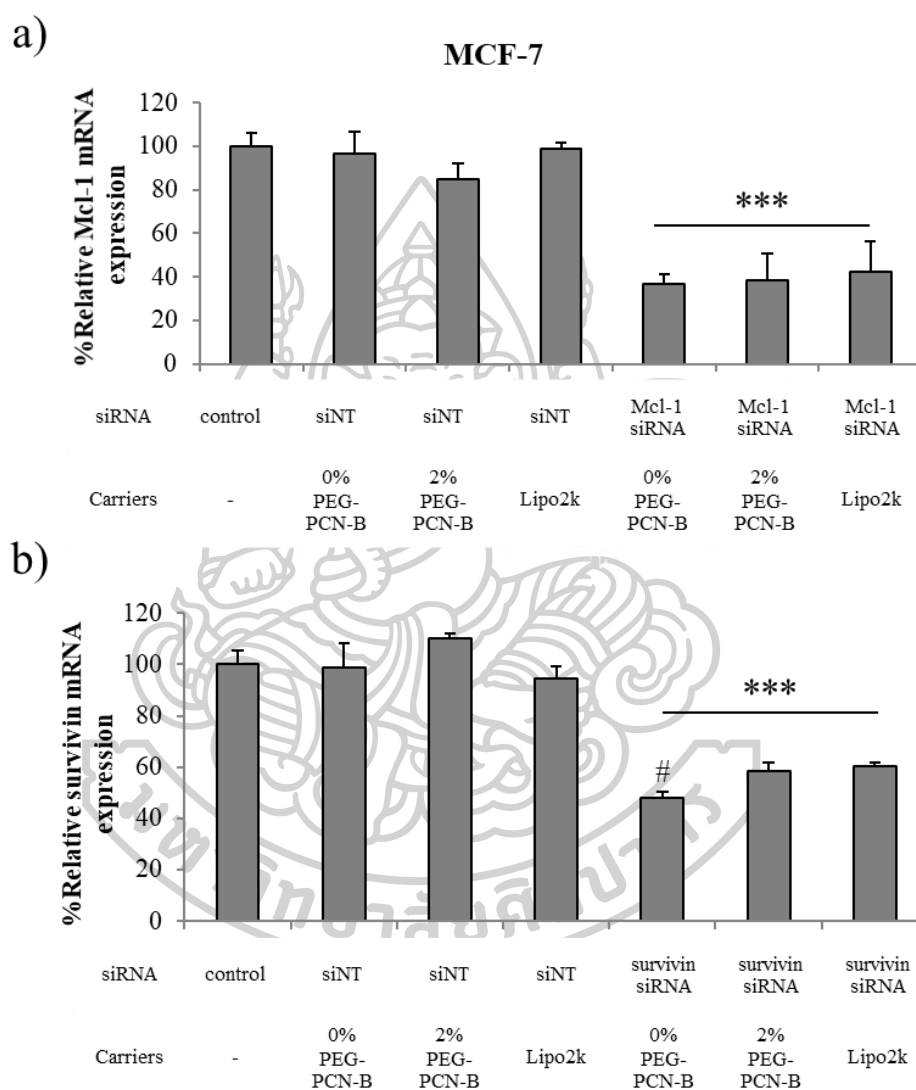


Figure 35 The relative mRNA expression study evaluated using the $2^{-\Delta\Delta CT}$ method which presented as a percentage; (a) relative Mcl-1 mRNA expression and (b) relative survivin mRNA expression in MCF-7. ***The data was significantly different from siNT complexes transfection at p-value < 0.001. #The data was significantly different from Lipo2k transfection at p-value < 0.05.

The relative mRNA of both targets was dramatically reduced by 80% in MDA-MB-231 cells which are depicted in Figure 36. The results suggested that 0% PEG-PCN-B and 2% PEG-PCN-B efficiently delivered and released siRNA to the desired target site. However, there are many factors involved in successful target silencing in different cell lines, such as internalization, siRNA release and intracellular trafficking.

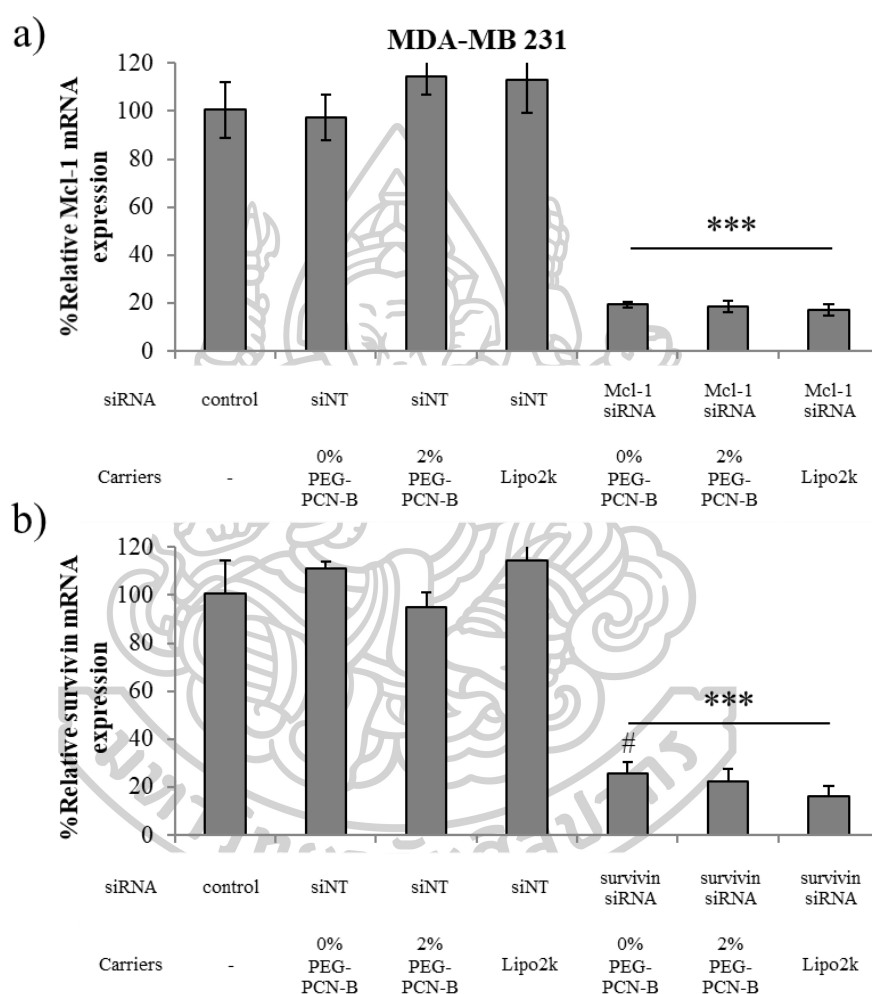


Figure 36 The relative mRNA expression study evaluated using the $2^{-\Delta\Delta CT}$ method which presented as a percentage; (a) relative Mcl-1 mRNA expression and (b) relative survivin mRNA expression in MDA-MB 231. ***The data was significantly different from siNT complexes transfection at p-value < 0.001. #The data was significantly different from Lipo2k transfection at p-value < 0.05.

4.4.3 Cytotoxicity of cationic niosomes

The IC₅₀ in MCF-7 and MDA-MB 231 cells was also investigated by MTT assay. From the IC₅₀ presented in Table 11, PEGylation at 2% was found to reduce the cytotoxicity and increase IC₅₀ about 1.5 times in both cell lines. These results confirmed that PEGylation was sufficiently utilized to reduce cytotoxicity on PCNs at 2%.

Table 11 The IC₅₀ of 0% PEG-PCN-B and 2% PEG-PCN-B in MCF-7 and MDA-MB 231 cells were presented as the mean ± SD of triplicates.

Cells	Cationic niosomes	IC ₅₀ (µg/mL)
MCF-7	0% PEG-PCN-B	30.90 ± 4.39
	2% PEG-PCN-B	45.91 ± 4.70
MDA-MB 231	0% PEG-PCN-B	19.34 ± 1.74
	2% PEG-PCN-B	29.21 ± 5.46

4.4.4 Inhibition of cell proliferation

The consequence of anti-apoptosis mRNA silencing was also confirmed by MTT assay to observe cell death induction by anti-apoptosis siRNA delivery. The weight ratio of carriers/anti-apoptosis siRNA was fixed at 15, and mock-treated cells were also performed in MCF-7 and MDA-MB 231 cells. The cells were treated with designed treatments for 24 h and observed after 72 h. The data in Figure 37a are presented as % cell viability compared with untreated cell control. This assay conducted by silencing anti-apoptotic gene i.e. Mcl-1, Bcl-2 and survivin siRNA. The results expressed that Bcl-2 and survivin silencing did not affect the cell viability in both cell lines. The data of Beh et al. (2009) depicted that Bcl-2 siRNA downregulated Bcl-2 mRNA but did not affect the cell viability in MDA-MB-231 and HeLa cells. The mRNA expression levels were lower than 30% compared with untreated MDA-MB-231 cells. Therefore, the investigation was further performed by applying Bcl-2 siRNA as a chemosensitizer in HeLa cells. This finding was hypothesized that due to the relatively long half-life of Bcl-2 protein, it would take considerable time to obviously observe the effect of protein reduction using mRNA degradation by siRNA (167). In 2005, Talaiezhadeh et al. investigated the effective Bcl-2 gene silencing in MCF-7 cells.

They found that the level of Bcl-2 mRNA was declined by siRNA approximately more than 90% but the level of apoptosis cells did not increase. They also suggested that Bcl-2 targeting might involve another cell death pathway which is autophagy. There is evidence that Bcl-2 protein can interact with Beclin 1 protein. Bcl-2 reduction results in releasing of Beclin1 and then activation of autophagy. Moreover, autophagy can interrupt the apoptosis pathway by breaking down intracellular building blocks including mitochondria which play an important role in the intrinsic pathway of apoptotic cascades (168). The study of Trabulo et al. (2011) investigated the effect of survivin siRNA by using Lipo2k as a delivery system in 3 cell lines including A549, HeLa and MCF-7. Transfection of Lipo2k/survivin siRNA downregulated survivin protein significantly in all cell lines. The cell viability of A549 and HeLa was reduced after the siRNA treatment. However, the cell viability of survivin siRNA/Lipo2k was not significantly different from Lipo2k/siNT in MCF-7 (169). In this study, the silencing of Mcl-1 noticeably induced cell death about 30% in MCF-7 cells, compared to mock-treated cells of each formulation (Figure 37a). On the contrary, the cell viability of Mcl-1 siRNA delivery in MDA-MB-231 cells showed flat effects. This effect was consistent with the previous study. Hamidreza et al. found that Mcl-1 siRNA delivery did not decline cell viability in MDA-231 but significantly decreased when it was combined with RPS6KA5 siRNA in MDA-MB 231 or treated resistant MDA-MB 231 (95). The effect of cell death induction was presented in Figure 37b. 0% PEG-PCN-B and 2% PEG-PCN-B could silence Mcl-1 mRNA and induce cell death which had efficiency as Lipo2k. These findings suggested that Mcl-1 downregulation might be a potential target for apoptosis induction. Mcl-1 has a high turnover rate and short half-life (i.e., 2-3 h) which is different from other Bcl-2 family protein. Therefore, it seems reasonable that Mcl-1 plays an important role in apoptosis which response to rapid changing of Mcl-1 expression (19, 170, 171). However, apoptosis is the sophisticated cell death regulation. There are many apoptotic regulators involving cell death decisions and understudying (10).

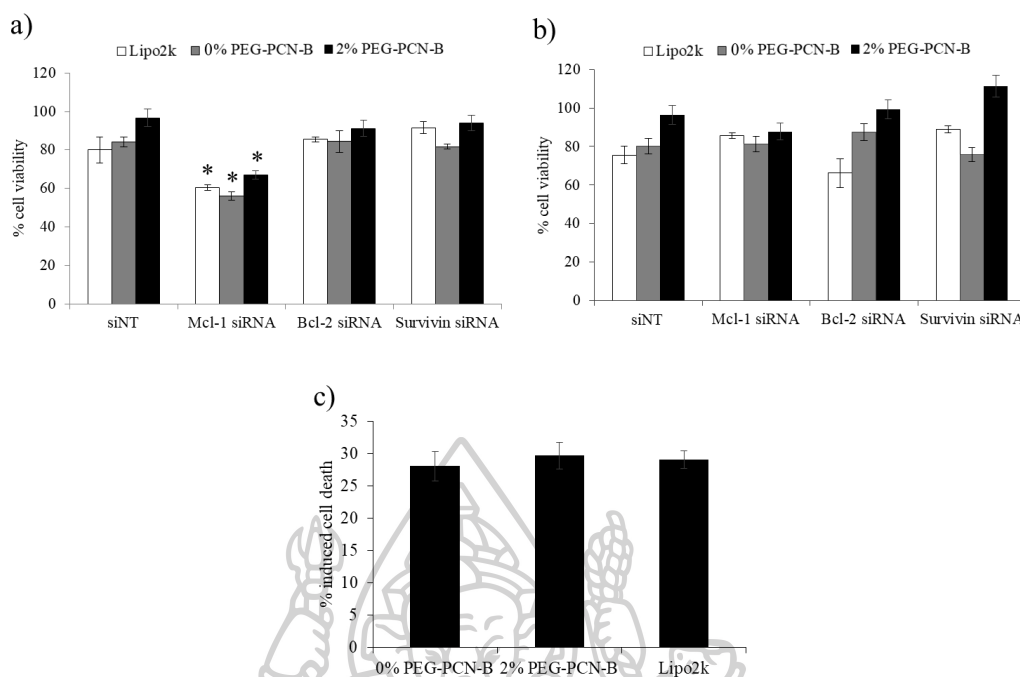
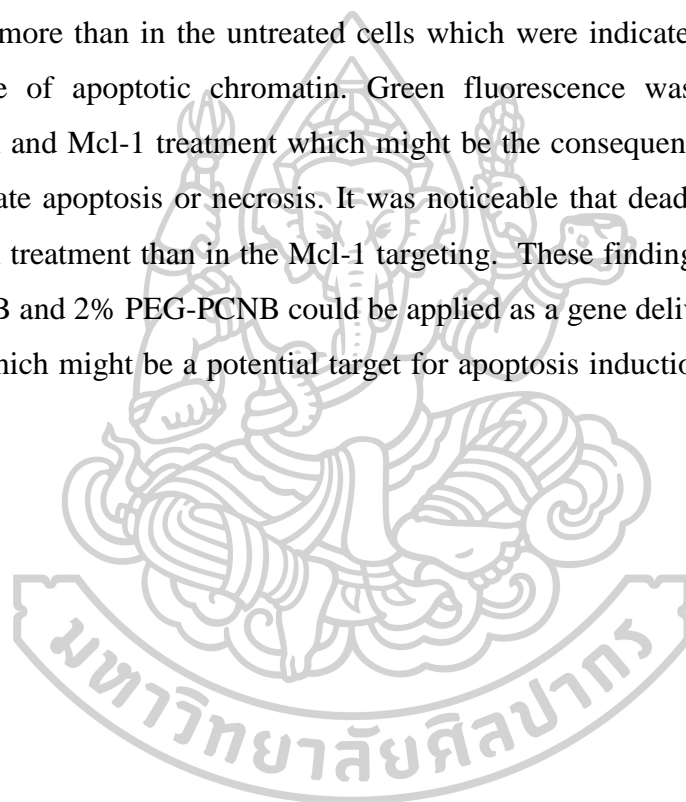


Figure 37 Cell viability of indicated siRNA targeting (Mcl-1, Bcl-2 and survivin) in (a) MCF-7 and (b) MDA-MB 231 cells. The percentage of induced cell death (c) was obtained from the comparison Mcl-1 siRNA complex with siNT complex treatment of each formulation in MCF-7 cells. *The data was significantly different from siNT complexes transfection at p-value < 0.05.

4.4.5 Double stain apoptosis detection: Hoechst 33342 and SYTOX™ Green

As a result of the inhibition of cell proliferation, Mcl-1 siRNA delivery significantly affected the cell viability in MCF-7 cells. Therefore, Apoptosis induction was also confirmed by double stain apoptosis detection assay for the condensed state of chromatin in apoptotic cells. Hoechst 33342 was used as a DNA labeling which is a permeable blue fluorescence dye through the cell membrane. The condensed chromatin is found in the cell undergoing apoptosis which its straining become more brightly than the chromatin in normal cells. SYTOX™ Green was applied for dead cell staining. The green fluorescence dye can easily penetrate into dead cells but it does not cross the live cell membrane. These staining can distinguish dead, live and apoptotic cells. The stained MCF-7 cells were observed under light and fluorescence microscope which depicted in Figure 38. Doxorubicin was used as a positive control in this study which

can induce apoptosis induction in MCF-7 cells (172). As in the fluorescence images, the morphology of untreated cells exhibited a smooth nucleus appearance, spheroid shape, normal chromatin, and uniform cells that were less presenting bright blue fluorescence, and the green fluorescence of dead cells were not found. In contrast, the dominant morphology of apoptotic cells was observed in the cell treated with doxorubicin and Mcl-1. The cell density was less than that of untreated cells. The volume of the nucleus and cytoplasm was decreased since cell shrinkage from apoptosis. Moreover, the chromatin condensation and DNA fragmentation significantly manifested more than in the untreated cells which were indicated by the bright blue fluorescence of apoptotic chromatin. Green fluorescence was found in both of doxorubicin and Mcl-1 treatment which might be the consequence of cell membrane rupture in late apoptosis or necrosis. It was noticeable that dead cells were found in doxorubicin treatment than in the Mcl-1 targeting. These findings suggested that 0% PEG-PCN-B and 2% PEG-PCNB could be applied as a gene delivery system for Mcl-1 siRNA which might be a potential target for apoptosis induction in the MCF-7 cell line.



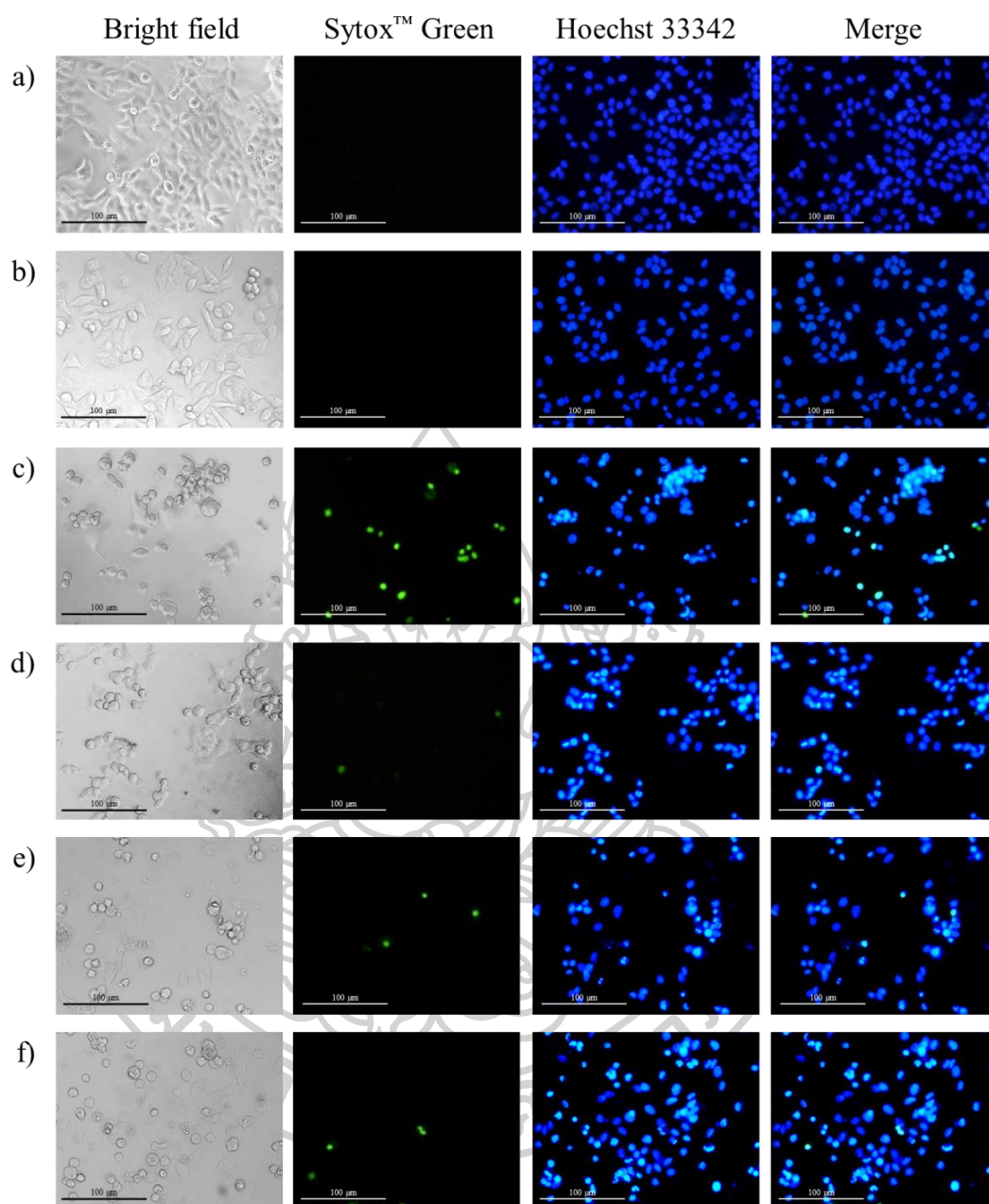


Figure 38 Double stain apoptosis detection was observed under Inverted fluorescence microscope (100X) after 24h of treatments. Untreated cell control (a); PCN-B/siNT (b); 0.8 μM of doxorubicin (c); Lipo2k/Mcl-1 siRNA (d); 0% PEG-PCN-B/Mcl-1 siRNA (e); 2% PEG-PCN-B/Mcl-1 siRNA (f)

CHAPTER 5

CONCLUSION

5.1 Formulation of cationic niosomes (PCN) containing plier-like cationic lipids (PCLs) as non-viral gene carriers

5.1.1 The molar ratio of PCL in cationic niosomes

The surface charge of cationic niosomes was influenced by the increase of molar ratios of cationic lipids. Increasing the molar ratios of cationic lipids resulted in more positive zeta potential. The particle sizes of PCN-A were declined when the molar ratios increased from 0.5-2, and PCN-A at a molar ratio of 2 had the smallest particle size. PCN-A at a molar ratio of 0.5 represented unstable niosome vesicles that had large particle size and a wide range of size distribution. Therefore, the formulations of the niosomes with PCL-A at the molar ratio of 2 mM having positive surface charge and nano-sized range were chosen for nucleic acid delivery.

5.1.2 Weight ratio of carriers/DNA siRNA complexes

Complex formation between cationic niosomes and nucleic acids employed the electrostatic interaction through neutralizing the negative charge of nucleic acids. The increase of weight ratio reaching positive charge was beneficial for nucleic acid complex formation and cellular attachment, resulting in the high transfection and silencing efficiency. However, the cytotoxicity can be caused by excessive positive charge from the delivery systems. The consequence from cytotoxicity may diminish the desired final outcomes. Therefore, the optimization of weight ratios used in gene delivery is an essential step to obtain the maximal cellular activity of gene delivery. This result indicated that PCN-A 2/DNA or PCN-A 2/siRNA at the weight ratios of 1 and 5, respectively, were able to form the complexes with high transfection efficiency and negligible cytotoxicity.

5.1.3 Structure of cationic lipids

Three different hydrophobic tail attributes of PCLs consist of saturated symmetric, saturated asymmetric and unsaturated asymmetric tails which are PCL-A, PCL-B and PCL-C, respectively. PCN-B provided the highest transfection efficiency and silencing efficiency comparing to PCN-A and PCN-C. The shorter chain lipid of PCN-A was associated with cytotoxicity. The lipid arrangement of PCN-C in the lipid bilayer was highly difficult for packing with other compositions, which the arch lipid (double bond area) could be the cause of the unstable bilayer. Therefore, a balance between fluidity and rigidity of the bilayer system is required for cationic lipid designs.

5.1.4 PEGylation cationic niosomes

PEGylation of PCN-B can provide steric stabilization preventing particle aggregations, non-specific binding, and increasing storage stability (173). However, the excessive amount of PCN-B PEGylation at 5% could decrease the transfection efficiency. PEGylation of PCN-B at 2% significantly reduced cytotoxicity and improved efficiency for both pDNA and siRNA delivery in HeLa cells. This study showed that PCN-B and 2% PEG-PCN-B gave high transfection and silencing efficiency even in the present of serum. PEGylation significantly increased storage stability probably providing a steric barrier and preventing particle aggregation. Therefore, the recommended storage condition of 0% PEG-PCN-B was 4 °C for 1 month, whereas 2% PEG-PCN-B and 5% PEG-PCN-B could be kept at both 4 °C or 25 °C for 4 months.

5.2 Cellular internalization mechanisms of PCNs

The major internalization pathways of asymmetric niosomes (PCN-B) were clathrin-mediated endocytosis followed by caveolae-mediated endocytosis and micropinocytosis. The internalization pathway of siRNA delivery was almost the same as DNA delivery. Remarkably, pretreatment with methyl- β -cyclodextrin, which depleted chol from the cell membrane showed the most inhibitory effect on DNA and siRNA delivery. Chol is important for cell membrane ruffle formation which is involved in the endocytosis of extracellular macromolecules, including

micropinocytosis and caveolae- and clathrin-mediated endocytosis (150-154). PCNs presented pH-sensitive properties which might contribute to intracellular endosomal escape for gene delivery applications.

5.3 Apoptosis-related siRNA in breast cancer cells including MCF-7 and MDA-MB 231 cells by PCNs.

In this study, the silencing of Mcl-1 mRNA noticeably reduced the cell viability of MCF-7 cells by approximately 30%. This finding suggested that Mcl-1 downregulation might be identified as a potential target in MCF-7 cells for apoptosis induction. PCN-B can convey Mcl-1 siRNA as efficient as Lipo2k which can silence Mcl-1 mRNA and induced cell death through apoptosis.

In this study novel PCLs as cationic niosomes were used to formulate PCNs which could be applied as gene delivery systems to get the expected therapeutic outcomes. PCNs could be an effective transfection reagent for not only pDNA but also siRNA in HeLa cells. PCN-B was successfully employed as siRNA carriers for anti-apoptotic targets in breast cancer cells that could deliver and release siRNA to the desired target site, silencing mRNA levels in both MCF-7 and MDA-MB-231 cells. Apoptosis targeting may increase tumor cell killing and therefore improve the outcome of patients with various cancer types. The utilization of siRNA targeting apoptosis could be applied for further study as an alternative approach in combination with current chemotherapies and targeted therapies to increase therapeutic outcomes and reduce resistance to the current therapies in cancers.

REFERENCES

1. National Cancer Institute. The Genetics of Cancer 2017 [Available from: <https://www.cancer.gov/about-cancer/causes-prevention/genetics>].
2. National Cancer Institute. Cancer Statistics 2018 [Available from: <https://www.cancer.gov/about-cancer/understanding/statistics>].
3. Siegel RL, Miller KD, Jemal A. Cancer statistics, 2020. *CA: A Cancer Journal for Clinicians*. 2020;70(1):7-30.
4. Breastcancer.org. U.S. Breast Cancer Statistics 2019 [cited 2019 20 Sep]. Available from: https://www.breastcancer.org/symptoms/understand_bc/statistics.
5. American Cancer Society. Breast Cancer Risk Factors You Cannot Change 2019 [cited 2019 24 Sep]. Available from: <https://www.cancer.org/cancer/breast-cancer/risk-and-prevention/breast-cancer-risk-factors-you-cannot-change.html>.
6. Favaloro B, Allocati N, Graziano V, Di Ilio C, De Laurenzi V. Role of apoptosis in disease. *Aging (Albany NY)*. 2012;4(5):330-49.
7. Wong RSY. Apoptosis in cancer: from pathogenesis to treatment. *Journal of Experimental & Clinical Cancer Research*. 2011;30(1):87.
8. Kerr JF, Wyllie AH, Currie AR. Apoptosis: a basic biological phenomenon with wide-ranging implications in tissue kinetics. *British journal of cancer*. 1972;26(4):239-57.
9. Sharma A, Boise LH, Shanmugam M. Cancer Metabolism and the Evasion of Apoptotic Cell Death. *Cancers (Basel)*. 2019;11(8):1144.
10. Williams MM, Cook RS. Bcl-2 family proteins in breast development and cancer: could Mcl-1 targeting overcome therapeutic resistance? *Oncotarget*. 2015;6(6):3519-30.
11. Resnier P, Montier T, Mathieu V, Benoit J-P, Passirani C. A review of the current status of siRNA nanomedicines in the treatment of cancer. *Biomaterials*. 2013;34(27):6429-43.
12. García-Aranda M, Pérez-Ruiz E, Redondo M. Bcl-2 Inhibition to Overcome Resistance to Chemo- and Immunotherapy. *Int J Mol Sci*. 2018;19(12):3950.
13. Akar U, Chaves-Reyez A, Barria M, Tari A, Sanguino A, Kondo Y, et al. Silencing of Bcl-2 expression by small interfering RNA induces autophagic cell death in MCF-7 breast cancer cells. *Autophagy*. 2008;4(5):669-79.

14. Lindeman GJ, Visvader JE. Targeting BCL-2 in breast cancer: exploiting a tumor lifeline to deliver a mortal blow? *Breast Cancer Management*. 2012;2(1):1-4.
15. Oh S, E X, Ni D, Pirooz SD, Lee JY, Lee D, et al. Downregulation of autophagy by Bcl-2 promotes MCF7 breast cancer cell growth independent of its inhibition of apoptosis. *Cell Death & Differentiation*. 2011;18(3):452-64.
16. Akar U, Chaves-Reyez A, Barria M, Tari A, Sanguino A, Kondo Y, et al. Silencing of Bcl-2 expression by small interfering RNA induces autophagic cell death in MCF-7 breast cancer cells. *Autophagy*. 2008;4(5):669-79.
17. Lindeman GJ, Visvader JE. Targeting BCL-2 in breast cancer: exploiting a tumor lifeline to deliver a mortal blow? *Breast Cancer Management*. 2013;2(1):1-4.
18. Xiang W, Yang CY, Bai L. MCL-1 inhibition in cancer treatment. *OncoTargets and therapy*. 2018;11:7301-14.
19. Akgul C. Mcl-1 is a potential therapeutic target in multiple types of cancer. *Cellular and Molecular Life Sciences*. 2009;66(8):1326-36.
20. Campbell KJ, Dhayade S, Ferrari N, Sims AH, Johnson E, Mason SM, et al. MCL-1 is a prognostic indicator and drug target in breast cancer. *Cell Death & Disease*. 2018;9(2):19.
21. Quinn BA, Dash R, Azab B, Sarkar S, Das SK, Kumar S, et al. Targeting Mcl-1 for the therapy of cancer. *Expert opinion on investigational drugs*. 2011;20(10):1397-411.
22. Xiang W, Yang C-Y, Bai L. MCL-1 inhibition in cancer treatment. *Onco Targets Ther*. 2018;11:7301-14.
23. Kennedy SM, O'Driscoll L, Purcell R, Fitz-simons N, McDermott EW, Hill AD, et al. Prognostic importance of survivin in breast cancer. *British journal of cancer*. 2003;88(7):1077-83.
24. Cong H, Xu L, Wu Y, Qu Z, Bian T, Zhang W, et al. Inhibitor of Apoptosis Protein (IAP) Antagonists in Anticancer Agent Discovery: Current Status and Perspectives. *Journal of Medicinal Chemistry*. 2019;62(12):5750-72.
25. Wheatley SP, Altieri DC. Survivin at a glance. *Journal of Cell Science*. 2019;132(7):jcs223826.
26. Chen X, Duan N, Zhang C, Zhang W. Survivin and Tumorigenesis: Molecular Mechanisms and Therapeutic Strategies. *J Cancer*. 2016;7(3):314-23.

27. Jha K, Shukla M, Pandey M. Survivin expression and targeting in breast cancer. *Surgical oncology*. 2012;21(2):125-31.
28. Sarti M, Pinton S, Limoni C, Carbone GM, Pagani O, Cavalli F, et al. Differential expression of testin and survivin in breast cancer subtypes. *Oncol Rep*. 2013;30(2):824-32.
29. Salzano G, Riehle R, Navarro G, Perche F, De Rosa G, Torchilin VP. Polymeric micelles containing reversibly phospholipid-modified anti-survivin siRNA: A promising strategy to overcome drug resistance in cancer. *Cancer letters*. 2014;343(2):224-31.
30. Hu Y, Xu K, Yagüe E. miR-218 targets survivin and regulates resistance to chemotherapeutics in breast cancer. *Breast Cancer Research and Treatment*. 2015;151(2):269-80.
31. Maslova O, Koliada A, Vaiserman A. *Gene Therapy. Reference Module in Biomedical Sciences*: Elsevier; 2019.
32. Farris E, Heck K, Lampe AT, Brown DM, Ramer-Tait AE, Pannier AK. Oral non-viral gene delivery for applications in DNA vaccination and gene therapy. *Current Opinion in Biomedical Engineering*. 2018;7:51-7.
33. Razi Soofiyan S, Baradaran B, Lottfipour F, Kazemi T, Mohammadnejad L. Gene therapy, early promises, subsequent problems, and recent breakthroughs. *Adv Pharm Bull*. 2013;3(2):249-55.
34. Chakraborty C, Sharma AR, Sharma G, Doss CGP, Lee SS. Therapeutic miRNA and siRNA: Moving from Bench to Clinic as Next Generation Medicine. *Mol Ther Nucleic Acids*. 2017;8:132-43.
35. Jones CH, Chen C-K, Ravikrishnan A, Rane S, Pfeifer BA. Overcoming nonviral gene delivery barriers: perspective and future. *Mol Pharm*. 2013;10(11):4082-98.
36. Durymanov M, Reineke J. Non-viral Delivery of Nucleic Acids: Insight Into Mechanisms of Overcoming Intracellular Barriers. *Front Pharmacol*. 2018;9:971-.
37. Yang N. Nonviral gene delivery system. *Int J Pharm Investig*. 2012;2(3):97-8.
38. Kamimura K, Suda T, Zhang G, Liu D. Advances in Gene Delivery Systems. *Pharmaceutical Medicine*. 2011;25(5):293-306.
39. Nayerossadat N, Maedeh T, Ali PA. Viral and nonviral delivery systems for gene delivery. *Adv Biomed Res*. 2012;1:27-.

40. Ibraheem D, Elaissari A, Fessi H. Gene therapy and DNA delivery systems. *International Journal of Pharmaceutics*. 2014;459(1):70-83.
41. Ginn SL, Amaya AK, Alexander IE, Edelstein M, Abedi MR. Gene therapy clinical trials worldwide to 2017: An update. *The Journal of Gene Medicine*. 2018;20(5):e3015.
42. Lares MR, Rossi JJ, Ouellet DL. RNAi and small interfering RNAs in human disease therapeutic applications. *Trends in biotechnology*. 2010;28(11):570-9.
43. Nandety RS, Kuo Y-W, Nouri S, Falk BW. Emerging strategies for RNA interference (RNAi) applications in insects. *Bioengineered*. 2015;6(1):8-19.
44. David S, Pitard B, Benoît JP, Passirani C. Non-viral nanosystems for systemic siRNA delivery. *Pharmacological research*. 2010;62(2):100-14.
45. Tekedereli I, Alpay SN, Akar U, Yuca E, Ayugo-Rodriguez C, Han HD, et al. Therapeutic Silencing of Bcl-2 by Systemically Administered siRNA Nanotherapeutics Inhibits Tumor Growth by Autophagy and Apoptosis and Enhances the Efficacy of Chemotherapy in Orthotopic Xenograft Models of ER (-) and ER (+) Breast Cancer. *Molecular therapy Nucleic acids*. 2013;2(9):e121.
46. Zhang Y, Wang Z, Gemeinhart RA. Progress in microRNA delivery. *Journal of controlled release : official journal of the Controlled Release Society*. 2013;172(3):962-74.
47. Rasoulianboroujeni M, Kupgan G, Moghadam F, Tahriri M, Boughdachi A, Khoshkenar P, et al. Development of a DNA-liposome complex for gene delivery applications. *Materials Science and Engineering: C*. 2017;75:191-7.
48. Zhi D, Bai Y, Yang J, Cui S, Zhao Y, Chen H, et al. A review on cationic lipids with different linkers for gene delivery. *Advances in Colloid and Interface Science*. 2018;253:117-40.
49. Paecharoenchai O, Teng L, Yung BC, Teng L, Opanasopit P, Lee RJ. Nonionic surfactant vesicles for delivery of RNAi therapeutics. *Nanomedicine (Lond)*. 2013;8(11):1865-73.
50. Karim K, Mandal A, Biswas N, Guha A, Chatterjee S, Behera M, et al. Niosome: A future of targeted drug delivery systems. *Journal of Advanced Pharmaceutical Technology & Research*. 2010;1(4):374-80.

51. Bartelds R, Nematollahi MH, Pols T, Stuart MCA, Pardakhty A, Asadikaram G, et al. Niosomes, an alternative for liposomal delivery. *PLoS One*. 2018;13(4):e0194179-e.
52. Chen S, Hanning S, Falconer J, Locke M, Wen J. Recent advances in non-ionic surfactant vesicles (niosomes): Fabrication, characterization, pharmaceutical and cosmetic applications. *European Journal of Pharmaceutics and Biopharmaceutics*. 2019;144:18-39.
53. Opanasopit P, Leksantikul L, Niyomtham N, Rojanarata T, Ngawhirunpat T, Yingyongnarongkul BE. Cationic niosomes an effective gene carrier composed of novel spermine-derivative cationic lipids: effect of central core structures. *Pharmaceutical development and technology*. 2017;22(3):350-9.
54. Pengnam S, Patrojanasophon P, Rojanarata T, Ngawhirunpat T, Yingyongnarongkul B-e, Radchatawedchakoon W, et al. A novel plier-like gemini cationic niosome for nucleic acid delivery. *Journal of Drug Delivery Science and Technology*. 2019;52:325-33.
55. Paecharoenchai O, Niyomtham N, Leksantikul L, Ngawhirunpat T, Rojanarata T, Yingyongnarongkul B-e, et al. Nonionic surfactant vesicles composed of novel spermine-derivative cationic lipids as an effective gene carrier in vitro. *AAPS PharmSciTech*. 2014;15(3):722-30.
56. Schroeder A, Levins CG, Cortez C, Langer R, Anderson DG. Lipid-based nanotherapeutics for siRNA delivery. *J Intern Med*. 2010;267(1):9-21.
57. Hirko A, Tang F, Hughes JA. Cationic lipid vectors for plasmid DNA delivery. *Current medicinal chemistry*. 2003;10(14):1185-93.
58. Grijalvo S, Puras G, Zárata J, Sainz-Ramos M, Qtaish NAL, López T, et al. Cationic Niosomes as Non-Viral Vehicles for Nucleic Acids: Challenges and Opportunities in Gene Delivery. *Pharmaceutics*. 2019;11(2):50.
59. Campani V, Salzano G, Lusa S, De Rosa G. Lipid Nanovectors to Deliver RNA Oligonucleotides in Cancer. *Nanomaterials (Basel)*. 2016;6(7):131.
60. Chan C-L, Ewert KK, Majzoub RN, Hwu Y-K, Liang KS, Leal C, et al. Optimizing cationic and neutral lipids for efficient gene delivery at high serum content. *The journal of gene medicine*. 2014;16(3-4):84-96.

61. Ewert K, Ahmad A, Evans HM, Schmidt HW, Safinya CR. Efficient synthesis and cell-transfection properties of a new multivalent cationic lipid for nonviral gene delivery. *Journal of medicinal chemistry*. 2002;45(23):5023-9.
62. Shirazi RS, Ewert KK, Leal C, Majzoub RN, Bouxsein NF, Safinya CR. Synthesis and characterization of degradable multivalent cationic lipids with disulfide-bond spacers for gene delivery. *Biochimica et Biophysica Acta (BBA) - Biomembranes*. 2011;1808(9):2156-66.
63. Martin B, Sainlos M, Aissaoui A, Oudrhiri N, Hauchecorne M, Vigneron JP, et al. The design of cationic lipids for gene delivery. *Current pharmaceutical design*. 2005;11(3):375-94.
64. Semple SC, Akinc A, Chen J, Sandhu AP, Mui BL, Cho CK, et al. Rational design of cationic lipids for siRNA delivery. *Nature biotechnology*. 2010;28(2):172-6.
65. Zhi D, Zhang S, Wang B, Zhao Y, Yang B, Yu S. Transfection Efficiency of Cationic Lipids with Different Hydrophobic Domains in Gene Delivery. *Bioconjugate Chemistry*. 2010;21(4):563-77.
66. Ojeda E, Puras G, Agirre M, Zarate J, Grijalvo S, Eritja R, et al. The influence of the polar head-group of synthetic cationic lipids on the transfection efficiency mediated by niosomes in rat retina and brain. *Biomaterials*. 2016;77:267-79.
67. Junquera E, Aicart E. Recent progress in gene therapy to deliver nucleic acids with multivalent cationic vectors. *Advances in colloid and interface science*. 2016;233:161-75.
68. Mochizuki S, Kanegae N, Nishina K, Kamikawa Y, Koiwai K, Masunaga H, et al. The role of the helper lipid dioleoylphosphatidylethanolamine (DOPE) for DNA transfection cooperating with a cationic lipid bearing ethylenediamine. *Biochimica et biophysica acta*. 2013;1828(2):412-8.
69. Pengnam S, Plianwong S, Singpanna K, Ni-yomtham N, Radchatawedchakoon W, Yingyongnarongkul BE, et al. PEGylated Plier-Like Cationic Niosomes on Gene Delivery in HeLa Cells. *Key Engineering Materials*. 2019;819:151-6.
70. Di Marzio L, Marianecchi C, Cinque B, Nazzarri M, Cimini AM, Cristiano L, et al. pH-sensitive non-phospholipid vesicle and macrophage-like cells: Binding, uptake and endocytotic pathway. *Biochimica et Biophysica Acta (BBA) - Biomembranes*. 2008;1778(12):2749-56.

71. Huth US, Schubert R, Peschka-Suss R. Investigating the uptake and intracellular fate of pH-sensitive liposomes by flow cytometry and spectral bio-imaging. *Journal of controlled release : official journal of the Controlled Release Society*. 2006;110(3):490-504.
72. Liu J, Bauer H, Callahan J, Kopeckova P, Pan H, Kopecek J. Endocytic uptake of a large array of HPMA copolymers: Elucidation into the dependence on the physicochemical characteristics. *Journal of controlled release : official journal of the Controlled Release Society*. 2010;143(1):71-9.
73. Li C, Samulski RJ. Engineering adeno-associated virus vectors for gene therapy. *Nature Reviews Genetics*. 2020;21(4):255-72.
74. Roma-Rodrigues C, Rivas-García L, Baptista PV, Fernandes AR. Gene Therapy in Cancer Treatment: Why Go Nano? *Pharmaceutics*. 2020;12(3):233.
75. Baghban R, Roshangar L, Jahanban-Esfahlan R, Seidi K, Ebrahimi-Kalan A, Jaymand M, et al. Tumor microenvironment complexity and therapeutic implications at a glance. *Cell Communication and Signaling*. 2020;18(1):59.
76. Yao Y, Dai W. Genomic Instability and Cancer. *J Carcinog Mutagen*. 2014;5:1000165.
77. Bajan S, Hutvagner G. RNA-Based Therapeutics: From Antisense Oligonucleotides to miRNAs. *Cells*. 2020;9(1).
78. Di Fusco D, Dinallo V, Marafini I, Figliuzzi MM, Romano B, Monteleone G. Antisense Oligonucleotide: Basic Concepts and Therapeutic Application in Inflammatory Bowel Disease. *Frontiers in Pharmacology*. 2019;10(305).
79. Pfeffer CM, Singh ATK. Apoptosis: A Target for Anticancer Therapy. *Int J Mol Sci*. 2018;19(2):448.
80. Fadok VA, Bratton DL, Frasch SC, Warner ML, Henson PM. The role of phosphatidylserine in recognition of apoptotic cells by phagocytes. *Cell Death & Differentiation*. 1998;5(7):551-62.
81. Mariño G, Kroemer G. Mechanisms of apoptotic phosphatidylserine exposure. *Cell Res*. 2013;23(11):1247-8.
82. Silva MT. Secondary necrosis: The natural outcome of the complete apoptotic program. *FEBS Letters*. 2010;584(22):4491-9.

83. Berghe TV, Vanlangenakker N, Parthoens E, Deckers W, Devos M, Festjens N, et al. Necroptosis, necrosis and secondary necrosis converge on similar cellular disintegration features. *Cell Death & Differentiation*. 2010;17(6):922-30.
84. Fares J, Fares MY, Khachfe HH, Salhab HA, Fares Y. Molecular principles of metastasis: a hallmark of cancer revisited. *Signal Transduction and Targeted Therapy*. 2020;5(1):28.
85. Guicciardi ME, Gores GJ. Life and death by death receptors. *The FASEB Journal*. 2009;23(6):1625-37.
86. Li J, Yuan J. Caspases in apoptosis and beyond. *Oncogene*. 2008;27(48):6194-206.
87. Wang Y, Tjandra N. Structural insights of tBid, the caspase-8-activated Bid, and its BH3 domain. *J Biol Chem*. 2013;288(50):35840-51.
88. Fouad YA, Aanei C. Revisiting the hallmarks of cancer. *Am J Cancer Res*. 2017;7(5):1016-36.
89. Meng XW, Lee S-H, Kaufmann SH. Apoptosis in the treatment of cancer: a promise kept? *Current Opinion in Cell Biology*. 2006;18(6):668-76.
90. Fernald K, Kurokawa M. Evading apoptosis in cancer. *Trends Cell Biol*. 2013;23(12):620-33.
91. Westhoff M-A, Marschall N, Grunert M, Karpel-Massler G, Burdach S, Debatin K-M. Cell death-based treatment of childhood cancer. *Cell Death & Disease*. 2018;9(2):116.
92. Carrington EM, Zhan Y, Brady JL, Zhang J-G, Sutherland RM, Anstee NS, et al. Anti-apoptotic proteins BCL-2, MCL-1 and A1 summate collectively to maintain survival of immune cell populations both in vitro and in vivo. *Cell Death & Differentiation*. 2017;24(5):878-88.
93. Huang K, O'Neill KL, Li J, Zhou W, Han N, Pang X, et al. BH3-only proteins target BCL-xL/MCL-1, not BAX/BAK, to initiate apoptosis. *Cell Res*. 2019;29(11):942-52.
94. Shamas-Din A, Kale J, Leber B, Andrews DW. Mechanisms of action of Bcl-2 family proteins. *Cold Spring Harb Perspect Biol*. 2013;5(4):a008714-a.

95. Aliabadi HM, Maranchuk R, Kucharski C, Mahdipoor P, Hugh J, Uludağ H. Effective response of doxorubicin-sensitive and -resistant breast cancer cells to combinational siRNA therapy. *Journal of Controlled Release*. 2013;172(1):219-28.
96. Long J, Ji Z, Jiang K, Wang Z, Meng G. miR-193b Modulates Resistance to Doxorubicin in Human Breast Cancer Cells by Downregulating MCL-1. *BioMed Research International*. 2015;2015:373574.
97. Nie S. Understanding and overcoming major barriers in cancer nanomedicine. *Nanomedicine (Lond)*. 2010;5(4):523-8.
98. Maheshwari N, Kumar Atreriya U, Tekade M, Sharma MC, Elhissi A, Tekade RK. Chapter 3 - Guiding Factors and Surface Modification Strategies for Biomaterials in Pharmaceutical Product Development. In: Tekade RK, editor. *Biomaterials and Bionanotechnology*: Academic Press; 2019. p. 57-87.
99. Shukla T, Upmanyu N, Pandey SP, Sudheesh MS. Chapter 14 - Site-specific drug delivery, targeting, and gene therapy. In: Grumezescu AM, editor. *Nanoarchitectonics in Biomedicine*: William Andrew Publishing; 2019. p. 473-505.
100. Hu B, Zhong L, Weng Y, Peng L, Huang Y, Zhao Y, et al. Therapeutic siRNA: state of the art. *Signal Transduction and Targeted Therapy*. 2020;5(1):101.
101. Vercauteren D, Rejman J, Martens TF, Demeester J, De Smedt SC, Braeckmans K. On the cellular processing of non-viral nanomedicines for nucleic acid delivery: Mechanisms and methods. *Journal of Controlled Release*. 2012;161(2):566-81.
102. Nabika H, Unoura K. Chapter 8 - Interaction between nanoparticles and cell membrane. In: Grumezescu AM, editor. *Surface Chemistry of Nanobiomaterials*: William Andrew Publishing; 2016. p. 231-63.
103. Rothen-Rutishauser B, Bourquin J, Petri-Fink A. Nanoparticle-Cell Interactions: Overview of Uptake, Intracellular Fate and Induction of Cell Responses. In: Gehr P, Zellner R, editors. *Biological Responses to Nanoscale Particles: Molecular and Cellular Aspects and Methodological Approaches*. Cham: Springer International Publishing; 2019. p. 153-70.
104. Zhang XX, McIntosh TJ, Grinstaff MW. Functional lipids and lipoplexes for improved gene delivery. *Biochimie*. 2012;94(1):42-58.

105. El-Andaloussi S, Lee Y, Lakhali-Littleton S, Li J, Seow Y, Gardiner C, et al. Exosome-mediated delivery of siRNA in vitro and in vivo. *Nature Protocols*. 2012;7(12):2112-26.
106. Artiga Á, Serrano-Sevilla I, De Matteis L, Mitchell SG, de la Fuente JM. Current status and future perspectives of gold nanoparticle vectors for siRNA delivery. *Journal of Materials Chemistry B*. 2019;7(6):876-96.
107. Yonezawa S, Koide H, Asai T. Recent advances in siRNA delivery mediated by lipid-based nanoparticles. *Adv Drug Deliv Rev*. 2020;154-155:64-78.
108. Lobovkina T, Jacobson GB, Gonzalez-Gonzalez E, Hickerson RP, Leake D, Kaspar RL, et al. In vivo sustained release of siRNA from solid lipid nanoparticles. *ACS Nano*. 2011;5(12):9977-83.
109. Yu YH, Kim E, Park DE, Shim G, Lee S, Kim YB, et al. Cationic solid lipid nanoparticles for co-delivery of paclitaxel and siRNA. *European Journal of Pharmaceutics and Biopharmaceutics*. 2012;80(2):268-73.
110. Riaz MK, Riaz MA, Zhang X, Lin C, Wong KH, Chen X, et al. Surface Functionalization and Targeting Strategies of Liposomes in Solid Tumor Therapy: A Review. *Int J Mol Sci*. 2018;19(1).
111. Xia Y, Tian J, Chen X. Effect of surface properties on liposomal siRNA delivery. *Biomaterials*. 2016;79:56-68.
112. Li L, Hou J, Liu X, Guo Y, Wu Y, Zhang L, et al. Nucleolin-targeting liposomes guided by aptamer AS1411 for the delivery of siRNA for the treatment of malignant melanomas. *Biomaterials*. 2014;35(12):3840-50.
113. Yonenaga N, Kenjo E, Asai T, Tsuruta A, Shimizu K, Dewa T, et al. RGD-based active targeting of novel polycation liposomes bearing siRNA for cancer treatment. *Journal of Controlled Release*. 2012;160(2):177-81.
114. Paecharoenchai O, Teng L, Yung BC, Teng L, Opanasopit P, Lee RJ. Nonionic surfactant vesicles for delivery of RNAi therapeutics. *Nanomedicine (Lond)*. 2013;8(11):1865-73.
115. Hemati M, Haghirsadat F, Yazdian F, Jafari F, Moradi A, Malekpour-Dehkordi Z. Development and characterization of a novel cationic PEGylated niosome-encapsulated forms of doxorubicin, quercetin and siRNA for the treatment of cancer by

using combination therapy. *Artificial cells, nanomedicine, and biotechnology*. 2019;47(1):1295-311.

116. Grijalvo S, Puras G, Zárata J, Sainz-Ramos M, Qtaish NAL, López T, et al. Cationic Niosomes as Non-Viral Vehicles for Nucleic Acids: Challenges and Opportunities in Gene Delivery. *Pharmaceutics*. 2019;11(2).

117. Yang C, Gao S, Song P, Dagnæs-Hansen F, Jakobsen M, Kjems J. Theranostic Niosomes for Efficient siRNA/MicroRNA Delivery and Activatable Near-Infrared Fluorescent Tracking of Stem Cells. *ACS Applied Materials & Interfaces*. 2018;10(23):19494-503.

118. Metwally AA, Pourzand C, Blagbrough IS. Efficient Gene Silencing by Self-Assembled Complexes of siRNA and Symmetrical Fatty Acid Amides of Spermine. *Pharmaceutics*. 2011;3(2):125-40.

119. Antimisiaris S, Mourtas S, Papadia K. Targeted si-RNA with liposomes and exosomes (extracellular vesicles): How to unlock the potential. *International Journal of Pharmaceutics*. 2017;525(2):293-312.

120. Mohamed M, Abu Lila AS, Shimizu T, Alaaeldin E, Hussein A, Sarhan HA, et al. PEGylated liposomes: immunological responses. *Sci Technol Adv Mater*. 2019;20(1):710-24.

121. Milla P, Dosio F, Cattel L. PEGylation of proteins and liposomes: a powerful and flexible strategy to improve the drug delivery. *Current drug metabolism*. 2012;13(1):105-19.

122. Zhou C, Mao Y, Sugimoto Y, Zhang Y, Kanthamneni N, Yu B, et al. SPANosomes as Delivery Vehicles for Small Interfering RNA (siRNA). *Molecular Pharmaceutics*. 2012;9(2):201-10.

123. Obeid MA, Elburi A, Young LC, Mullen AB, Tate RJ, Ferro VA. Formulation of Nonionic Surfactant Vesicles (NISV) Prepared by Microfluidics for Therapeutic Delivery of siRNA into Cancer Cells. *Molecular Pharmaceutics*. 2017;14(7):2450-8.

124. Obeid MA, Dufès C, Somani S, Mullen AB, Tate RJ, Ferro VA. Proof of concept studies for siRNA delivery by nonionic surfactant vesicles: in vitro and in vivo evaluation of protein knockdown. *Journal of Liposome Research*. 2019;29(3):229-38.

125. Sun M, Yang C, Zheng J, Wang M, Chen M, Le DQS, et al. Enhanced efficacy of chemotherapy for breast cancer stem cells by simultaneous suppression of multidrug resistance and antiapoptotic cellular defense. *Acta Biomaterialia*. 2015;28:171-82.
126. Rajput S, Puvvada N, Kumar BNP, Sarkar S, Konar S, Bharti R, et al. Overcoming Akt Induced Therapeutic Resistance in Breast Cancer through siRNA and Thymoquinone Encapsulated Multilamellar Gold Niosomes. *Molecular Pharmaceutics*. 2015;12(12):4214-25.
127. Hemati M, Haghirsadat F, Yazdian F, Jafari F, Moradi A, Malekpour-Dehkordi Z. Development and characterization of a novel cationic PEGylated niosome-encapsulated forms of doxorubicin, quercetin and siRNA for the treatment of cancer by using combination therapy. *Artificial Cells, Nanomedicine, and Biotechnology*. 2019;47(1):1295-311.
128. Paecharoenchai O, Niyomtham N, Ngawhirunpat T, Rojanarata T, Yingyongnarongkul B-e, Opanasopit P. Cationic niosomes composed of spermine-based cationic lipids mediate high gene transfection efficiency. *Journal of Drug Targeting*. 2012;20(9):783-92.
129. dos Santos T, Varela J, Lynch I, Salvati A, Dawson KA. Quantitative assessment of the comparative nanoparticle-uptake efficiency of a range of cell lines. *Small* (Weinheim an der Bergstrasse, Germany). 2011;7(23):3341-9.
130. Lee SJ, Kim MJ, Kwon IC, Roberts TM. Delivery strategies and potential targets for siRNA in major cancer types. *Advanced drug delivery reviews*. 2016;104:2-15.
131. López-García J, Lehocký M, Humpolíček P, Sába P. HaCaT Keratinocytes Response on Antimicrobial Atelocollagen Substrates: Extent of Cytotoxicity, Cell Viability and Proliferation. *J Funct Biomater*. 2014;5(2):43-57.
132. Desigaux L, Sainlos M, Lambert O, Chevre R, Letrou-Bonneval E, Vigneron J-P, et al. Self-assembled lamellar complexes of siRNA with lipidic aminoglycoside derivatives promote efficient siRNA delivery and interference. *Proceedings of the National Academy of Sciences*. 2007;104(42):16534.
133. Schroeder A, Levins CG, Cortez C, Langer R, Anderson DG. Lipid-based nanotherapeutics for siRNA delivery. *Journal of internal medicine*. 2010;267(1):9-21.

134. Wang X-L, Jensen R, Lu Z-R. A novel environment-sensitive biodegradable polydisulfide with protonatable pendants for nucleic acid delivery. *Journal of Controlled Release*. 2007;120(3):250-8.
135. Weecharangsan W, Opanasopit P, Ngawhirunpat T, Apirakaramwong A, Rojanarata T, Ruktanonchai U, et al. Evaluation of chitosan salts as non-viral gene vectors in CHO-K1 cells. *International journal of pharmaceutics*. 2008;348(1-2):161-8.
136. Sahay G, Alakhova DY, Kabanov AV. Endocytosis of nanomedicines. *Journal of controlled release : official journal of the Controlled Release Society*. 2010;145(3):182-95.
137. Vercauteren D, Rejman J, Martens TF, Demeester J, De Smedt SC, Braeckmans K. On the cellular processing of non-viral nanomedicines for nucleic acid delivery: mechanisms and methods. *Journal of controlled release : official journal of the Controlled Release Society*. 2012;161(2):566-81.
138. LeCher JC, Nowak SJ, McMurry JL. Breaking in and busting out: cell-penetrating peptides and the endosomal escape problem. *Biomol Concepts*. 2017;8(3-4):131-41.
139. Chang Kang H, Bae YH. Co-delivery of small interfering RNA and plasmid DNA using a polymeric vector incorporating endosomolytic oligomeric sulfonamide. *Biomaterials*. 2011;32(21):4914-24.
140. Bolcato-Bellemin A-L, Bonnet M-E, Creusat G, Erbacher P, Behr J-P. Sticky overhangs enhance siRNA-mediated gene silencing. *Proceedings of the National Academy of Sciences*. 2007;104(41):16050.
141. Bouxsein NF, McAllister CS, Ewert KK, Samuel CE, Safinya CR. Structure and Gene Silencing Activities of Monovalent and Pentavalent Cationic Lipid Vectors Complexed with siRNA. *Biochemistry*. 2007;46(16):4785-92.
142. Li W, Szoka FC. Lipid-based Nanoparticles for Nucleic Acid Delivery. *Pharmaceutical Research*. 2007;24(3):438-49.
143. Scholz C, Wagner E. Therapeutic plasmid DNA versus siRNA delivery: common and different tasks for synthetic carriers. *Journal of controlled release : official journal of the Controlled Release Society*. 2012;161(2):554-65.
144. Satya Ranjan Sarker, Takeoka S. Amino acid-based liposomal assemblies: Intracellular plasmid DNA delivery

nanoparticles. *J Nanomed*. 2018;2:1008.

145. Koynova R, Tenchov B, Wang L, Macdonald RC. Hydrophobic moiety of cationic lipids strongly modulates their transfection activity. *Molecular pharmaceutics*. 2009;6(3):951-8.

146. Heyes JA, Niculescu-Duvaz D, Cooper RG, Springer CJ. Synthesis of Novel Cationic Lipids: Effect of Structural Modification on the Efficiency of Gene Transfer. *Journal of Medicinal Chemistry*. 2002;45(1):99-114.

147. Meka RR, Godeshala S, Marepally S, Thorat K, Reddy Rachamalla HK, Dhayani A, et al. Asymmetric cationic lipid based non-viral vectors for an efficient nucleic acid delivery. *RSC Advances*. 2016;6(81):77841-8.

148. Nantz MH, Dicus CW, Hilliard B, Yellayi S, Zou S, Hecker JG. The benefit of hydrophobic domain asymmetry on the efficacy of transfection as measured by in vivo imaging. *Molecular pharmaceutics*. 2010;7(3):786-94.

149. Zhou C, Mao Y, Sugimoto Y, Zhang Y, Kanthamneni N, Yu B, et al. SPANosomes as delivery vehicles for small interfering RNA (siRNA). *Molecular pharmaceutics*. 2012;9(2):201-10.

150. Fielding CJ, Fielding PE. Cholesterol and caveolae: structural and functional relationships. *Biochimica et biophysica acta*. 2000;1529(1-3):210-22.

151. Fielding CJ, Fielding PE. Relationship between cholesterol trafficking and signaling in rafts and caveolae. *Biochimica et Biophysica Acta (BBA) - Biomembranes*. 2003;1610(2):219-28.

152. Rodal SK, Skretting G, Garred O, Vilhardt F, van Deurs B, Sandvig K. Extraction of cholesterol with methyl-beta-cyclodextrin perturbs formation of clathrin-coated endocytic vesicles. *Molecular biology of the cell*. 1999;10(4):961-74.

153. Ormerod KG, Rogasevskaia TP, Coorssen JR, Mercier AJ. Cholesterol-Independent Effects of Methyl- β -Cyclodextrin on Chemical Synapses. *PLOS ONE*. 2012;7(5):e36395.

154. Mahammad S, Parmryd I. Cholesterol depletion using methyl-beta-cyclodextrin. *Methods in molecular biology (Clifton, NJ)*. 2015;1232:91-102.

155. dos Santos T, Varela J, Lynch I, Salvati A, Dawson KA. Effects of transport inhibitors on the cellular uptake of carboxylated polystyrene nanoparticles in different cell lines. *PLoS One*. 2011;6(9):e24438.
156. Mayle KM, Le AM, Kamei DT. The intracellular trafficking pathway of transferrin. *Biochimica et biophysica acta*. 2012;1820(3):264-81.
157. Creusat G, Rinaldi AS, Weiss E, Elbaghdadi R, Remy JS, Mulherkar R, et al. Proton sponge trick for pH-sensitive disassembly of polyethylenimine-based siRNA delivery systems. *Bioconjugate chemistry*. 2010;21(5):994-1002.
158. Gabrielson NP, Pack DW. Acetylation of polyethylenimine enhances gene delivery via weakened polymer/DNA interactions. *Biomacromolecules*. 2006;7(8):2427-35.
159. Sato Y, Hatakeyama H, Sakurai Y, Hyodo M, Akita H, Harashima H. A pH-sensitive cationic lipid facilitates the delivery of liposomal siRNA and gene silencing activity in vitro and in vivo. *Journal of Controlled Release*. 2012;163(3):267-76.
160. *Encyclopedia of Surface and Colloid Science*. 2nd ed. Somasudaran P, editor: Taylor & Francis
161. Fröhlich E. The role of surface charge in cellular uptake and cytotoxicity of medical nanoparticles. *Int J Nanomedicine*. 2012;7:5577-91.
162. Ran R, Liu Y, Gao H, Kuang Q, Zhang Q, Tang J, et al. Enhanced gene delivery efficiency of cationic liposomes coated with PEGylated hyaluronic acid for anti P-glycoprotein siRNA: A potential candidate for overcoming multi-drug resistance. *International journal of pharmaceutics*. 2014;477(1):590-600.
163. Huang Y, Rao Y, Chen J, Yang VC, Liang W. Polysorbate cationic synthetic vesicle for gene delivery. *J Biomed Mater Res A*. 2011;96(3):513-9.
164. Heurtault B, Saulnier P, Pech B, Proust JE, Benoit JP. Physico-chemical stability of colloidal lipid particles. *Biomaterials*. 2003;24(23):4283-300.
165. Junyaprasert VB, Teeranachaideekul V, Supaperm T. Effect of charged and non-ionic membrane additives on physicochemical properties and stability of niosomes. *AAPS PharmSciTech*. 2008;9(3):851-9.
166. Xu L, Wempe MF, Anchordoquy TJ. The effect of cholesterol domains on PEGylated liposomal gene delivery in vitro. *Ther Deliv*. 2011;2(4):451-60.

167. Beh CW, Seow WY, Wang Y, Zhang Y, Ong ZY, Ee PL, et al. Efficient delivery of Bcl-2-targeted siRNA using cationic polymer nanoparticles: downregulating mRNA expression level and sensitizing cancer cells to anticancer drug. *Biomacromolecules*. 2009;10(1):41-8.
168. Talaiezhadeh A, jalali F, Galehdari H, Khodadadi A. Time depended Bcl-2 inhibition might be useful for a targeted drug therapy. *Cancer Cell International*. 2015;15(1):105.
169. Trabulo S, Cardoso AM, Santos-Ferreira T, Cardoso AL, Simões S, Pedroso de Lima MC. Survivin Silencing as a Promising Strategy To Enhance the Sensitivity of Cancer Cells to Chemotherapeutic Agents. *Molecular pharmaceutics*. 2011;8(4):1120-31.
170. Quinn BA, Dash R, Azab B, Sarkar S, Das SK, Kumar S, et al. Targeting Mcl-1 for the therapy of cancer. *Expert opinion on investigational drugs*. 2011;20(10):1397-411.
171. Williams MM, Cook RS. Bcl-2 family proteins in breast development and cancer: could Mcl-1 targeting overcome therapeutic resistance? *Oncotarget*. 2015;6(6):3519-30.
172. Pilco-Ferreto N, Calaf GM. Influence of doxorubicin on apoptosis and oxidative stress in breast cancer cell lines. *International journal of oncology*. 2016;49(2):753-62.
173. Steffes VM, Zhang Z, MacDonald S, Crowe J, Ewert KK, Carragher B, et al. PEGylation of Paclitaxel-Loaded Cationic Liposomes Drives Steric Stabilization of Bicelles and Vesicles thereby Enhancing Delivery and Cytotoxicity to Human Cancer Cells. *ACS Applied Materials & Interfaces*. 2020;12(1):151-62.

VITA

NAME Supusson Pengnam

DATE OF BIRTH 15 August 1992

PLACE OF BIRTH Bangkok, Thailand

INSTITUTIONS ATTENDED Faculty of Pharmacy, Silpakorn University

HOME ADDRESS 21/845 Nawamin 42-9 road, Bungkum distinct, Bangkok, Thailand, 10240

PUBLICATION

INTERNATIONAL JOURNAL

Supusson Pengnam, Samawadee Plainwong, Prasopchai Patrojanasophon, Theerasak Rojanarata, Tanasait Ngawhirunpat, Widchaya Radchatawedchakoon, Nattisa Niyomtham, Boon-Ek Yingyongnarongkul, Praneet Opanasopit. Effect of hydrophobic tails of plier-like cationic lipids on nucleic acid delivery and intracellular trafficking. *Int J Pharm.* 2020;5;573:118798.

Supusson Pengnam, Prasopchai Patrojanasophon, Theerasak Rojanarata, Tanasait Ngawhirunpat, Boon-ek Yingyongnarongkul, Widchaya Radchatawedchakoon, Praneet Opanasopit. A novel plier-like gemini cationic niosome for nucleic acid delivery. *J Drug Deliv Sci Technol.* 2019;52:325-33.

Supusson Pengnam, Samawadee Plainwong, Kanokwan Singpanna, Nattisa Niyomtham, Widchaya Radchatawedchakoon, Boon-Ek Yingyongnarongkul and Praneet Opanasopit. PEGylated plier-like cationic niosomes on gene delivery in HeLa cells. *Key Eng Mater.* 2019; 819:169-174.

Supusson Pengnam, Praneet Opanasopit, Theerasak Rojanarata, Nattisa Ni-yomtham, Boon-Ek Yingyongnarongkul and Samarwadee Plianwong. Niosomes containing spermine-based cationic lipid with different linkers for siRNA delivery. *Key Eng Mater.* 2019;819:169-174.

Supusson Pengnam, Lalita Leksantikul, Prasopchai Tonglairoom, Praneet Opanasopit, Nattisa Ni-yomtham, Boon-Ek Yingyongnarongkul and Samarwadee Plianwong. Influence of serum on DNA protection ability and transfection efficiency of cationic lipid-based nanoparticles for gene delivery. *MATEC Web Conf.* 2018;192:01025.

THAI JOURNAL

AWARD RECEIVED

Supusson Pengnam, Prasopchai Tonglairoum, Nattisa Ni-yomtham, Boon-ek Yingyongnarongkul, Praneet Opanasopit, Samarwadee Plianwong. Effects of squalane on the spermine-based cationic niosomes for gene delivery. *Thai Bull Pharm Sci.* 2018;13(2):13-24.
2ND PLACE ORAL PRESENTATION AWARDS
The 6th International Conference on Advanced Pharmaceutical Research (6th ICAPH 2019), Rangsit University, Bangkok, Thailand.

OUTSTANDING POSTER PRESENTATION AWARD ENTITLED

The 34th International Annual Meeting in Pharmaceutical Sciences and 2nd CU FPhS -RIKEN CDB Symposium: Advances in Cellular and Molecular Biology, Arnoma grand hotel, Bangkok, Thailand.

BEST ORAL PRESENTATION AWARDS

The 10th Walailak Research National Conference, Walailak University, Nakhonsithammarat, Thailand.

